FOOD WEBS IN SPACE!

A Dissertation

Presented to the Faculty of the Graduate School

of Cornell University

In Partial Fulfillment of the Requirements for the Degree of

Doctor of Philosophy

by

Joseph Lawrence Simonis

January 2013

FOOD WEBS IN SPACE!

Joseph Lawrence Simonis, Ph. D.

Cornell University 2013

All organisms engage in trophic interactions, as consumers of or as resources for other organisms in a food web. And all organisms move through space, sometimes dispersing to a new location, where they still engage in trophic interactions, but in a different food web. As a result, dispersal connects not just populations of organisms across space, but also the food webs in which they exist. This dissertation comprises five studies examining how dispersal and trophic interactions combine to influence the spatial dynamics of populations and food webs. In addressing this topic, I utilize theoretical and empirical approaches, with the empirical component focused on a system of freshwater rock pools on Appledore Island, Maine, USA.

In Chapter One, I use a set of mathematical models describing a simple two-patch predator-prey metapopulation to show that the inherent variation in the timing of demographic events (called *demographic stochasticity*) qualitatively alters the effect of dispersal on trophic interactions. Chapter Two describes the dominant food chain in the Appledore rock pools and shows how the age structure of the apex predator (*Trichocorixa*) population drives within-pool trophic dynamics through allometric increases in *per capita* consumption rates. I begin exploring dispersal in the Appledore pools in Chapter Three, where I examine the ability of *Larus* gulls to disperse invertebrates between pools. I combine experimental and observational studies to show that gull-mediated dispersal occurs frequently enough to homogenize the taxonomic composition of the pools and may be the main mode of dispersal for many taxa that cannot actively disperse. The apex predator *Trichocorixa*, however, can

fly among pools, and their flight is the focus of Chapter Four, where I show that *Trichocorixa*'s high, yet variable, dispersal rate combines with high, and variable, rates of population turnover to cause complex spatial population dynamics. And in Chapter Five, I explore how *Trichocorixa*'s actions as a frequent disperser and a voracious predator may combine to drive the spatial dynamics of their prey *Moina*. In particular, because *Trichocorixa* emigrates frequently more when *Moina* are in lower densities, they are not likely to drive local *Moina* populations extinct, potentially promoting spatial food-web persistence.

BIOGRAPHICAL SKETCH

Joseph Lawrence Simonis was born July 30, 1984 in Libertyville, Illinois to Lawrence Lee and Sandra Hope Thomson Simonis, the youngest of three children. Joe grew up in Northern Illinois, spending most of the first 18 years of his life in Mundelein, a quiet(ish) town on the edge of the Chicago suburbs, passing his time by being a general nerd, playing sports, drumming, and enjoying the outdoors.

After graduating from Mundelein High School in 2002, Joe headed west to start college at the University of California: San Diego, determined to become a biomedical engineer. That determination was short-lived, however, and Joe found himself switching majors to Ecology, Behavior, and Evolution after two quarters. Joe studied at UCSD for two years before deciding it was time to move back to the Midwest, and transferred to the University of Illinois: Urbana-Champaign at the start of his junior year, where he majored in Integrative Biology. While at UIUC, Joe became engaged in research for the first time as an assistant in Andy Suarez's Lab, helping Chad Tillberg on a project looking at food web position of an invasive ant using stable isotopes. From that moment on, Joe knew he wanted to be an ecologist. Joe conducted his senior honors project in the lab of Carol Shearer, with assistance from Huzefa Raja, looking at the enzymatic capabilities of freshwater fungi. During his time at UIUC, Joe also had the opportunity to be a summer REU researcher at the Kellogg Biological station, working with Carla Cáceres and Spencer Hall to examine host-parasite interactions in *Daphnia*. That summer, Joe went to his first Ecological Society of America meeting (that year in Montreal), where he met Carla's former PhD advisor, and the man who would later become Joe's own PhD advisor, Nelson Hairston, Jr. But before he and Nelson would work together, Joe took a year off from school and moved down to Tallahassee, Florida to work as a technician in Nora Underwood's lab at Florida State University, on a project examining population density effects in plant-insect interactions using *Solanum*.

Joe entered Cornell University in Fall 2007 as a graduate student in Ecology and Evolutionary Biology, passing his candidacy exam in May 2009. Joe had always intended to study spatial community ecology in aquatic systems for his PhD, but a chance conversation with former Shoals Marine Laboratory (SML) director Jim Morin took Joe's mind off of vernal ponds in Upstate New York and moved it to freshwater rock pools on an island off the coast of Maine. Joe visited Appledore Island (home of SML) with Jim for the first time in May 2008 and was hooked on the place and the rock pools. Joe spent four summers (2008 – 2011) on Appledore studying dispersal and trophic interactions in the pools and those studies are the empirical focus of this thesis.

Never a system-focused person and having spent enough time in the Eastern Time Zone for now, Joe is ready to move back to Illinois and on to another project. She begins a post-doctoral position at the Alexander Center for Applied Population Biology at the Lincoln Park Zoo in Chicago, Illinois as soon as this dissertation is accepted.

To my parents, for everything.

ACKNOWLEDGMENTS

"It takes a village to raise a child."

In whatever capacity I am allowed to use this analogy, as I have never had a child before, this dissertation is my baby. And I didn't raise it alone. This was a multi-team effort, and so I have lots of folks to thank for making this work possible.

My thesis committee was incredibly awesome, and I am honored to have gotten the opportunity to work with them for these past five-plus years. Nelson Hairston, Jr. was the best advisor I could have hoped for, exactly the balance of support and *laissez faire* I needed to get through graduate school with a sense of who I am as an independent scientist. Nelson is an inspiration both as an ecologist and as a person, and I will cherish everything I learned from him (including that predate *is* actually a word that means "eat"). Steve Ellner has been a fantastic mentor, specifically with respect to quantitative skills, but more generally, as well. Steve is an incredibly intelligent and eloquent ecologist and one of the nicest people I have ever met. I came to Cornell with the hopes of learning how to combine theoretical and empirical ecology from Steve and Nelson, and I am so thankful that they took me under their wings. I hope I'm ready to fledge. Alex Flecker was incredibly invaluable and just awesome to work with. Perhaps the most enjoyable, critical, and productive discussions I had in graduate school took place in Alex's office. I tell you, get two circuitously talking ecologists in a room together and magic happens (although it can take a while…). Alex also provided field equipment and training and a home-away-from-home in the Flecker lab, all of which I am incredibly thankful for. Anurag Agrawal is the closest thing I have to an outside member on my committee, and I am grateful for the alternative viewpoints he always brought to the table, forcing me to step out of my comfort zone and think about things from a different angle.

More generally, the faculty of Cornell's EEB Department are all top-notch researchers

and wonderful people, and I am thankful for everything that they have taught me. In particular Monica Geber, David Winkler, Jed Sparks, and Harry Greene were all great mentors and friends.

This department is just the latest set in a life full of really fantastic science teachers. I am the product of a public school education (well, plus whatever Cornell counts as), and I am thankful for all of the teachers at Mechanics Grove Elementary School, Carl Sandburg Middle School, Mundelein High School, the University of California: San Diego, the University of Illinois: Urbana-Champaign, Florida State University, and Cornell University who imparted upon me the wisdom, curiosity, and critical thinking skills that I have today. Having grown up in a family of teachers, I am inspired by those who give of themselves to impart knowledge. Teachers make the world go 'round.

I was also the member of a number of really awesome ecology labs that helped me get to Cornell. At UIUC, Andy Suarez and Chad Tillberg gave me my first lab job, and I am so thankful for the opportunity. Carol Shearer was a fantastic undergraduate mentor and she and Huzefa Raja were very helpful in getting me my first first-authored scientific paper. Carla Cáceres was an incredible teacher and mentor. I am thankful that the stars aligned for me to take Limnology with Carla, otherwise I would never have gotten the opportunity to be an REU at Kellogg Biological Station and work with her and Spencer Hall, nor would I have met Nelson at ESA in Montreal. Spencer is perhaps the best science role model I have ever had, seemingly seamlessly combining rigorous math with cool natural history to answer interesting questions, and I am grateful to have had the opportunity to work with and learn from him while at Kellogg. At Florida State, the Underwood Lab provided me with a stimulating job, an opportunity to take a break from school for a year, and a nice respite from freshwater research! Stacey Halpern and Nora Underwood were both fantastic bosses and mentors.

While at Cornell, I've been lucky to call the Hairston Zoo home. All of the members past and present have been supportive, intelligent, helpful folks. In particular, I cannot thank

Colleen Kearns and Lindsay Schaffner enough for all that they did and do to make the lab run smoothly and effectively. Lindsay was also an immense rock star of a helper with formatting this thesis. It would not have been done on time without her. Oh, and she's one of my best friends, and arguably my derby wife. We're not in a relationship, but seriously, she rocks. All of the post-docs and grad students have also made the Hairston Lab a fantastic place to get science done. Lutz Becks, Mikael Gyllstrom, Aldo Barreiro, Teppo Hiltunen, Masato Yamaichi, Brooks Miner, Becky Doyle-Morin, Rebecca Dore, Mike Booth, Cayelan Carey, Sarah Collins, Chris Dalton, and Katie Siriani, you rock! The Flecker lab was also a great sister-lab, and I thank Krista Capps, Jen Moslemi, and Marita Davidson for welcoming me. Both labs were great places to get feedback on ideas, talks, and papers. Never again I worry about formatting a talk as much as I did before presenting at the Flecker lab.

I resided in three different offices in Corson Hall, each full of fantastic people that kept me distracted, happy, and entertained, as well as provided great sounding boards for all of my hair-brained ideas. Although the giant office was a difficult place to work sometimes, I enjoyed sharing a space with Erica Larson, Fin Ransler, Mike Booth, Paulo Llambias, Marissa Weiss, Morgan Mouchka, and Chris Dalton. I found a great, and more productive, home with April Melvin, Susan Cook, and Danica Lombardozzi, all of whom shared sage advice on finishing grad school and were awesome officemates. Finally, MG Weber and Colin Edwards were fantastic foster officemates after I got moved for my final semester. I am so happy to have had even just a few months working together, and wish I could have had more.

I had the pleasure of spending work (and not-work) time with an incredible group of friends including (but not limited to…sorry if I forgot!) Sarah Collins, Rayna Bell, Chris Dalton, Dave Baker, Morgan Mouchka, Willie Fetzer, Ben Dalziel, MG Weber, Jon DeCoste, Nancy Chen, Jen Koslow, Stuart Campbell, Mike Stastny, Mike Booth, Sam Chamberlain, Lindsay Schaffner, Yula Kapetanakos, Anna Forsman, Ezra Lencer, Ginny Howick, Sarah States, April Melvin, Susan Cook, Danica Lombardozzi, Krista Capps, Erica Larson, Findley

Ransler, and Angela Early.

Music and sports have been two of my favorite pastimes throughout my life and grad school was no exception. Ben Dalziel and Scott Callan were a pure joy to play music with on a (semi-)regular schedule, and I cherish everything we created. I wish I had played more music with Thea Whitman, Tyler Cullender, and Emily Goldman than time allowed, but I'm glad that those opportunities happened! I very much appreciate Mike Booth, Jen Koslow, and Paulo Llambias taking me rock climbing (and forcing me to stick at it) my first year. And learning how to skate for derby has been an incredible experience this year, one that I'm so glad to have shared with Lindsay Schaffner. I'm sad to be leaving ILWR behind (before bouting, no less!), but am thankful for everything they've taught me, on and off the track.

The empirical components of my thesis would not have been possible at all without the staff of the Shoals Marine Laboratory. Director Willy Bemis and his staff facilitated my spending four fantastic summers on Appledore, for which I am incredibly grateful. In particular, Mike Rosen, Kevin Wells, Zak Robinson, Kevin Jerram, Hal Weeks, Ian Hewson, Amy Broman, Dan Broman, Phil Thompson, Kipp Quinby, Meg Eastwood, Heather Anne Wright, Hilary Kates, Carter Terry, Captain Tom, Val Anderson, Hanna Wingard, Ian Whipple, Lauren Q, Chef Ryan, Chef Matt, Todd Draper, Chef Charlotte, Christine Bogdanowicz, and countless work interns supported all of this research in many ways, not the least of which was keeping me fed, supplied, and entertained while living on an island for four months at a time. My Kiggins Basement Lab-mates were always a fantastic bunch. In particular, Christine, Q-Bert, Justin, Riley, Elise, Andrew Powers, Kara, and the Hewson lab were fantastic. Phil was always welcome. It was a joy getting to work out on the rocks with Julie Ellis and David Bonter (and the whole gull crew, really). Kara Pellowe was a fantastic intern and a wonderful person to get to work with for two years. I am so lucky to have had the opportunity to mentor Kara and am incredibly thankful to Krista Capps for putting up in touch with each other. Former SML directors JB Heiser and Jim Morin provided sage advice

and critical feedback on my ideas. This work would not at all have been possible without the work Jim (and four undergraduates) did in cataloging and categorizing the rock pool system. Their studies laid the groundwork for my thesis and helped me accomplish a lot of empirical work in relatively short order. And Jim introduced me to the pools, Appledore, and SML.

David Bonter, Sarah Collins, Willie Fetzer, Nelson Hairston Jr., Jess Hewitt, Ian Hewson, Natalie Koskal, Kara Pellowe, Lauren Quevillion, Mike Rosen, Justin Stillwell, Phil Thompson, and Christine Wilkinson provided sweet field assistance on various projects, including Phil, Lauren, and Kara sampling while I was off-island. Ben Dalziel, Daniel Fink, Matt Holden, Paul Hurtado, Dan Rabosy, and David Winkler provided computational, mathematical, and statistical suggestions and advice. Steve Bogdanowicz and Erica Larson provided incredibly helpful tutelage and assistance with the genetics project. My committee, Mike Booth, Krista Capps, Sarah Collins, Ben Dalziel, and Sandy Simonis gave helpful comments and suggestions on earlier versions of these chapters.

This work was financially supported by the Andrew W. Mellon Foundation, the Cornell University Biogeochemistry and Environmental Biocomplexity Program, the Cornell University Ecology and Evolutionary Biology Department, the Cornell University Graduate School, the National Science Foundation (GRFP; DEB-1110545), the Orenstein Family, and the Shoals Marine Laboratory.

Finally, my family, and my parents in particular, have always been supportive of everything I've done, and this thesis is no exception. Lar and Sam have always been in my corner, ready to help or lend support whenever needed. They worked incredibly hard to raise three children into pretty darn good people. They have also been moving champions, helping me get all over the country in multiple directions, including getting me from Ithaca back to Illinois as I frantically try to finish my thesis before I start a new job. My mother also copy edited this thesis (and the manuscripts in it) more times than I can count, and for that I am eternally grateful.

TABLE OF CONTENTS

LIST OF FIGURES

Chapter One

Chapter Two

Chapter Three

Chapter Four

Chapter Five

Appendix

LIST OF TABLES

Chapter One

Chapter Two

Chapter Three

Chapter Four

LIST OF EQUATIONS

Chapter One

Chapter Two

Chapter Four

Appendix

CHAPTER 1

DEMOGRAPHIC STOCHASTICITY REDUCES THE SYNCHRONIZING EFFECT OF DISPERSAL IN PREDATOR–PREY METAPOPULATIONS[1]

[1] Published as: Simonis, Joseph L. 2012. Demographic stochasticity reduces the synchronizing effect of dispersal in predator–prey metapopulations. *Ecology* 93:1517–1524.

ABSTRACT

Dispersal may affect predator–prey metapopulations by rescuing local sink populations from extinction or by synchronizing population dynamics across the metapopulation, increasing the risk of regional extinction. Dispersal is likely influenced by demographic stochasticity, however, particularly because dispersal rates are often very low in metapopulations. Yet the effects of demographic stochasticity on predator–prey metapopulations are not well known. To that end, I constructed three models of a two-patch predator–prey system. The models constitute a hierarchy of complexity, allowing direct comparisons. Two models included demographic stochasticity (pure jump process [PJP] and stochastic differential equations [SDE]), and the third was deterministic (ordinary differential equations [ODE]). One stochastic model (PJP) treated population sizes as discrete, while the other (SDE) allowed population sizes to change continuously. Both stochastic models only produced synchronized predator–prey dynamics when dispersal was high for both trophic levels. Frequent dispersal by only predators or prey in the PJP and SDE spatially decoupled the trophic interaction, reducing synchrony of the non-dispersive species. Conversely, the ODE generated synchronized predator–prey dynamics across all dispersal rates, except when initial conditions produced anti-phase transients. These results indicate that demographic stochasticity strongly reduces the synchronizing effect of dispersal, which is ironic because demographic stochasticity is often invoked *post hoc* as a driver of extinctions in synchronized metapopulations.

INTRODUCTION

Dispersal is a fundamental process in predator–prey metapopulations, as the movements of individuals connect spatially separated patches of locally interacting prey and

predators (Hanski 1998). Dispersing individuals can increase metapopulation persistence by rescuing local populations (subpopulations) from extinction or recolonizing patches after local extinctions (Brown and Kodric-Brown 1977). In these situations, dispersal is able to overcome the risk of local extinction that would otherwise occur as the result of either deterministic factors or demographic stochasticity. The benefits of dispersal come with a potential cost, however, as dispersing individuals may synchronize predator–prey dynamics across patches. If local dynamics are cyclical, for example classic predator–prey cycles, dispersal can synchronize patches in ‘‘phase lock’’ (local dynamics are synchronized with 0-time lag) (Jansen 1999). As a result, all subpopulations will be small, and thus susceptible to demographic stochasticity, at the same time (Earn *et al.* 2000; Hastings 2001). In such situations, rescue is unlikely and the entire metapopulation may go extinct due to simultaneous local extinctions, each the result of local demographic stochasticity.

Although demographic stochasticity contributes to local and metapopulation-wide extinction risk, it may also influence predator–prey dynamics at both spatial scales (Chesson 1978; Bonsall and Hastings 2004). Demographic stochasticity has the largest effect when population events (*e.g.*, births) are infrequent due to small population sizes, low per capita rates, or both. If local predator–prey dynamics are cyclic, local population sizes will often be small enough for demographic stochasticity to affect local dynamics. In addition, *per capita* dispersal rates are generally very low in metapopulations, often orders of magnitude lower than birth or mortality rates (Hanski 1998). Dispersal and, by extension, regional dynamics are therefore likely to be strongly affected by demographic stochasticity, even when subpopulations are large enough that demographic stochasticity does not influence local dynamics (Chesson 1978).

Despite the potential influence of demographic stochasticity on dispersal, we currently know little about its effects on metapopulations. Most models of predator–prey metapopulations are based on deterministic equations, particularly ordinary differential

equations (ODEs), which show that any amount of dispersal by either trophic level will eventually synchronize local dynamics unless patches differ in quality (Murdoch *et al.* 1992, Jansen 1999; Hastings 2001). Although ODE models provide a tractable starting point and useful deterministic comparison, they cannot directly speak to the effects of demographic stochasticity.

This study aims to determine the effect of demographic stochasticity on the ability of dispersal to synchronize dynamics in a predator–prey metapopulation. To that end, I developed three models of a predator–prey metapopulation: two with demographic stochasticity and a deterministic model for comparison. The first stochastic model was a pure jump process (PJP) model, which treated all population processes (*e.g.*, births) as Poisson processes. As a result, population sizes were integers only and changed via discrete jumps with inherent stochasticity. The second model utilized stochastic differential equations (SDEs), and was the continuous approximation to the PJP. In the SDE, population sizes changed continuously, but still with intrinsic stochasticity. The two stochastic models were compared to an ODE, in which population sizes changed deterministically and continuously. The ODE was the law of large numbers approximation of the SDE model. The three models thus form a hierarchy of complexity and exhibit the same mean-field behavior, and so were directly comparable. The PJP and SDE generated similar results, which differed qualitatively and quantitatively from those of the ODE, suggesting that demographic stochasticity strongly alters metapopulation dynamics by reducing the synchronizing effect of dispersal and spatially decoupling trophic interactions.

METHODS

I based my study on a two-patch extension of the Rosenzweig-MacArthur (1963) predator–prey model (RM model), which has been used to study dispersal and synchrony

(*e.g.*, Hastings 2001) and has been applied to empirical systems (*e.g.*, Vasseur and Fox 2009). Locally, prey (*N*) grew according to logistic growth, prey were consumed by predators (*P*) via a Holling Type-II functional response then converted into predators, and predators experienced density-independent mortality. Local dynamics occurred similarly in the two patches (*i* and *j*), and between-patch dispersal for both trophic levels was linear and density independent.

In order to model demographic stochasticity appropriately, both the PJP and SDE models required that all population processes (*e.g.*, births) be represented as independent terms. This necessitated two algebraic rearrangements (detailed in Appendix 1.A) of the classical ODE version of the RM model. First, logistic population growth actually represents the combination of two demographic processes: births and deaths (independent of predation). I decomposed the prey logistic growth term into separate terms for prey birth and predator independent prey mortality, assuming that birth was density dependent and mortality was density independent (as it was for the predators; see Appendix 1.A). Second, the predation term in the prey equation combines predation events that do and do not directly lead to the birth of a new predator. That is, not all of the prey required to produce a new predator are consumed exactly when that new predator is born. Thus, I decomposed the predation term in the prey equation into separate terms for predation events that do and do not lead to predator birth, assuming that the birth of a predator is linked to the consumption of a single (final) prey individual (see Appendix 1.A).

As a result of these rearrangements, the two-patch version of the RM system I used here was represented via 14 separate demographic processes (listed in Table 1). All three representations of the RM model (PJP, SDE, ODE) derived directly from these 14 processes (Table 1.1). Next, I briefly outline the three models, see Appendix 1.A for additional details.

Table 1.1. State changes and propensities (or rates) for each of the 14 population processes in the two-patch predator-prey model.

Process, k	State Change, $(\mathbf{\Delta X})_k$	Propensity or rate, $p_k(\mathbf{X})$
Prey birth, patch i	$(1,0,0,0)^{\mathrm{T}}$	$\left[m_N + r\left(1 - \frac{N_i}{K_N}\right)\right] N_i$
Prey mortality, patch i	$(-1,0,0,0)^{\mathrm{T}}$	$m_N N_i$
Predation, no predator birth, patch i	$(-1,0,0,0)^{\mathrm{T}}$	$\frac{(1-c)aN_iP_i}{N_i + h_N}$
Predation, predator birth, patch i	$(-1,1,0,0)^{\mathrm{T}}$	$\frac{caN_iP_i}{N_i + h_N}$
Predator mortality, patch i	$(0,-1,0,0)^{\mathrm{T}}$	$m_P P_i$
Prey birth, patch j	$(0,0,1,0)^{\mathrm{T}}$	$\left[m_N + r\left(1 - \frac{N_j}{K_N}\right)\right] N_j$
Prey mortality, patch j	$(0,0,-1,0)^{\mathrm{T}}$	$m_N N_j$
Predation, no predator birth, patch j	$(0,0,-1,0)^{\mathrm{T}}$	$\frac{(1-c)aN_jP_j}{N_j + h_N}$
Predation, predator birth, patch j	$(0,0,-1,1)^{\mathrm{T}}$	$\frac{caN_jP_j}{N_j + h_N}$
Predator mortality, patch j	$(0,0,0,-1)^{\mathrm{T}}$	$m_P P_j$
Prey dispersal, patch i to j	$(-1,0,1,0)^{\mathrm{T}}$	$\delta_N N_i$
Prey dispersal, patch j to i	$(1,0,-1,0)^{\mathrm{T}}$	$\delta_N N_j$
Predator dispersal, patch i to j	$(0,-1,0,1)^{\mathrm{T}}$	$\delta_P P_i$
Predator dispersal, patch j to i	$(0,1,0,-1)^{\mathrm{T}}$	$\delta_P P_j$

Notes. The first five processes occur within patch i, the next five processes occur within patch j, and the final four processes occur between patches. $\mathbf{X}^{\mathrm{T}}$ is a vector of the four population sizes (N_i, P_i, N_j, P_j) and the vector $(\mathbf{\Delta X})_k{}^{\mathrm{T}}$ represents the change in the population sizes for process k. For the PJP and SDE models, p_k represents the propensity of k. For the ODE model, p_k represents the rate of k. For all simulations, the following within-patch parameter values were used: prey intrinsic growth rate r = 0.5 d^{-1}, prey mortality rate m_N = 0.1 d^{-1}, prey carrying capacity K_N = 950 prey ind., conversion rate c = 0.2 prey ind. predator ind. $^{-1}$, maximum predator attack rate a = 1.1 prey ind. d^{-1}, predator half-saturation level h_N = 320 prey ind., and predator mortality m_P = 0.1 d^{-1}. Dispersal rates for prey (δ_N) and predators (δ_P) varied across simulations.

Pure Jump Process (PJP) Model

PJP models are a variety of continuous-time Markov chain models, which restrict population sizes to integers and treat all population processes as occurring via discrete ‘‘jumps’’ in continuous time (Kurtz 1970; Gillespie 1977; Allen 2011). In the PJP, each demographic process k was described by two entities: the state-change vector $(\mathbf{\Delta X})_k$, which described how all population sizes would change as a result of k occurring, and the propensity function $p_k(\mathbf{X})$, which determines the likelihood of k happening given the current state of the population $\mathbf{X}$ (Table 1.1), specifically that the probability of k happening in a small time interval Δt is $p_k(\mathbf{X})\Delta t$. For example, take the process of predator mortality in patch i. This process occurred with propensity $p(\mathbf{X}) = m_P P_i$ and resulted in the state change $(\mathbf{\Delta X}) = (0, -1, 0, 0)$, where $(\mathbf{\Delta X})$ = the change in population sizes of N_i, P_i, N_j, and P_j, respectively (only the predator subpopulation in patch i changed in size).

I used Gillespie’s (1977) ‘‘direct method’’ version of the stochastic simulation algorithm to implement the PJP. At time t, the waiting time until the next event (τ) was randomly drawn from an exponential distribution with an expected value equal to $[p_0(\mathbf{X})]^{-1}$, where $p_0(\mathbf{X})$ was the sum of all the propensity functions given $\mathbf{X}$ (Table 1.1). The specific type of that event (*i.e.*, which demographic process occurred) was then determined randomly, where the probability of the event being of process type k is $p_k(\mathbf{X})/p_0(\mathbf{X})$. The system was then updated by replacing t with $t + \tau$ and $\mathbf{X}$ with $\mathbf{X} + (\mathbf{\Delta X})_k$.

Stochastic Differential Equation (SDE) Model

A continuous-state, but still stochastic, analog to a PJP model is an SDE model, which is derived through a Gaussian approximation for the net effect of the many discrete jumps that occur in each small time interval when the population size is large (Kurtz 1978). This

approximation is analogous to the central limit theorem for the sum of many independent random variables, and resulted in each demographic process *k* being represented as a continuous diffusion process whose mean and variance approximate those of the PJP when the population size is large. The system described by the PJP model was thus approximated by the SDE in the sense of Itô:

$$d\mathbf{X}_t = \mu(\mathbf{X}_t)\mathrm{d}t + \mathbf{C}(\mathbf{X}_t)\mathrm{d}\mathbf{B}_t \quad (1.1)$$

in matrix–vector notation (see Appendix 1.A for a full depiction of the model), where the mean $\mu(\mathbf{X}_t) = \sum_k p_k(\mathbf{X})(\mathbf{\Delta X})_k$, **C** was the square-root of the covariance matrix ($\mathbf{C}^2$), which accounted for the variability of demographic events as well as any correlations among events (*e.g.*, dispersal of prey from patch *i* to patch *j*), and $\mathbf{B}_t$ was a vector of independent Brownian motions (one for each population process) (Kurtz 1978; Allen 2011).

Thus, the first term on the right-hand side of Equation 1.1 describes the expected values of the changes in population sizes given the current state of the populations, $\mathbf{X}_t$, and the second term describes the variation in those changes. The variation (stochasticity) in the SDE derived directly from the underlying demographic process.

Ordinary Differential Equation (ODE) Model

Finally, the familiar ODE version of the two-patch RM model can be formulated as a continuous-state, deterministic analog to the PJP and SDE models by taking the limit as population sizes approach infinity (Kurtz 1970). As a result of the law of large numbers approximation, the variance surrounding the population processes became infinitesimal and dropped out of the model. Because the resulting ODE was entirely deterministic, the algebraic rearrangements outlined above canceled out (see Appendix 1.A), and the model was

$$\frac{\mathrm{d}N_i}{\mathrm{d}t} = rN_i\left(1 - \frac{N_i}{K_N}\right) - \frac{aN_iP_i}{N_i + h_N} + \delta_N\left(N_j - N_i\right) \quad (1.2)$$

$$\frac{\mathrm{d}P_i}{\mathrm{d}t} = \frac{caN_iP_i}{N_i + h_N} - m_P P_i + \delta_P\left(P_j - P_i\right) \quad (1.3)$$

where N_i were prey and P_i were predator densities in patch i. Patch j was described by a similar set of equations with the subscripts i and j switched. Other variables are dispersal rates for prey (δ_N) and predators (δ_P), prey intrinsic growth rate (r), mortality rate for predators (m_P), prey carrying capacity (K_N), conversion rate (c), maximum predator attack rate a, and predator half-saturation level h_N.

Model Comparison

Because the SDE and ODE models were formulated through subsequent simplifications that did not affect the (approximate) mean-field behavior of the RM model system as described by the PJP, direct comparisons of the outputs from the three models were valid (Kurtz 1970; Kurtz 1978; Allen 2011; see also Appendix 1.A). For each of the three models, I conducted simulations to evaluate the influence of dispersal on between-population synchrony. I chose values for the within-patch parameters (see Table 1.1) that generated unstable, cyclical local predator–prey dynamics (Rosenzweig and MacArthur 1963), and thus represented a situation where dispersal among patches could synchronize dynamics in phase lock. To focus on how dispersal influences synchrony in each model, without the effect of local extinctions, I chose parameter values that did not cause population sizes to cycle too close to 0. In a single-patch version of the ODE, prey cycled between 95 and 567 individuals and predators between 119 and 245 individuals. Single-patch versions of the PJP and SDE displayed similar dynamics (Appendix 1.B).

For all three models, I ran simulations using two initial conditions. First, following Hastings (2001), I started with one patch empty and the other near a peak in the predator–prey cycle (prey = 420 individuals, predators = 240 individuals). These conditions are likely to arise in situations when a local population has gone extinct or a new patch has just opened and may result in transient dynamics where the two patches are nearly out of phase (antiphase) for an extended period of time (Hastings 2001). The second set of initial conditions was with both patches at the same densities near the cycle peak (prey = 420 individuals, predators = 240 individuals). Because the ODE model is entirely deterministic, the only possible result for the latter set of initial conditions is complete in-phase synchrony, regardless of dispersal rates. Due to stochasticity, such a result is not guaranteed for the PJP or SDE models.

For these two starting conditions, I explored the effects of dispersal by varying δ_N and δ_P values from 0.0001 to 1.0 d^{-1} (or 0.1% to 1000% of the mortality rates), covering the dispersal parameter space evenly on a $\log_{10}$ scale. For the ODE model, I used a 100 × 100 grid (10,000 parameter combinations). The computational intensity of the PJP and SDE models limited the number of simulations I could conduct, so I used a 19 × 19 grid (361 combinations). I ran each simulation for 1000 model days, enough for ~ 20 cycles in the single-patch system.

The models produced data at varying frequencies: I conducted simulations of the ODE and SDE models using a time interval of 0.01 day, and the PJP model generated data after each event (variable number of data per model day). To standardize the data sets across the three models, I censused all population sizes at the beginning of each model day, generating 1001 data points for each simulation. For all analyses, I used the second half of each time series (days 500 to 1000) to eliminate the influence of short-term aperiodic transients, instead focusing on long-term dynamical behavior, including persistent transients. I calculated synchrony between the two subpopulations independently for prey and predators using the Pearson product-moment correlation coefficient on raw abundances with a 0-time lag, which

is an appropriate metric for measuring in-phase synchrony when patches do not differ in parameter values (Bjørnstad *et al.* 1999; Liebhold *et al.* 2004), as is the case here. To account for variability in the PJP and SDE, I ran 10 replicate simulations per parameter combination and summarized the replicates using the mean between-patch correlation for each trophic level. Ten replicates were sufficient to characterize the dynamics and the mean was an appropriate summary statistic (Appendix 1.C).

All simulations were conducted in R (R Development Core Team 2010) using the odesolve (Setzer 2008), GillespieSSA (Pineda-Krch 2008; Pineda-Krch 2010) and yuima (YUIMA Project Team 2012) packages for the ODE, PJP, and SDE, respectively.

RESULTS

Despite the three models describing the same system, they generated quite different results (Figure 1.1). In particular, the stochastic PJP (Figure 1.1A, B) and SDE (Figure 1.1C, D) models produced nearly identical results, which differed qualitatively from the results of the deterministic ODE model (Figure 1.1E, F). Hence, the SDE approximation captures important features of the dynamics of the PJP model not captured by the ODE approximation.

For the initial condition where one patch was full and the other empty, most dispersal rates in the ODE model generated very strong synchrony between patches for both prey and predators (Figure 1.1E, F). Indeed, 90% of all parameter combinations used with the ODE under these initial conditions gave correlations over 0.9 for both trophic levels. The remainder of the parameter combinations generated out-of-phase dynamics for the ODE (areas of blue in Figure 1.1E, F). Both areas of antiphase were long-term transients caused by the prey in patch j initially exceeding the typical local maximum prey density (Appendix 1.B). When $\delta_N = \delta_P = 0.0001$ d^{-1}, the populations became synchronized but not until ~ 33,000 model days (Appendix 1.B). When $\delta_N = 0.00022$ d^{-1} and $\delta_P = 0.0025$ d^{-1}, the populations became

Figure 1.1. Correlation in sizes between the two subpopulations for the (A, C, E) prey and (B, D, F) predators as a function of prey and predator dispersal rates (on a $\log_{10}$ scale). Data are from simulations initiated with one patch full and one empty for the (A, B) pure jump process (PJP), (C, D) stochastic differential equations (SDE), and (E, F) ordinary differential equations (ODE) models. (See Appendix 1.D for results from simulations where both patches started full.) Correlations are from the second half of the time series and the PJP and SDE data are means of the 10 replicate simulations. The boxed data points in panels A–D relate to the data shown as time series in Figure 1.2; for each boxed point, the lowercase letter (a–h) indicates the corresponding panel in Figure 1.2. Lines mark the mortality rates for the two trophic level (0.1 d^{-1} for both).

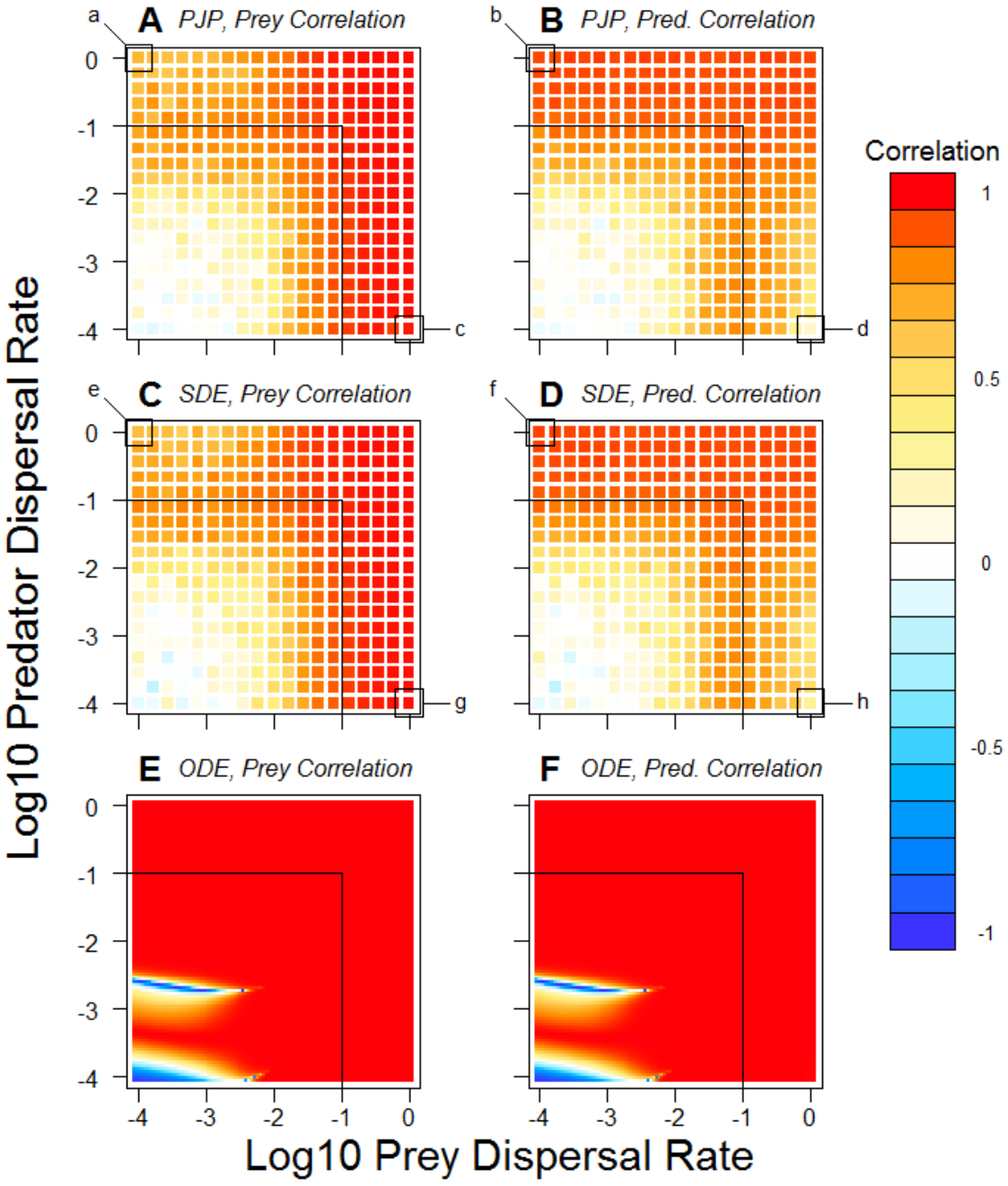
A PJP, Prey Correlation
B PJP, Pred. Correlation
C SDE, Prey Correlation
D SDE, Pred. Correlation
E ODE, Prey Correlation
F ODE, Pred. Correlation
a
b
c
d
e
f
g
h
Correlation
1
0.5
0
-0.5
-1
Log10 Predator Dispersal Rate
Log10 Prey Dispersal Rate
0
-1
-2
-3
-4

synchronized after ~ 2000 model days (Appendix 1.B). The presence of these antiphase transient dynamics in the ODE was sensitive to the initial conditions (previously noted by Hastings 2001), as the simulations where both patches started full were perfectly correlated for all dispersal values (Appendix 1.D).

In contrast to the ODE, both the PJP and SDE models generated much less synchrony over the dispersal parameter space, never resulted in antiphase dynamics, and were not sensitive to initial conditions (Figure 1.1; also see Appendix 1.D for sensitivity to initial conditions). Rather, the areas of asynchrony in the PJP and SDE were due exclusively to the values of the dispersal parameters. In the PJP model when one patch started full and the other empty, only 34.9% and 18.6% of dispersal parameter combinations gave between-patch correlations over 0.9 for the prey and predators, respectively. Similarly for the SDE, 35.3% (prey) and 19.3% (predators) of parameter combinations generated correlation values > 0.9. High correlations were similarly uncommon when both patches started full for both models (PJP, 34.9% for prey and 18.8% for predators; SDE, 35.2% for prey and 18.6% for predators; Appendix 1.D).

Asynchronous dynamics in the PJP and SDE models were located in the same three areas of the dispersal parameter space (Figure 1.1A–D). Naturally, low dispersal rates by both predators and prey caused both trophic levels to be uncorrelated between the patches (lower left corners of Figure 1.1A–D). The additional areas of asynchrony were less intuitive: low dispersal by prey coupled with high dispersal by predators gave low prey correlation only (upper left corners of Figure 1.1A, C) and low dispersal by predators coupled with high dispersal by prey gave low predator correlation only (lower right corners of 1.1B, D). This was again in contrast to the ODE, where the two trophic levels had near-identical correlation values for all dispersal rates. The situations in the PJP and SDE where only one of the species was tightly correlated were the result of a hump-shaped relationship between the dispersal rate of the more dispersive species and the correlation of the less dispersive species (correlation

first increases then decreases along the *y*-axis in Figure 1.1A, C and along the *x*-axis in Figure 1.1B, D). The decrease in correlation with very high dispersal rates of only one trophic level resulted from a spatial decoupling of the predator–prey interaction (as predicted from general theory; see Van de Koppel *et al.* [2005]).

For example, when prey had a very low dispersal rate (0.0001 d^{-1}) and predators were highly dispersive (1.0 d^{-1}) (PJP, Figure 1.2a, b; SDE, Figure 1.2e, f), predators interacted with the prey regionally, yet the prey were interacting with predators locally. Under these conditions, an increase in prey in patch 1 (due to births) led to an increase in predators in patch 1 (via consumption and conversion), but because the predator dispersal rate was so high, the new predators were instantly split equally between the two patches. As a result, there were fewer predators (and a lower predation rate) in patch 1 and more predators (and a higher predation rate) in patch 2 than expected, given the change in local prey densities. The increase in predation that occurred in patch 2 was unrelated to the prey density in patch 2. This mechanism could be thought of as a spatial variation of apparent competition (*sensu* Holt, l977), where two subpopulations of prey share a "common" predator, which is acting as a single population due to high dispersal. Under lower predator dispersal rates (~ 0.1d^{-1}), predators moved enough to correlate their subpopulations, but were more coupled to the local prey populations through the trophic interaction, and the dispersal of predators was able to synchronize the prey.

A similar mechanism generated the other area of asynchrony, where prey disperse frequently and predators rarely (PJP, Figure 1.2c, d; SDE, Figure 1.2g, h). Under this scenario, an increase in predators in one patch led to a decrease in prey in that same patch, but this effect was quickly split between the two patches as prey dispersed from the second patch to the first, equalizing the prey densities. As a result, the effect of predation was less in the first patch than would be expected, and there was an effect of predation in the second patch even though none was expected. The effect of predation experienced in the second patch was

Figure 1.2. Representative time series of (a, c, e, g) prey and (b, d, f, h) predator subpopulations from (a–d) PJP and (e–h) SDE model simulations where dispersal rates spatially decouple the trophic interaction: (a, b, e, f) high predator dispersal and low prey dispersal or (c, d, g, h) low predator dispersal and high prey dispersal. Panel letters (a–h) coincide with the regions of parameter space marked in Figure 1.1. For each panel, the letter indicates the region in Figure 1.1 marked with the corresponding letter. The two patches are represented by different line colors, and the data are from the second half of the time series. High dispersal by predators (1.0 d^{-1}) and low dispersal by prey (0.0001 d^{-1}) resulted in correlations of (a, b) 0.623 for prey and 0.940 for predators in the PJP, compared to (e, f) 0.631 for prey and 0.923 for predators in the SDE. Low dispersal by predators (0.0001 d^{-1}) and high dispersal by prey (1.0 d^{-1}) resulted in correlations of (c, d) 0.986 for prey and 0.210 for predators in the PJP, compared to (g, h) 0.982 for prey and 0.324 for predators in the SDE.

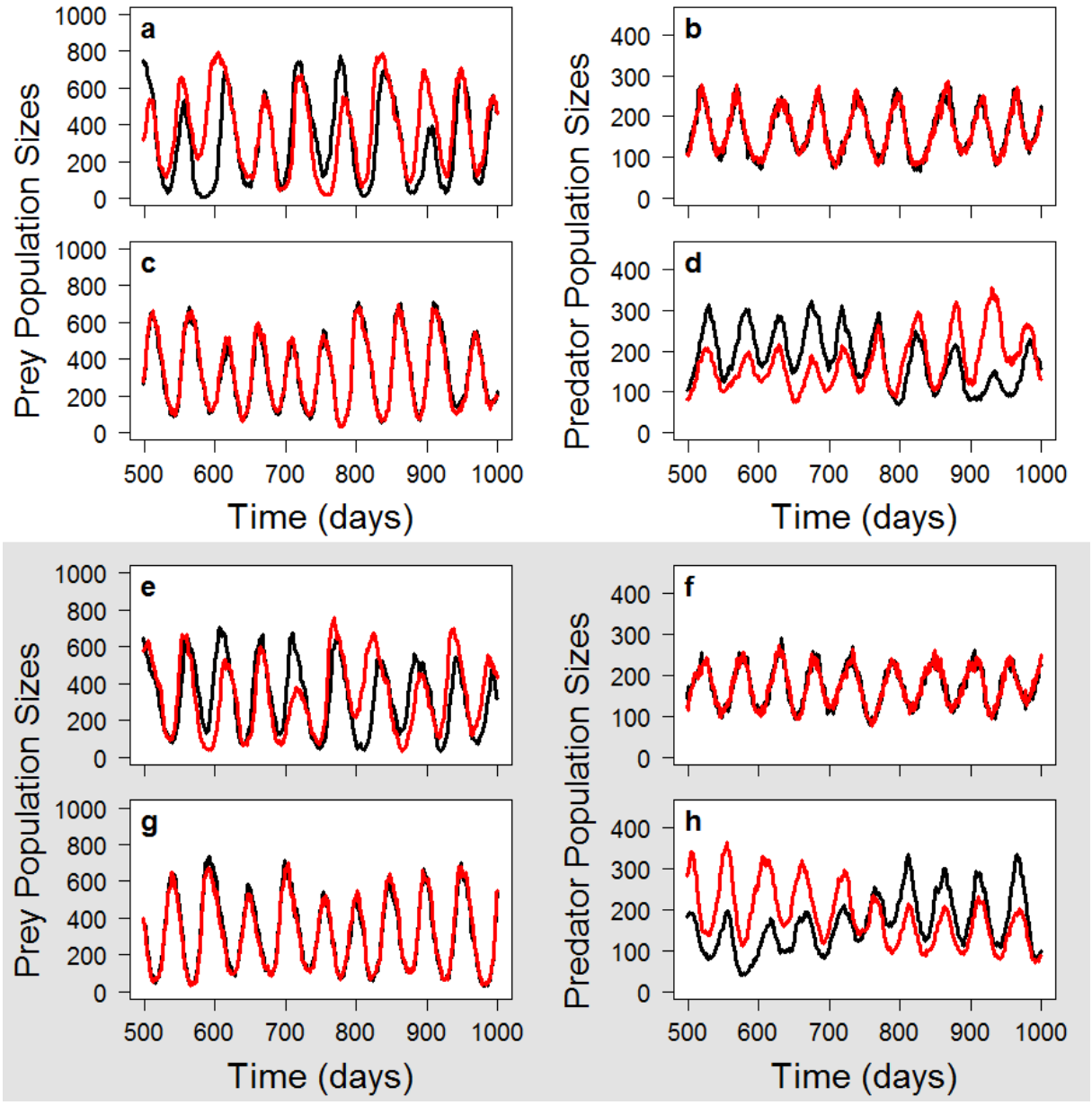
a
b
c
d
e
f
g
h
Prey Population Sizes
Predator Population Sizes
Time (days)
0
100
200
300
400
600
800
1000
500
700
900

independent of the local predator population density, and again the trophic interaction was spatially decoupled. The equalization of prey densities through dispersal led to the predator subpopulations experiencing identical per capita growth rates, but the predator densities were free to drift because predator dispersal was too infrequent to equalize them (hence the similar, but offset, trajectories in Figure 1.2d, h). This mechanism is quite similar to classical competition, where the two subpopulations of predators were sharing a "common" prey resource, which was dispersing so frequently as to act as a single population. Similar to the predators, when prey dispersed less frequently ($\delta_N \approx 0.1\ d^{-1}$), they still moved enough to correlate their subpopulations, but were more coupled to the local predator populations through the trophic interaction, and were able to synchronize the predators. Thus, for dispersal of one trophic level to synchronize the other in the presence of demographic stochasticity, they must disperse enough to synchronize themselves, but not so much that they spatially decouple the trophic interaction. When both prey and predators were highly dispersive, the "local" trophic interaction scaled directly to the regional level.

DISCUSSION

When modeling populations, it is often convenient to use deterministic systems, such as ODEs, making the simplifying assumption that demographic stochasticity does not strongly alter dynamics. When populations are large and events occur frequently, the ODE approach is a valid approximation (Kurtz 1970; Allen 2011). This assumption may not be appropriate for predator–prey metapopulations, however, where per capita dispersal rates are low and populations are often small (Hanski 1998). I have shown here that instead formulating the metapopulation using a model including demographic stochasticity substantially reduced the synchronizing effect of dispersal, at least when one or both trophic levels had low dispersal rates.

The reduction in synchrony occurred even though local dynamics were not significantly affected by the addition of demographic stochasticity (Appendix 1.B; one-patch versions of the three models gave similar dynamics), suggesting that the driver of the differences between the deterministic and stochastic models was dispersal between patches. Specifically, dispersal was a much weaker synchronizing force in the stochastic models than in the deterministic model. Stochastic dispersal was unable to synchronize predator–prey dynamics unless dispersal rates of both trophic levels were very high (Figure 1.1), despite subpopulation sizes rarely being very small (Figure 1.2). This finding agrees with previous theoretical research showing that demographic stochasticity can have pervasive effects even when subpopulation sizes are large, if *per capita* dispersal rates are small (Chesson 1978). Considering that demographic stochasticity is often invoked *post hoc* as a potential driver of regional extinctions in synchronized metapopulations (*e.g.*, Earn *et al.* 2000; Hastings 2001) it is ironic that building it into the model *a priori* reduced the synchronizing effect of dispersal, limiting the role of demographic stochasticity in causing regional extinctions.

The striking similarity between the PJP and SDE, relative to the ODE, (Figures 1.1, 1.2; Appendix 1.A) suggests that the differences between the stochastic and deterministic models were driven exclusively by the presence or absence of demographic stochasticity, rather than the discreteness of the PJP or some combination of discreteness and stochasticity. Compared to the deterministic approximation (transitioning from stochastic SDE to deterministic ODE), which caused a marked change in dynamics, the continuous approximation (transitioning from discrete PJP to continuous SDE) did not alter the ability of dispersal to synchronize predator–prey dynamics in the simulations I conducted. This is not to say that the discreteness of individuals never alters metapopulation dynamics, however. For example, the discreteness of individuals could likely affect both local and regional dynamics if population sizes were regularly low enough to generate extinctions. However, it is currently unknown if the discreteness of individuals will alter predator–prey metapopulation dynamics

on top of the influence of demographic stochasticity, and how small subpopulations must be to enact this effect.

Predators and prey in metapopulations often have very different dispersal rates, typically with predators being more dispersive (Van de Koppel *et al.* 2005). It is therefore significant that the deterministic and stochastic models differed in their predicted dynamics for situations when one trophic level was much more dispersive than the other. In the PJP and SDE models, having only one highly dispersive species spatially decoupled the trophic interaction and altered metapopulation dynamics by introducing a spatial analog to competition or apparent competition (Holt 1977). This result is entirely unexpected from an ODE-perspective, which instead predicts that dispersal of either trophic level should synchronize both (Murdoch *et al.* 1992; Jansen 1999), but agrees with verbal theory predicting a decoupling of trophic interactions when consumers and resources vary in their spatial scales or dispersal rates (Van de Koppel *et al.* 2005).

Although I restricted the model system to two patches and only considered one set of local parameters, the stochastic and deterministic models generated qualitatively distinct outcomes. This divergence needs to be explored in situations of increasing model complexity: additional patches, varying parameters between patches, environmental stochasticity, and more reticulated food webs. It is currently unknown if adding complexity will exacerbate or lessen the difference between the models. Further, the ecological relevance of these results remains to be tested explicitly and empirically, especially considering that the divergence between the deterministic model and the stochastic models depends on the rates of dispersal: the stochastic models differed from the ODE except when dispersal rates were high for both trophic levels. Laboratory microcosms particularly lend themselves to testing the predictions of the models formulated here as dispersal rates can be directly manipulated, confounding factors like the abiotic environment can be controlled tightly, and they generate large amounts of data necessary for model fitting and selection (*e.g.*, Bonsall and Hastings 2004; Vasseur

and Fox 2009).

These demographically stochastic modeling approaches are also applicable to field systems (*e.g.*, Pineda-Krch *et al.* 2007) and may provide important insights into metapopulation dynamics *in situ*. Considering that synchrony is a major concern for species persistence in fragmented landscapes (Earn *et al.* 2000), determining the biological relevance of these theoretical results has significant implications for the management and conservation of predator–prey metapopulations. Under conservation planning guided by a PJP or SDE model, dispersal could be promoted to facilitate persistence without having to worry about synchrony and regional extinctions as much as previously thought based on ODE models.

ACKNOWLEDGMENTS

I am grateful for the advice of Stephen Ellner, Paul Hurtado, Ben Dalziel, Sarah Collins, and Nelson Hairston, Jr. Additionally, the Hairston lab group, Sandra Simonis, and anonymous reviewers provided helpful comments on earlier versions of the manuscript. Many thanks to the yuima team (in particular Stefano Iacus) for assistance with programming the SDE model. I was supported by an NSF Graduate Research Fellowship during the preparation of this manuscript.

REFERENCES

Allen, L. J. S. 2011. An introduction to stochastic processes with applications to biology. CRC Press, New York.

Bjørnstad, O., R. Ims, and X. Lambin. 1999. Spatial population dynamics: analyzing patterns and processes of population synchrony. Trends in Ecology and Evolution 14:427–432.

Bonsall, M. B. and A. Hastings. 2004. Demographic and environmental stochasticity in predator–prey metapopulation dynamics. Journal of Animal Ecology 73:1043–1055.

Brown, J. H. and A. Kodric-Brown. 1977. Turnover rates in insular biogeography: effect of immigration on extinction. Ecology 58:445–449.

Chesson, P. 1978. Predator–prey theory and variability. Annual Review of Ecology and Systematics 9:323–347.

Earn, D. J. D., S. A. Levin, and P. Rohani. 2000. Coherence and conservation. Science 290:1360–1364.

Gillespie, D. T. 1977. Exact stochastic simulation of coupled chemical reactions. Journal of Physical Chemistry 81:2340–2361.

Hanski, I. 1998. Metapopulation dynamics. Nature 396:41–49.

Hastings, A. 2001. Transient dynamics and persistence of ecological systems. Ecology Letters 4:215–220.

Holt, R. D. 1977. Predation, apparent competition, and the structure of prey communities. Theoretical Population Biology 12:197–229.

Jansen, V. A. A. 1999. Phase locking: another cause of synchronicity in predator–prey systems. Trends in Ecology and Evolution 14:278–279.

Kurtz, T. G. 1970. Solutions of ordinary differential equations as limits of pure jump Markov processes. Journal of Applied Probability 7:49–58.

Kurtz, T. G. 1978. Strong approximation theorems for density dependent Markov chains. Stochastic Processes and their Applications 6:223–240.

Liebhold, A., W. D. Koening, and O. N. Bjørnstad. 2004. Spatial synchrony in population dynamics. Annual Review of Ecology, Evolution, and Systematics 35:467–490.

Murdoch, W. M., C. J. Briggs, R. M. Nisbet, W. S. Gurney, and A. Stewart-Oaten. 1992. Aggregation and stability in metapopulation models. American Naturalist 140:41–58.

Pineda-Krch, M. 2008. GillespieSSA: implementing the stochastic simulation algorithm in R. Journal of Statistical Software 25:1–18.

Pineda-Krch, M. 2010. GillespieSSA: Gillespie's Stochastic Simulation Algorithm (SSA). R package version 0.5-4. http://CRAN.R-project.org/package=GillespieSSA.

Pineda-Krch, M., H. Blok, U. Dieckmann, and M. Doebeli. 2007. A tale of two cycles: distinguishing quasi-cycles and limit cycles in finite predator–prey populations. Oikos 116:53–64.

R Development Core Team. 2010. R: a language and environment for statistical computing. R Foundation for Statistical Computing, Vienna, Austria. www.r-project.org

Rosenzweig, M. L. and R. H. MacArthur. 1963. Graphic representation and stability conditions of predator–prey interaction. American Naturalist 97:209–223.

Setzer, R. W. 2008. odesolve: Solvers for Ordinary Differential Equations. R package version 0.5-20.

Van de Koppel, J., R. D. Bardgett, J. Bengtsson, C. Rodriguez- Barrueco, M. Rietkerk, M. J. Wassen, and V. Wolters. 2005. The effects of spatial scale on trophic interactions. Ecosystems 8:801–807.

Vasseur, D. A. and J. W. Fox. 2009. Phase-locking and environmental fluctuations generate synchrony in a predator–prey community. Nature 460:1007–1010.

YUIMA Project Team. 2012. yuima: The YUIMA Project package (unstable version). R package version 0.1.195/r198. http://R-Forge.R-project.org/projects/yuima/.

CHAPTER 2

PREDATOR ONTOGENY DETERMINES TROPHIC CASCADE STRENGTH IN FRESHWATER ROCK POOLS

ABSTRACT

Ontogenetic changes in consumers can influence the magnitude and outcome of direct and indirect ecological interactions. Although most research has focused on qualitative changes in diet (*i.e.*, shifts in trophic guild between life-history stages), quantitative effects of ontogeny, such as allometric scaling in *per capita* consumption rates, could also influence food webs by modulating the relative importance of top-down control. I examined the effect of predator ontogeny on *per capita* consumption rates, selectivity between prey species, and the resulting food-web consequences using a system of freshwater rock pools on Appledore Island, Maine, USA. The rock pools house a simple tri-trophic food chain consisting of chlorophyte algae consumed by cladoceran grazers (*Moina macrocopa* and *Daphnia pulex*), which are then preyed upon by the aquatic insect *Trichocorixa verticalis* (Corixidae). Lab studies showed that *Trichocorixa* grows substantially during its life history, with allometric increases in *per capita* predation rates (consuming both *Moina* and *Daphnia*). Predation rates were significantly higher on *Moina* than *Daphnia* in single-prey experiments and all instars of *Trichocorixa* significantly preferred *Moina* in choice experiments. In a mesocosm experiment, predation by *Trichocorixa* on zooplankters created a top-down trophic cascade by releasing phytoplankton from grazing and the strength of the cascade increased significantly with *Trichocorixa* life-history stage. Further, adult *Trichocorixa* were strong enough predators to reduce cladoceran densities over the duration of the experiment. Similar trophic dynamics appear to occur in the field, as the densities of *Moina* populations in three separate pools decreased markedly after the local *Trichocorixa* population molted into adults. Taken together, these results indicate that consumer ontogeny can affect food-web and ecosystem dynamics without qualitative niche shifts if *per capita* feeding rates change substantially over the consumer's life history. Given the prevalence of both allometrically scaling consumption rates and dynamically structured predator populations, top-predator demography may be an

important driver of the trophic structure and dynamics of food webs.

INTRODUCTION

Most animal species grow substantially as they develop from neonate to adult (Peters 1983; Werner 1988), and many key ecological and physiological parameters, such as *per capita* consumption rate and metabolism, scale allometrically with body size (Mittelbach 1981; Peters 1983; Kooijman 1993; Brown *et al.* 2004). As a result, the strengths and outcomes of ecological interactions may change as a function of the size distributions of interacting species (Werner and Gilliam 1984; Persson 1987; Persson *et al.* 1998; Cohen *et al.* 2003; Hildrew *et al.* 2007a). At the extreme, ontogenetic changes result in individuals qualitatively shifting their diet or habitat use at a critical point in their life history (*e.g.*, metamorphosis), a phenomenon that is known as an ontogenetic niche shift (Werner and Gilliam 1984) and can have significant effects on the dynamics of populations, food webs, and ecosystems (Polis and Strong 1996; Woodward and Hildrew 2002; Rudolf 2007; Rudolf and Lafferty 2011). However, even if individuals do not shift their diet or niche qualitatively as the grow, individual growth often results in important quantitative changes in vital rates (Kooijman 1993; Brown *et al.* 2004) which may influence the strength of ecological interactions.

In particular, many predators show strong increases in *per capita* consumption rates as they develop and grow (Thompson 1975; Mittelbach 1981; Peters 1983; Shine 1991; Kooijman 1993; Aljetlawi *et al.* 2004). Although common, increased consumption with size is not universal among predators: some species show negative or hump-shaped relationships between individual size and *per capita* consumption rate (*e.g.*, Persson 1987; Byström and Andersson 2005). Regardless of the specific relationship between size and consumption, any ontogenetic change in the *per capita* predation rate may influence population and food-web

dynamics by altering the strength of the predator-prey trophic link and the relative importance of top-down control in the food web (Alford 1989; de Roos *et al.* 2003). However, the broader ecological effects of any ontogenetic changes in individual vital rates depend upon the size-structure of the population, particularly whether it is stable or dynamic (Kooijman 1993).

For example, if the size structure of a predator population is stable, the overall rate of consumption by the population will depend only on population density, even if larger predators consume more prey items *per capita*. Conversely, if the size distribution of the predator population is dynamic (*e.g.*, due to non-overlapping generations or size-dependent mortality rates) and individuals display an ontogenetic change in predation rate, the overall rate of consumption will fluctuate as a function of the size distribution, even if the total population size remains constant. As a result, consumer demography may play an important role in dictating the dynamics of consumer-resource interactions by causing fluctuations in predation strength and may even introduce novel, destabilizing feedbacks between consumer populations and their resources (de Roos *et al.* 1990; Persson *et al.* 1998; de Roos and Persson 2002; de Roos *et al.* 2003). Given the complexity of ecosystems, however, the trophic consequences of predator ontogeny and related changes in individual consumption rates will likely depend upon the food-web context in which the consumer-resource interaction occurs (Hairston and Hairston 1997; Hildrew *et al.* 2007b; Jones and Jeppesen 2007).

In a simple food chain with three trophic levels, consumption by the top predator is predicted to decrease the density of intermediate consumers, potentially indirectly increasing the biomass of the basal resource via a trophic cascade (Hairston *et al.* 1960; Paine 1980; Strong 1992; Polis 1999; Schmitz *et al.* 2000; Shurin *et al.* 2002). It may therefore be expected that more voracious predators with stronger trophic links (higher *per capita* predation rates) will cause stronger trophic cascades, all else being equal (Paine 1980; Pace *et al.* 1999). Indeed, variation in consumption rates among apex predators is a major factor

influencing the presence and strength of trophic cascades across ecosystems (Hairston and Hairston 1993; Polis 1999; Borer *et al.* 2005; Hambright *et al.* 2007). Similarly, ontogenetically driven variation in a particular top predator's consumption rate may shift the relative importance of top-down and bottom-up control within the food chain and determine if a trophic cascade occurs in that ecosystem. However, despite the near ubiquity of ontogenetic growth of consumers and relationships between body size and *per capita* consumption rate, the effects of ontogenetic changes in predator consumption rates on trophic dynamics within ecosystems remain poorly studied (de Roos *et al.* 2003).

Here I examine the role of predator ontogeny, and thus size, on the rate of predation and the strength of top-down control in a system of freshwater rock pools on Appledore Island, Maine, USA. The pools contain a simple tri-trophic food chain of phytoplankton (primarily chlorophyte algae) consumed by herbivorous zooplankton (primarily *Moina macrocopa* and *Daphnia pulex* [Cladocera, Daphniidae]) which are in turn preyed upon by *Trichocorixa verticalis* (Hemiptera, Corixidae) (J.G. Morin *et al.*, *unpub. data*). *Trichocorixa* is a potentially voracious consumer (Wurtsbaugh 1992) that grows substantially in size during its ontogeny (Kelts 1979; see also *Results*). Adult *Trichocorixa* prey strongly enough upon *Artemia* (brine shrimp) in the Great Salt Lake, USA to release diatoms from grazing pressure and cause a trophic cascade (Wurtsbaugh 1992). However, little else is known about the trophic ecology of this geographically widely distributed and highly invasive aquatic insect (Tones and Hammer 1975; Tones 1977; Kelts 1979; Wurtsbaugh and Berry 1990; Van de Meutter *et al.* 2010).

Putatively a "generalist omnivore" (Kelts 1979), *Trichocorixa* possesses piercing and sucking mouthparts typical of Hemiptera that make it capable of consuming a wide range of resources (*e.g.*, filamentous algae, zooplankton, dipertan larvae). In the rock pools studied here, Cladocera (*Moina* in particular) are by far the most abundant and available potential resource for *Trichocorixa*, as filamentous algae are not found in the pools and the chironomid

larvae present construct protective cases that deter predation (Dillon 1985; J. L. Simonis, *pers. obs.*). By comparison, the cladocerans are widely distributed among pools and often reach densities exceeding 1,000 individuals L^{-1} (Simonis 2012) due to the high productivity of the pools (Loder *et al.* 1996). However, the two species of Cladocera present are not necessarily equally accessible prey for *Trichocorixa*, as *Daphnia* individuals are nearly 4.4 times larger than *Moina* individuals (by mass, see *Results*) and also exhibit a much lower intrinsic rate of population growth (J. L. Simonis, *unpub. data*). Therefore, the cascading effects of *Trichocorixa* predation on the food web may depend upon which species of cladoceran is present in the rock pool.

The goals of this study were to determine the effect of top-predator ontogeny on predation rate and trophic structure in the Appledore rock-pool ecosystem. I used laboratory feeding experiments to show that all life history stages of *Trichocorixa* consume both prey species (*Daphnia* and *Moina*), yet prefer *Moina*, and that *per capita* consumption rates scale allometrically with predator body size. This increase in predation rate with ontogeny led to a significant increase in the strength of top-down control in a mesocosm experiment. The trophic effect of *Trichocorixa* ontogeny was evident in unmanipulated rock pools as well, as cladoceran densities decreased markedly after *Trichocorixa* developed into adults. These results indicate that even without a qualitative shift in feeding niche, top predator ontogeny can influence food-web structure and trophic dynamics.

METHODS

Study System

Trichocorixa (Hempitera, Corixidae) is an aquatic insect that is native to saline and freshwater habitats across North America (Tones and Hammer 1975; Tones 1977; Kelts 1979;

Wurtsbaugh and Berry 1990) and has also invaded wetlands in Iberia, Africa, and New Caledonia (Jansson 1982; Sala and Boix 2005; Van de Meutter *et al.* 2010). Its ontogeny includes seven life-history stages: egg, five juvenile instars (each lasting 5 – 10 days), and adult. *Trichocorixa* overwinters as eggs, hatching commences in spring or early summer, and there are typically two or three partially-overlapping generations per year, resulting in a dynamic population age structure (Tones 1977; Kelts 1979; see also *Results*). Individuals grow substantially over their ontogeny from approximately 1 mm (body length) as first instar juveniles to approximately 5 mm as adults (Kelts 1979; see also *Results*). On the Isles of Shoals Archipelago (Gulf of Maine, USA), *Trichocorixa* is commonly found in freshwater rock pools that sit above the high tide line. Appledore, the largest island in the archipelago and home to the Shoals Marine Laboratory (SML), is 38.5 ha with approximately 1,500 rock pools, which range in size from *ca*. 1.0 to 30,000 L. The Appledore pools contain a relatively simple food web that is dominated by a tri-trophic food chain of chlorophyte algae, consumed by *Moina* and *Daphnia*, which are, in turn, preyed upon by *Trichocorixa* (J. G. Morin *et al.*, *unpub. data*). Although other species of aquatic invertebrates are found in the pools (*e.g.*, chironomids, ostracods, and cyclopoid copepods), the most abundant prey for *Trichocorixa* are cladocerans, and in particular, *Moina* (Simonis 2012).

All *Trichocorixa* used in experiments reported here were collected from rock pools on Appledore Island in May and June 2009, held in 20 L plastic buckets in the laboratory at SML, and fed *ad libitum* on a mixture of *Daphnia* and *Moina*. Individual *Trichocorixa* used in the experiments were identified to instar based on body shape, size, color, and wing development, following Kelts (1979). Separate laboratory cultures of *Daphnia* and *Moina* for use as prey in experiments were maintained in 20 L buckets and fed rock-pool algae.

Characterizing Predator and Prey Sizes

To determine the length and weight of each non-egg *Trichocorixa* life-history stage, I removed 22 individuals of each instar from the laboratory culture and placed them separately into 20 mL scintillation vials containing filtered well water for 24 hours prior to freeze-killing them at -20° C. After thawing, I measured each individual's length using digital calipers under a dissecting microscope (4-10 × magnification), then after drying at 60° C for 48 hours, I weighed each individual on an ultra-micro balance (Sartorius SE2). I fit a standard length-weight regression to the individual-level data using non-linear least squares regression in R (nls function; R Core Development Team 2011) and calculated the average length and dry weight for each instar. I also used the laboratory cultures to determine the average sizes of *Daphnia* and *Moina*. I photographed 20 non-gravid female individuals of each species under a dissecting microscope (4-10 × magnification), measured their lengths using ImageJ software (Abramoff *et al.* 2004), and converted the lengths to dry weights using published relationships (McCauley 1984).

Functional Response Experiments

I used a set of functional response experiments to quantify predation rates and determine how they are influenced by predator age class and prey species identity. Single *Trichocorixa* individuals of known instar were placed into glass jars containing 100 mL of filtered (0.45 µm) well water and non-gravid, adult female prey of either *Daphnia* or *Moina*. To standardize hunger levels among predators, I starved all *Trichocorixa* individuals for the 24 hours preceding the start of a feeding trial. Prey abundances used were 1, 2, 4, 8, 10, 12, 15, 20, 25, 30, 40, 50, 75, and 100 individuals per jar, giving densities between 10 and 1,000 prey L^{-1}, which spans most of the range seen in the Appledore rock pools (Simonis 2012). Experimental jars were placed in a temperature-stable room (mean: 18 °C, range: 16-20 °C) with fluorescent lamps ("plant and aquarium", Phillips 40W) on a 12:12 light:dark cycle.

After 24 hours, I removed the predators from the jars and enumerated the remaining prey. I did not replace prey during the trials and no predators or prey were reused between trials. I conducted duplicate trials for each of the six predator instars at each of the 14 prey densities for the two prey species, giving 336 total trials.

I fit the data using the Rogers Random Predator Equation, which is a Type-II functional response adapted to account for depletion of prey during feeding (Rogers 1972). To test if handling time or attack rate (the functional response parameters) changed with predator ontogeny, I allowed both parameters to scale allometrically with predator mass (using the average dry mass for each instar). I included both prey species in the same analysis and used a dummy variable approach to test if either the intercept values or the allometric scaling of the functional response parameters varied between prey species. For example with attack rate, *a*:

$$a = (a_i + d \times \Delta a_i) \times mass^{(a_s + d \times \Delta a_s)} \qquad (2.1)$$

where a_i is the intercept attack rate when consuming *Moina*, a_s is the scaling effect of predator mass on attack rate when consuming *Moina*, *d* is the dummy variable to account for prey species identity (equal to 0 when prey were *Moina*, equal to 1 when prey were *Daphnia*), and Δa_i and Δa_s are the differences in the intercept and scaling parameters, respectively, between *Daphnia* and *Moina* prey items. Model fitting was conducted using maximum likelihood and the mle2 function in the R package bbmle (Bolker and R Core Development Team 2011), and the significance of each parameter was determined using Likelihood Ratio Tests (LRTs) based on corrected AIC (AICc) values.

Prey Choice Experiment

I determined the preference of each *Trichocorixa* instar for the two prey species (*Daphnia* and *Moina*) using a choice experiment. Predators of known instar were starved for 24 hours, then placed singly into glass jars containing 200 mL of filtered (0.45 µm) well water and 20 non-gravid, adult females each of *Daphnia* and *Moina* (40 cladocerans total, the only density used) and the jars were placed in the same temperature and light conditions as above. After 24 hours, I removed the predators and counted the remaining prey. I conducted ten replicate trials for each *Trichocorixa* instar, for 60 total trials. I did not replace prey during the trials and did not reuse any predators or prey.

I quantified predator preference using the Chesson-Manly alpha metric (hereafter: α_{CM}; Manly 1974, Chesson 1978) with Manly's (1974) approximation to account for prey depletion. The expected value of α_{CM} under no preference with two prey types is 0.50 for both species, if predators attack the prey types equally. However, *Trichocorixa* have a much higher predation rate on *Moina* than *Daphnia* (see *Results*; attack rate on *Moina* is 2.84 × attack rate on *Daphnia*), perhaps due to differences in size or behavior between prey species, which caused greater detection of the former. Accounting for the difference in attack rates, I recalculated the expected value of α_{CM} to be 0.7399 for *Moina* and 0.2601 for *Daphnia* (following the methods of Chesson 1983, which are appropriate for situations with prey depletion). I calculated the selectivity of each *Trichocorixa* instar towards *Moina* and evaluated the significance of these selectivities using *t*-tests with $\mu_0 = 0.7399$. I also regressed α_{CM} against instar to determine if selectivity changed with ontogeny.

Food Web Mesocosm Experiment

I then used a mesocosm experiment to determine if predation by *Trichocorixa* is strong enough to affect zooplankton population densities and cascade to indirectly affect algal biomass, and if the age-structure of the *Trichocorixa* population mediates the strength of the

cascade. Four *Trichocorixa* treatment levels were used: predators absent, small juveniles (2nd and 3rd instars), large juveniles (4th and 5th instars), and adults. First instar *Trichocorixa* were not used in this experiment due to their high mortality rates in captivity. In July 2009, I collected and combined water from five representative rock pools around Appledore Island. I filtered (30 µm) the water, removing all zooplankton and *Trichocorixa*, but leaving the phytoplankton. Mesocosms (40 L Rubbermaid totes) were placed outdoors in an experimental array and filled with 30 L of the rock-pool water mixture that had an initial phytoplankton density of 800 µg chlorophyll-*a* L^{-1}. I then inoculated all of the mesocosms with a mixture of zooplankton from the same five pools (supplemented with individuals from the zooplankton lab cultures) to create initial densities of 40 *Daphnia* L^{-1} and 125 *Moina* L^{-1}. These phytoplankton and zooplankton densities are within the range of rock pools on Appledore (Simonis 2012; see *Results*).

The mesocosm communities were left to equilibrate for four days before the *Trichocorixa* treatment was established. To minimize any among-mesocosm variation that might have developed during these four days, I removed 5 L from each mesocosm, combined and homogenized this volume in a large bucket, removed a small volume (1 L total) to quantify chlorophyll and zooplankton densities (following methods described below), and then redistributed the remaining volume equally back among the mesocosms. I then added fifteen *Trichocorixa* individuals to each of the predator-present mesocosms according to the treatment levels outlined above. Each treatment level was replicated four times, for 16 total mesocosms, and the treatment levels were arranged physically in a 4 × 4 Latin Square design. I covered all of the mesocosms with 1 mm mesh screening to prevent any immigration or emigration by *Trichocorixa* or other organisms and reinforced the mesh with chicken wire to exclude gulls (*Larus* spp.). The experiment ran for 12 days after the addition of *Trichocorixa*, which likely encompassed three generations of the dominant prey species, *Moina* (Nandini and Sarma 2000). I checked the mesocosms every three days and removed and replaced any

Trichocorixa that had molted out of their treatment-level instar class or had died.

On the final day of the experiment, I sampled the mesocosms for phytoplankton and zooplankton densities. Prior to sampling, I gently stirred the mesocosms to homogenize the water column without resuspending flocculent detritus. I sampled chlorophyll-*a* as a proxy for phytoplankton biomass (Wetzel and Likens 2000) by collecting duplicate water samples from each mesocosm and filtering them onto glass-fiber filters (Whatman GF-F), with a pre-filtration step using a 75 µm sieve to remove zooplankton. The GF-F filters were kept frozen and dark until analyzed. I extracted chlorophyll-*a* from the filters in the dark for 24 hr in cold ethanol (90%) and measured fluorescence on a desktop fluorometer (Turner Designs TD-700), with HCl acidification to correct for phaeopigments (Nusch 1980). To estimate zooplankton densities, I filtered each mesocosm in its entirety through a 75 µm mesh and preserved the contents in 95% ethanol until I counted them under a dissecting microscope. When necessary due to high densities, I subsampled the zooplankton samples following standard protocols (Wetzel and Likens 2000). The reported and analyzed grazer densities for were total cladocerans (*Moina* and *Daphnia* together), due to the very low densities of *Daphnia* in all mesocosms (see *Results*).

I analyzed the phytoplankton and zooplankton data separately using ANOVAs to determine the overall significance of the *Trichocorixa* effect and incorporating two independent *a priori* contrasts (Gotelli and Ellison 2004) to address my specific, directional hypotheses. The first contrast tested whether the presence of *Trichocorixa* (of any instar) induced a trophic cascade. That is, did the three treatment levels with *Trichocorixa* present have significantly lower densities of zooplankton and significantly higher densities of phytoplankton than the no-*Trichocorixa* controls? The second contrast used a linear ordered term to test if older instars caused significantly stronger top-down effects. That is, did later instar treatment levels have significantly lower zooplankton densities and significantly higher phytoplankton densities? Both the zooplankton and phytoplankton data were $\log_{10}$-

transformed prior to analyses to homogenize variances and normalize residuals. I conducted the ANOVAs (with *a priori* contrasts) in R (R Core Development Team 2011).

Trophic Dynamics in the Field

Finally, I explored the trophic consequences of *Trichocorixa* predation and ontogeny *in situ* by sampling a set of three rock pools every 2 – 4 days from 22 May to 15 August 2009 (29 sample dates). At each pool on a sample date, I collected duplicate 500 mL samples haphazardly from throughout the water column using a large-bulb pipette, removed all invertebrates from the water via a 75-µm mesh sieve, and preserved the plankton in 95% ethanol until I enumerated the samples under a dissecting microscope. If any species were present in high densities, I counted replicate representative subsamples. I also identified all *Trichocorixa* present to instar, based on size and morphology (Kelts 1979; see also *Results*). I quantified algal biomass in all three pools on each sample date, by collecting a small volume of water from each pool (typically < 50 mL) and processing using the methods described above for chlorophyll-*a*. The volumes of the pools were all approximately 300 L, thus each sampling removed only ~ 0.3% of any population present at that time.

RESULTS

Predator and Prey Sizes

Trichocorixa grew substantially during its ontogeny (Figure 2.1), with first instar juveniles weighing 0.020 ± 0.002 mg (dry weight) and measuring 1.24 ± 0.02 mm (max. length), compared to adults, who were nearly 45 times heavier and over four times as long at 0.864 ± 0.070 mg and 5.07 ± 0.09 mm (all data means ± SEM, N = 22 individuals per instar).

This growth corresponded to individuals approximately doubling their body weight at each of the five molts. Despite the generally good fit of the instar-specific means and the overall length-weight regression to the raw data (92% of deviance explained), there was substantial variation among individuals within each instar (mean within-instar coefficient of variation [CV] for dry weight = 0.34). However, this variation remained relatively constant across life history stages (range in dry weight CV: 0.26 - 0.40) and did not change predictably as a

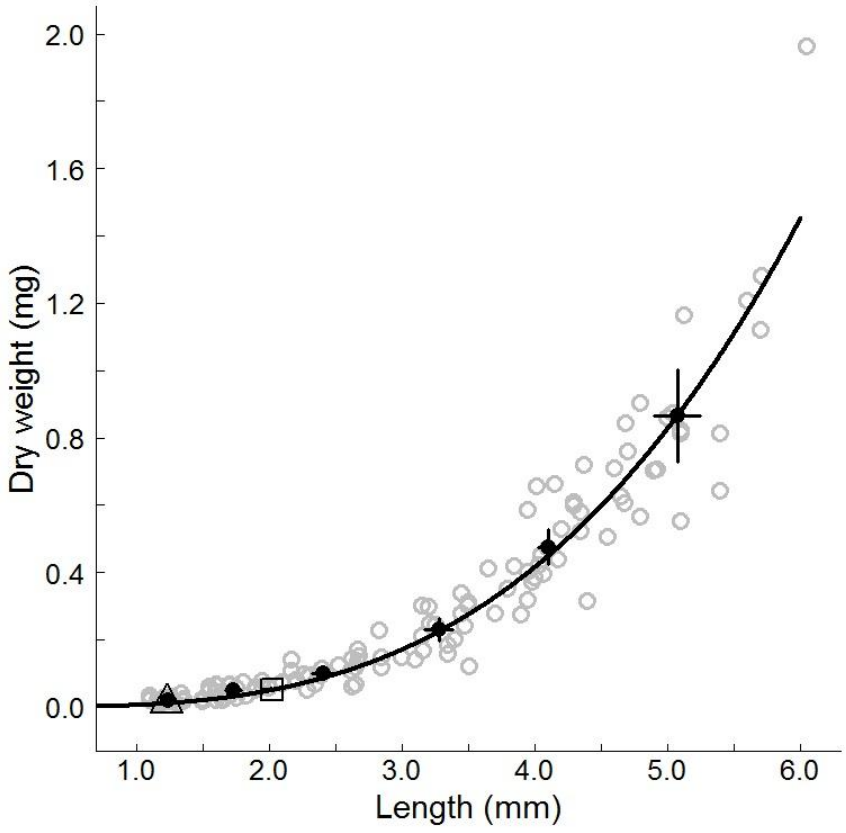

Figure 2.1. Length-weight relationship for *Trichocorixa* (N = 132; 22 individuals from each of six instars). The grey open circles are individual data and the black filled circles are instar means with 95% CIs (the first instar is the smallest, and each subsequent instar is larger). The solid line is the length-weight regression fit to the individual data: dry weight = 0.00586 × length$^{3.077}$. The open triangle and square are the mean length-weight for *Moina* and *Daphnia* (respectively) used in the laboratory experiments.

function of ontogeny (regression of dry weight CV against instar, $P = 0.38$).

The size of the prey used in the experiments was both consistent within, and quite different between, the two species (Figure 2.1), with *Daphnia* (0.053 ± 0.003 mg, 2.02 ± 0.05 mm, mean ± SEM, N = 20) being substantially larger than *Moina* (0.012 ± 0.001 mg, 1.23 ± 0.02 mm, mean ± SEM, N = 20). As a result, individuals from the two prey species potentially represented large differences in energetic rewards for the predator, depending on conversion efficiency. Also, *Trichocorixa* individuals grow through the size spectrum of the prey: first instar *Trichocorixa* are nearly identical in size to *Moina* but not until the third instar were individual predators larger than *Daphnia* (Figure 2.1). This overlap in predator and prey sizes does not necessarily preclude consumption, as *Trichocorixa* uses piercing mouth parts to fluid-feed on its prey and so is not limited by mouth gape size. However, the predator-prey size overlap could still influence the ability of different predator instars to capture and subdue their prey.

Functional Response Experiments

All six instars of *Trichocorixa* were able to feed on both prey species and the functional response curves took a saturating (Type II) shape (Figure 2.2). Attack rate and handling time both had significant intercept values (Table 2.1; $a_i = 1.642$, $h_i = 0.0114$, both $P < 0.001$) and scaled allometrically: attack rate increased and handling time decreased as functions of predator mass ($a_s = 0.483$, $h_s = -0.6162$, both $P < 0.001$). Three of the four parameters differed significantly between the prey species, all showing increased predation rates on *Moina*. *Trichocorixa* had a higher attack rate intercept and a lower handling time intercept when preying upon *Moina* compared with upon *Daphnia* (respectively, $\Delta a_i = -1.065$, $P < 0.001$; $\Delta h_i = 0.0111$, $P = 0.007$) and *Trichocorixa*'s handling time decreased more rapidly with increasing predator biomass when consuming *Moina* compared with *Daphnia*

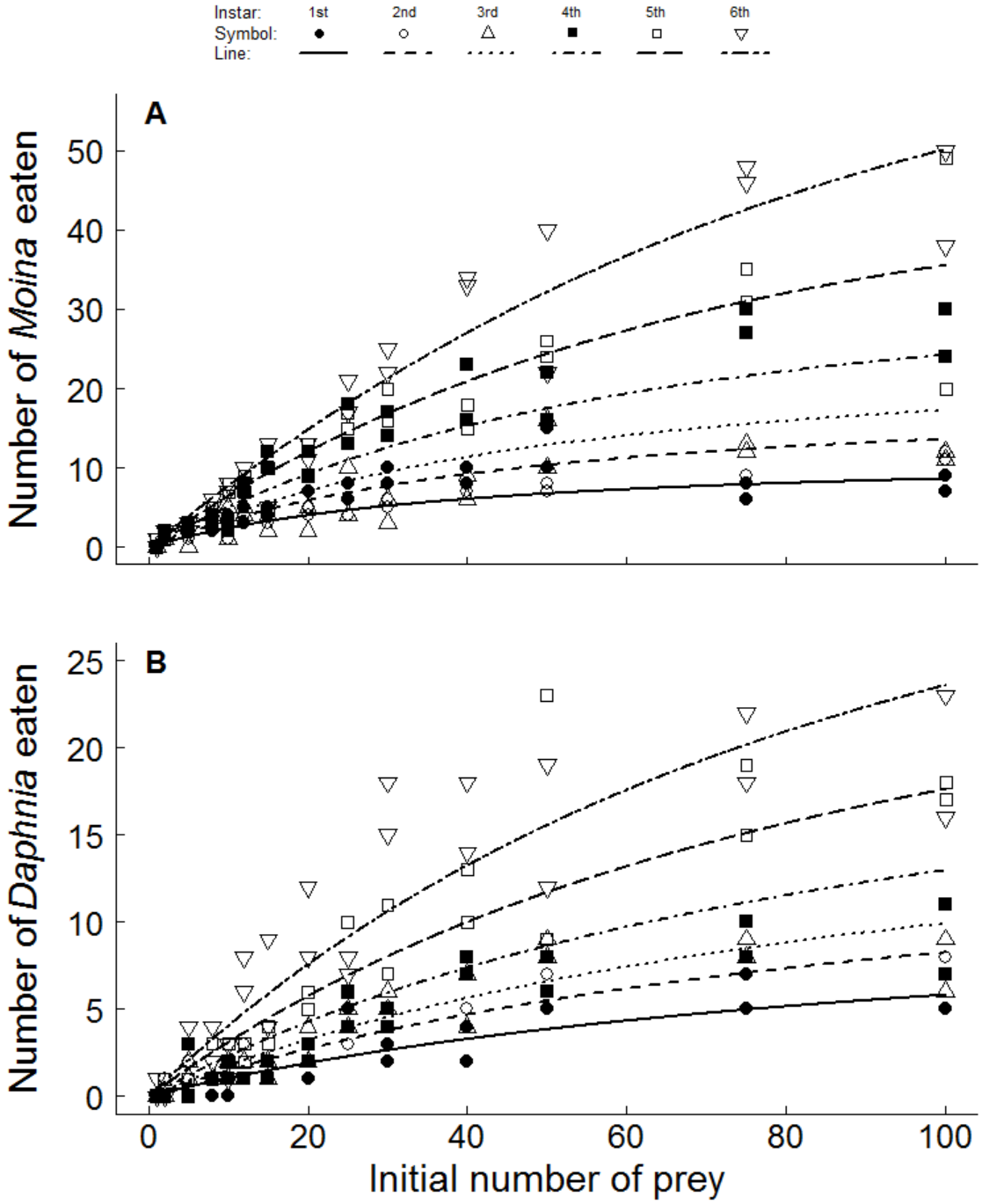

Figure 2.2. Functional responses for each of six *Trichocorixa* instars feeding on (A) *Moina* or (B) *Daphnia*. All data were fit with a single model based on the Rogers Random Predator Equation with allometric scaling of parameters across instars and differences in all parameters between prey species (see *Methods*, Equation 2.1, and Table 2.1). Note the difference in y-axes between (A) and (B).

(Δh_s = 0.2074, P = 0.047). The scaling of attack rate with predator mass did not significantly differ between the prey species (Δa_s; $P > 0.05$).

Although *per capita* predation was much higher on *Moina* than on *Daphnia* for all six *Trichocorixa* instars (Figure 2.2, Table 2.2), the total mass of *Daphnia* consumed was substantially higher than the total mass of *Moina* consumed, a result of the size difference between the prey species (*Daphnia* is 4.4 times larger than *Moina* in dry weight; Figure 2.1). Consequently, mass-specific consumption (mass of prey consumed ÷ mass of predator) was much higher for *Trichocorixa* of all instars when preying upon *Daphnia* than when preying upon *Moina* (Table 2.2). Despite the increase in the number of prey consumed with predator ontogeny, the increase in prey mass consumed by each instar was less than the growth in

Table 2.1. Best fit parameters from the functional response model.

Parameter	Estimate	Std. Error	P
a_i	1.642	0.112	< 0.001
Δa_i	-1.065	0.108	< 0.001
a_s	0.483	0.039	< 0.001
h_i	0.0114	0.0012	< 0.001
Δh_i	0.0111	0.0042	0.007
h_s	-0.6162	0.0586	< 0.001
Δh_s	0.2074	0.1043	0.047

Notes. Both attack rate and handling time were allowed to scale allometrically with predator biomass (Equation 2.1) and the resulting four parameters could differ between prey species. The scaling term for attack rate (a_s) did not differ significantly between the prey species (Δa_s; LRT, $P > 0.05$) and thus was removed from the model. Translation of these parameters into instar- and prey-specific functional response parameters is shown in Table 2.2

predator biomass between instars, causing predator mass-specific consumption to decrease monotonically with increasing instar (Table 2.2).

Table 2.2. Estimated functional response parameters and amount of prey eaten by each *Trichocorixa* instar.

	Predator				Predicted Prey Eaten		
Prey	Instar	Mass (mg. dry wt.)	Attack Rate (d^{-1})	Handling Time (d)	Number	Mass (mg. dry wt.)	Predicted DSC (%)
M	1	0.0381	0.339	0.085	8.61	0.1042	273.8
	2	0.0850	0.500	0.052	13.61	0.1646	193.7
	3	0.1297	0.613	0.040	17.25	0.2087	160.9
	4	0.2410	0.826	0.027	24.27	0.2936	121.8
	5	0.4945	1.169	0.018	35.55	0.4301	87.0
	6	0.9916	1.635	0.011	50.18	0.6071	61.2
D	1	0.0381	0.119	0.086	5.81	0.3069	806.3
	2	0.0850	0.176	0.062	8.26	0.4361	513.2
	3	0.1297	0.215	0.052	9.93	0.5241	404.0
	4	0.2410	0.291	0.040	12.97	0.6846	284.0
	5	0.4945	0.411	0.030	17.61	0.9300	188.1
	6	0.9916	0.575	0.023	23.58	1.2448	125.5

Notes. *M*: *Moina*; *D*: *Daphnia*. See Equation 2.1 for parameters. The predicted number and dry weight of prey eaten was determined using the functional responses with 100 initial prey. Predicted daily specific consumption (DSC) was calculated as the predicted mass of prey eaten divided by the average mass of the *Trichocorixa* instar and displayed as a percentage.

Prey Choice Experiment

When given both prey species together, *Trichocorixa* strongly preferred *Moina* over *Daphnia* (across all predator instars, α_{CM} for *Moina* = 0.9296 ± 0.0141, mean ± SEM, N = 60) and all six *Trichocorixa* instars displayed significant preference for *Moina*, even after accounting for the difference in their attack rates between the two prey species (Figure 2.3A; $P < 0.001$ for the first four juvenile instars, $P = 0.026$ for fifth instar juveniles, $P = 0.019$ for adults). Despite all predator instars preferring *Moina*, older *Trichocorixa* were significantly less selective towards *Moina* than were younger individuals (regression of α_{CM} against instar, slope = -0.032, $P < 0.001$). As expected given the functional responses (Figure 2.2), older predators consumed significantly more prey individuals in total (Poisson regression of total prey eaten against instar, slope = 0.18, $P < 0.001$). There was also a significant positive correlation between the number of prey individuals consumed from the two species (Figure 2.3B; $r = 0.45$, $P < 0.001$).

Food Web Mesocosm Experiment

The *Trichocorixa* treatment had significant effects on the densities of cladoceran grazers ($F_{3,12} = 4.53$, $P = 0.02$) and phytoplankton ($F_{3,12} = 3.66$, $P = 0.04$) in the mesocosm experiment (Figure 2.4). Regardless of instar, the presence of *Trichocorixa* led to a decrease in the density of cladocerans and an increase in the density of phytoplankton (*a priori* contrasts between treatments with and without *Trichocorixa*, cladocerans: contrast = -0.116, $P = 0.009$; phytoplankton: contrast = 0.074, $P = 0.024$; Figure 2.4). Further, the strength of both responses was significantly greater in the treatments containing later life-history stages of the predators (*a priori* linear contrasts among treatments with *Trichocorixa*, cladocerans: contrast = -0.344, $P = 0.019$; phytoplankton: contrast = 0.207, $P = 0.049$; Figure 2.4). In the control

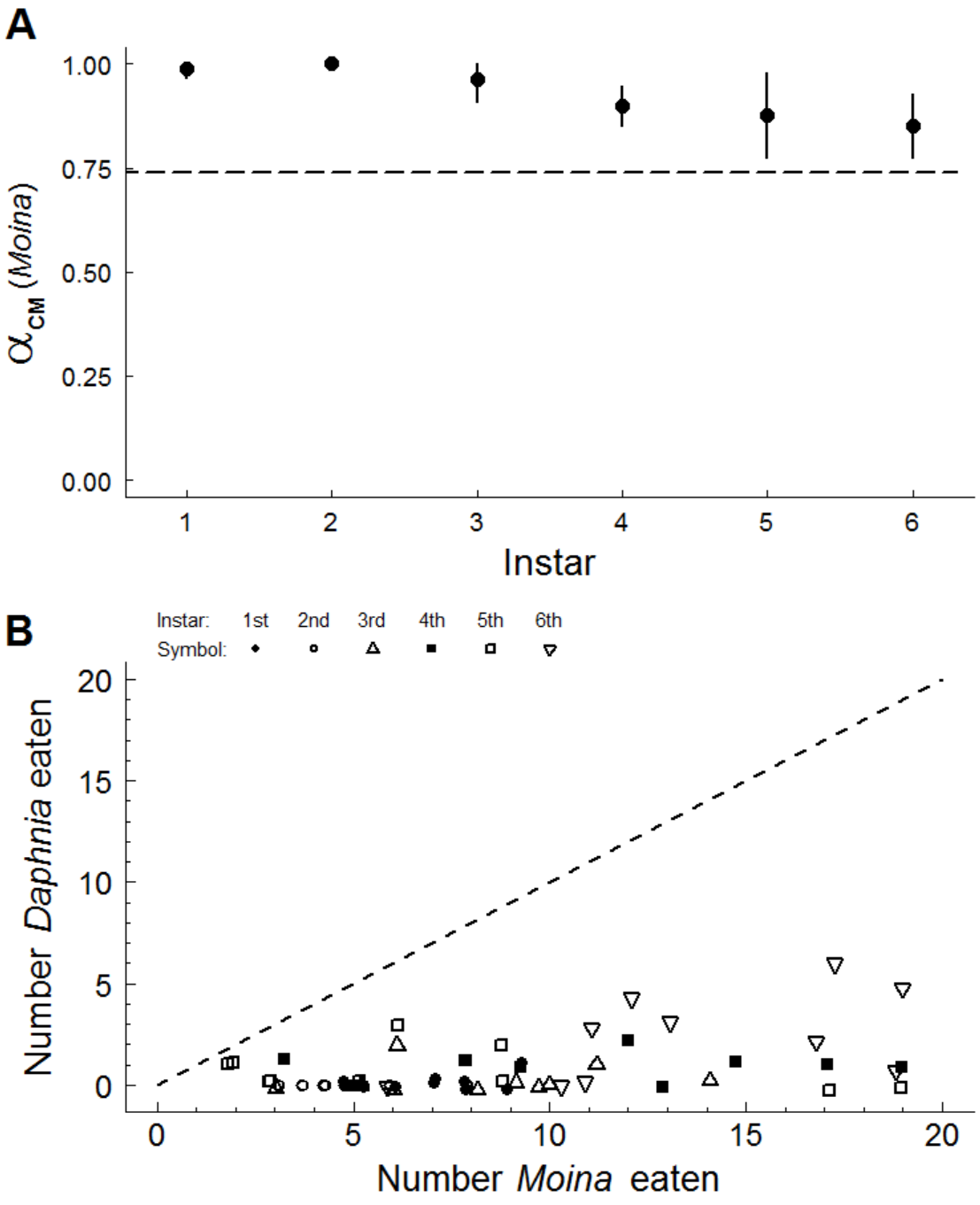

Figure 2.3. *Trichocorixa* choice between prey species (*Daphnia* and *Moina*) across *Trichocorixa* instars. (A) Preference of each *Trichocorixa* instar for *Moina* (as measured by α_{CM}; points are means with 95% CIs) in relation to the expected value given the differences in attack rates on the two species (dashed horizontal line; $\alpha_{CM} = 0.7399$). (B) Individual predator data showing the relationship between the number of prey consumed from each species. Data in (B) were slightly jittered in both the X and Y directions and the 1:1 line was added to aid interpretation.

mesocosms, the density of cladocerans increased and phytoplankton decreased substantially from the start of the experiment (dashed lines in Figure 2.4), indicating that the zooplankton can suppress phytoplankton densities in the absence of *Trichocorixa*. This effect also appeared to occur before the addition of *Trichocorixa*, as algal concentrations dropped from 800 to 719 µg chlorophyll-*a* L^{-1} during the four day equilibration period. In contrast, adult *Trichocorixa* on average slightly suppressed the density of the zooplankton trophic level, leading to a small average increase in phytoplankton density relative to the starting densities (Figure 2.4; three of four "adult" mesocosms had reduced zooplankton densities and increased phytoplankton densities). The increase in phytoplankton density observed in the presence of adult *Trichocorixa* was almost certainly not the result of excretion by the predators or grazers, since nutrient concentrations are extremely high in the Appledore rock pool water as the result of a steady input of gull guano (Sze 1981; Loder *et al.* 1996).

Despite the strong preference of *Trichocorixa* for *Moina* and the higher rate of predation on *Moina* compared to *Daphnia*, all of the mesocosms were dominated by *Moina* at the end of the experiment. Indeed, *Daphnia* was only found in three of the mesocosms and always at much lower densities than *Moina*. There was no clear relationship between the *Trichocorixa* treatment level and the presence of *Daphnia*: they were found in one mesocosm containing adult predators (17 *Daphnia* L^{-1}) and two containing small juvenile predators (1 and 2 *Daphnia* L^{-1}). This decrease in *Daphnia* densities appears to have begun before the predator treatment was imposed: during the four day equilibration period, the density of *Daphnia* decreased from 40 to 18 individuals L^{-1} (compared to an increase in *Moina* from 125 to 205 individuals L^{-1}). This suggests that some aspect of the mesocosm environment was unfavorable for *Daphnia*. One likely factor may have been the high phytoplankton densities, as *Daphnia* is not commonly found in rock pools with over 250 µg chlorophyll-*a* per L (J. L. Simonis, *unpub. data*). Also present in the mesocosms were *Brachionus* (rotifer), *Acanthocyclops* (copepod), and chironomid larvae. However, these taxa were generally at

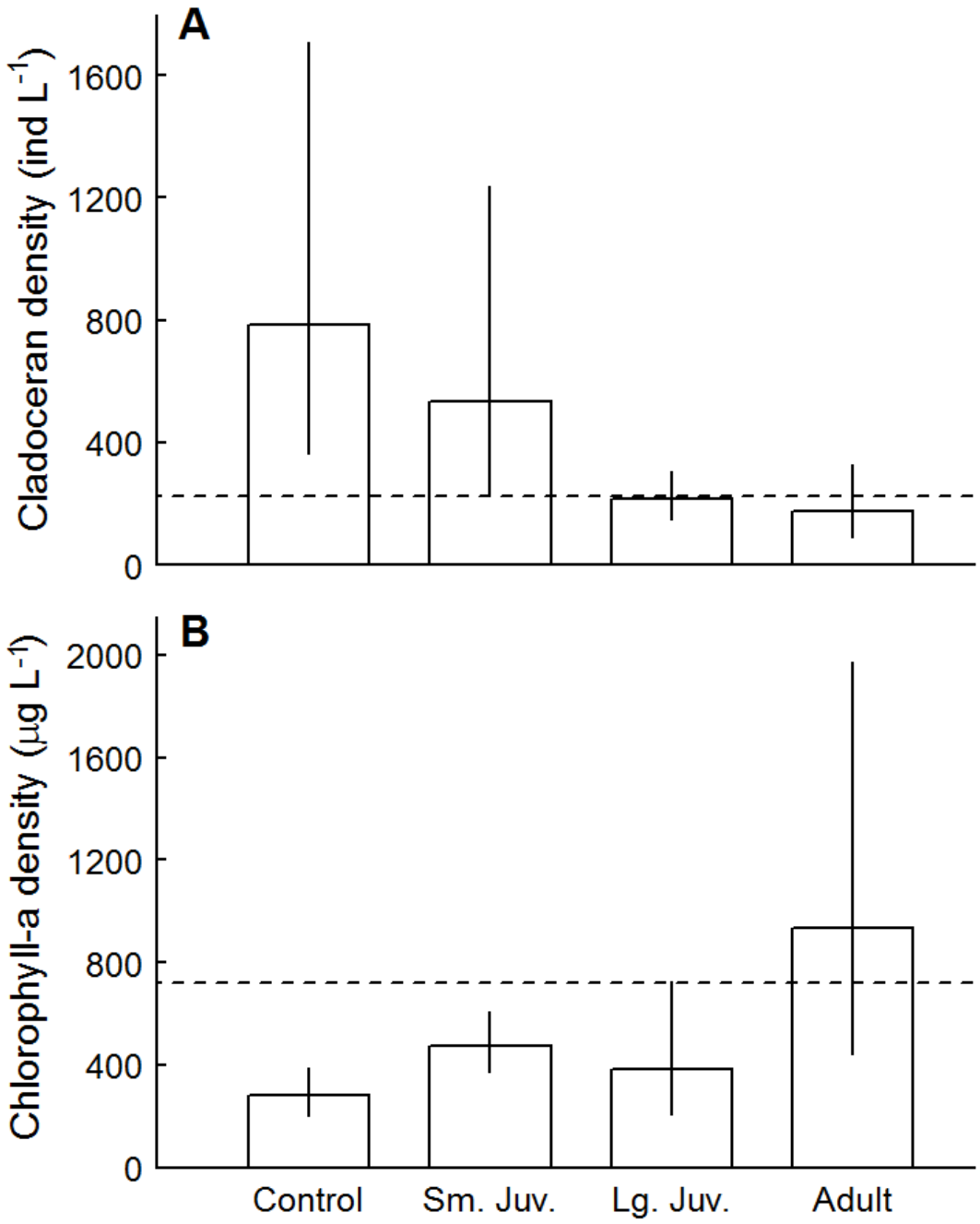

Figure 2.4. Influence of *Trichocorixa* presence and stage on the density of (A) cladocerans (*Moina* and *Daphnia* combined) and (B) phytoplankton (measured as chlorophyll-*a*) after 12 days (data are back-transformed means ± standard deviations; N = 4 for each treatment level). The dashed horizontal lines represent the density of each trophic level just prior to *Trichocorixa* addition (A: 223 cladocerans L^{-1}; B: 719 µg chlorophyll-*a* L^{-1}). Treatments are represented along the x-axis: Control (no *Trichocorixa*), Small Juveniles (2^{nd} and 3^{rd} instars), Large Juveniles (4^{th} and 5^{th} instars), and Adults.

low densities and none displayed changes in density significantly associated with the predator treatment (data not shown).

Trophic Dynamics in the Field

All three pools followed in the field survey had populations of chlorophyte algae, *Moina*, and *Trichocorixa*, but no *Daphnia* (Figure 2.5). There were also populations of *Brachionus* and populations chironomid larvae in all three pools. However, the chironomids were at relatively low densities (average: 8.6 ind. L^{-1}) and typically in protective cases attached to the benthos, which prevent predation by *Trichocorixa* (J. L. Simonis, *pers. obs.*). The survey began when the first generation of *Trichocorixa* was in the 3^{rd} – 5^{th} instars and lasted through the hatching and partial development of a second generation (Figure 2.6). The first generation reached adulthood 2 – 2.5 weeks into the survey (Figure 2.5B). *Trichocorixa* population densities were relatively constant at near 5 individuals L^{-1} during the survey period (Figure 2.5A), except when the population densities temporarily exploded (*ca.* Julian Date 190-210, maximum of 116 individuals L^{-1}) due to the hatching of the second generation (Figure 2.6). However, the second *Trichocorixa* generation appears to have experienced high mortality among the youngest instars, as population densities decreased markedly after the hatching and there was relatively low recruitment to later instar stages (Figures 2.5A, 2.6). In all three pools, *Moina* densities were high at the beginning of the survey, decreased quickly after *Trichocorixa* populations became dominated by adults, and increased again later in the summer following the mass mortality of the second generation of *Trichocorixa* (Figures 2.5C, 2.7). All three *Moina* populations experienced large decreases in their intrinsic growth rates following the development of *Trichocorixa* into adults (based on the four sample dates immediately preceding and the four dates immediately following the date on which *Trichocorixa* adults were first found; average change in growth rate was -0.3473 d^{-1}, and the

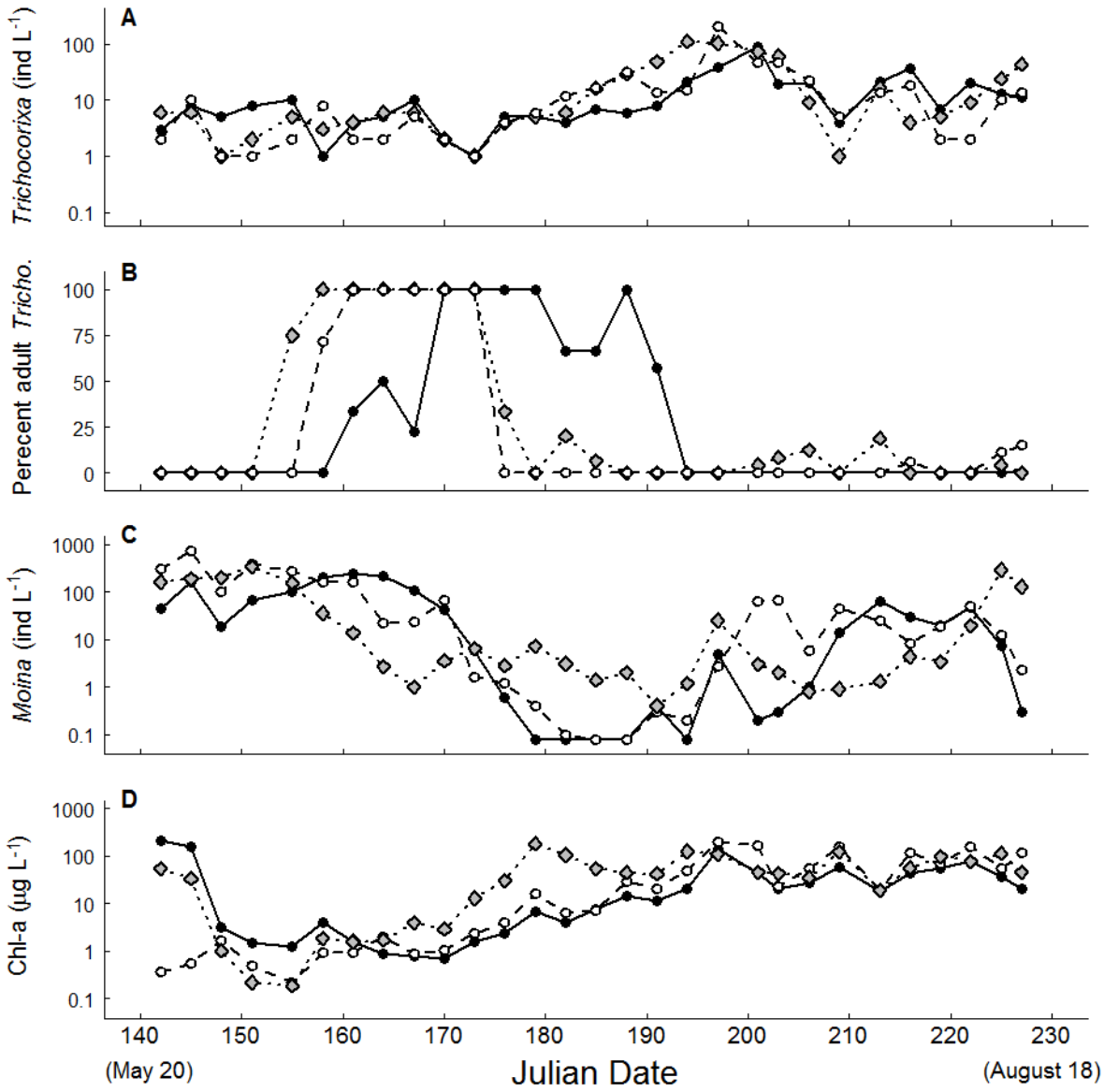

Figure 2.5. Time series of (A, B) *Trichocorixa*, (C) *Moina*, and (D) algae densities in three rock pools during the summer of 2009. Panel (B) shows the percentage of adults in the three *Trichocorixa* populations. Each set of point and line types represents a different pool and are consistent across panels. Note the $\log_{10}$ scales of the y-axes in (A, C, D).

Figure 2.6. Combined age distribution of the three *Trichocorixa* field populations. Successive instars are stacked on top of each other (darkness increasing with stage from white for 1st instar to black for adults).

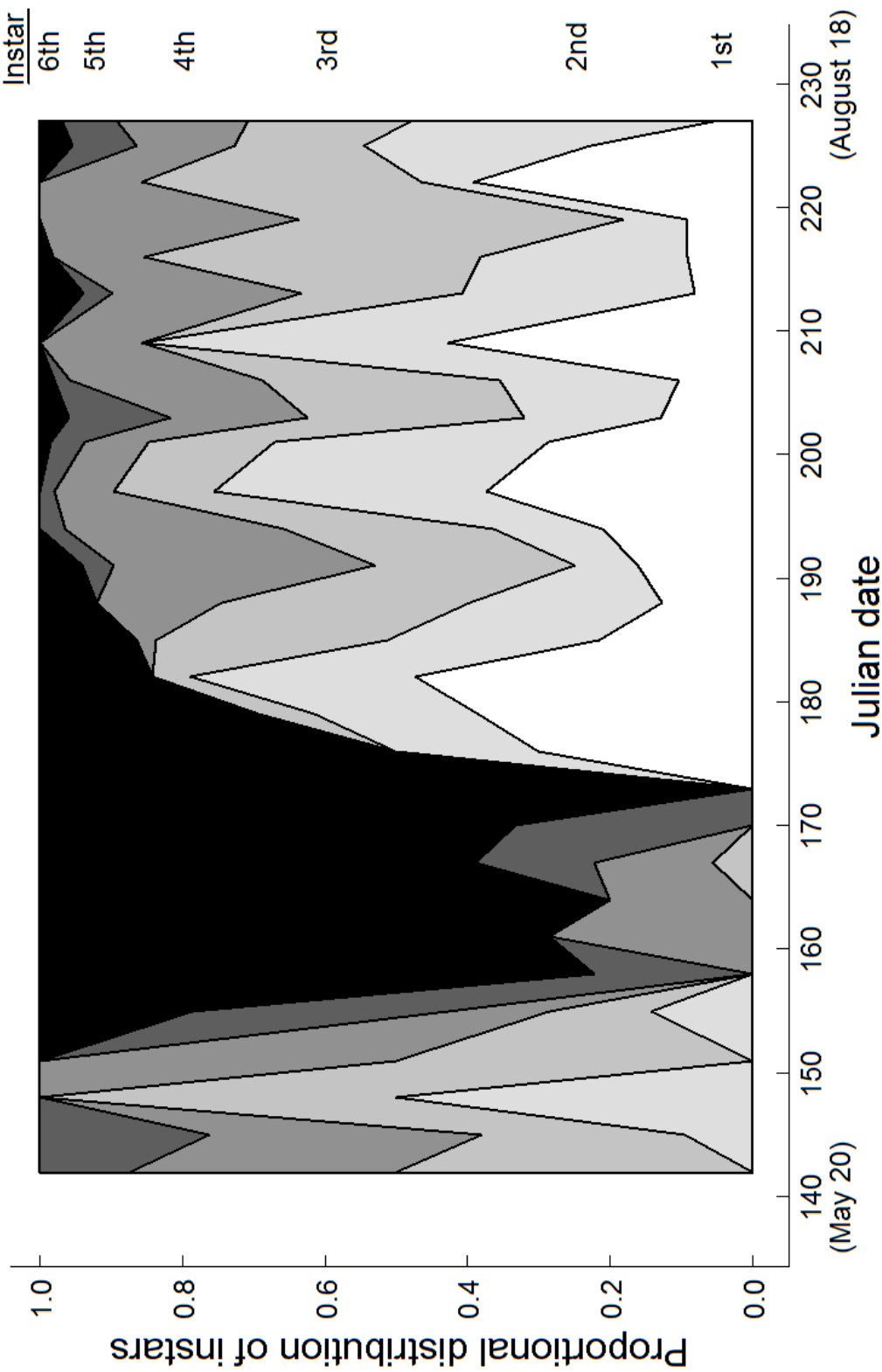
Instar
6th
5th
4th
3rd
2nd
1st
Proportional distribution of instars
0.0
0.2
0.4
0.6
0.8
1.0
140
(May 20)
150
160
170
180
190
200
210
220
230
(August 18)
Julian date

three populations declined from 0.135 d^{-1} to -0.194 d^{-1}, from 0.056 d^{-1} to -0.208 d^{-1}, and from -0.001 d^{-1} to -0.450 d^{-1}). The decrease in *Moina* density after the occurrence of *Trichocorixa* adults was also followed by the expected increase in algal density (Figures 2.5D, 2.7), reflecting the trophic cascade seen in the mesocosm experiment (Figure 2.4). The temporal dynamics of all three trophic levels were strongly synchronized across the three pools (Figure 2.7): average cross-correlation coefficients were 0.685 for the algae, 0.579 for *Moina*, and 0.690 for *Trichocorixa* (using a 0-time lag with $\log_{10}$ densities and averaging the three possible pairwise cross-correlation coefficients for each trophic level). And despite small among-pool differences in the timing of *Trichocorixa* developing into the adult stage, the resulting grazer-algal dynamics are quite similar in amplitude and duration, as shown by the consumer-resource phase planes (Figure 2.7).

DISCUSSION

Here I have combined lab and field experiments with field survey data in a freshwater ecosystem to highlight the role that ontogenetic changes in top predator consumption rates play in structuring food webs. Similar to many other predator taxa, *Trichocorixa* grew substantially during its life history, with concomitant increases in consumption rates (Thompson 1975; Mittelbach 1981; Peters 1983; Shine 1991; Kooijman 1993; Aljetlawi *et al.* 2004). The allometric increase in *per capita* consumption by *Trichocorixa* manifested in the rock-pool food web as an increase in top-down control with predator ontogeny, as demonstrated experimentally and observed in field data. Similar to other field populations of *Trichocorixa* (Tones 1975; Kelts 1979), the populations surveyed here showed a non-stable stage structure with partially overlapping generations (Figure 2.6), which led to a dynamic rate of predation and caused the strengths of direct and indirect effects of *Trichocorixa* predation on lower trophic levels to fluctuate through time. This type of demographically

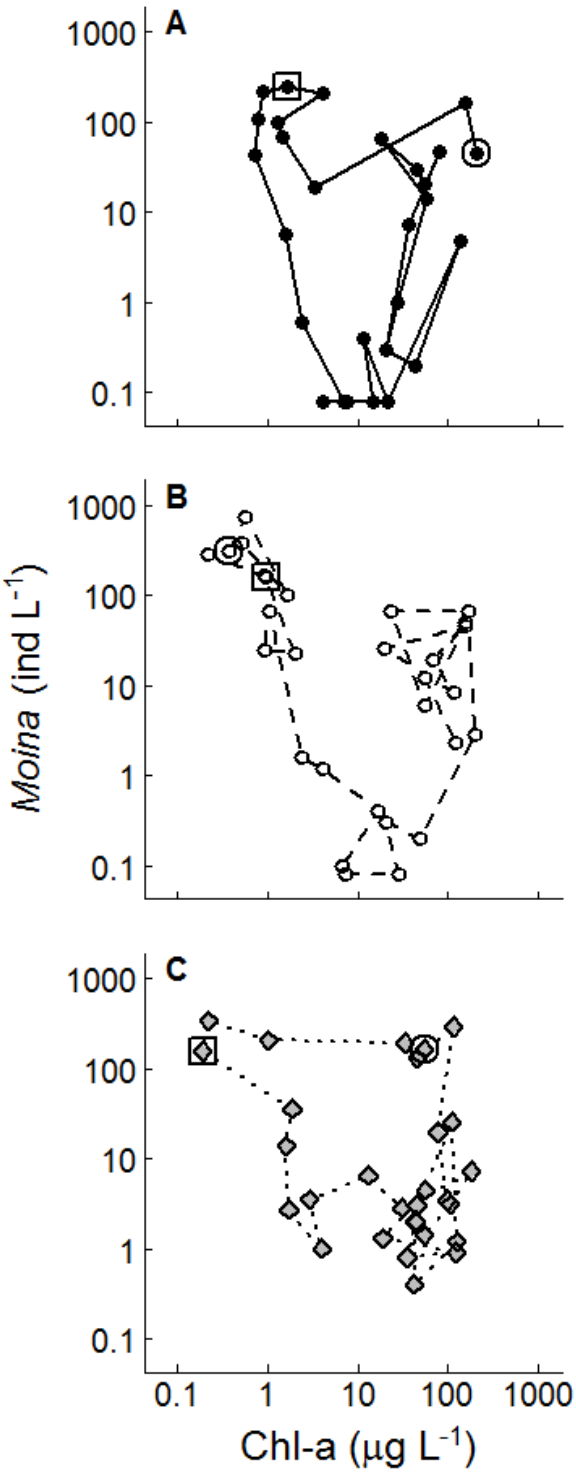

Figure 2.7. Phase planes depicting the relationship between *Moina* and algae densities in each of the three pools shown in Figure 2.5 (point and line types matching those in Figure 2.5). The circled point is the beginning of the time series and the boxed point represents the first day adult *Trichocorixa* were found in the pool.

driven variation in predation strength may be common given the prevalence of both allometrically scaling consumption rates and dynamically structured predator populations (Peters 1983; Ebenman and Persson 1988; Werner 1988; Kooijman 1993), and indicates that the inclusion of stage- or size-specific information may be important for understanding the trophic structure and dynamics of food webs (Alford 1989; Hairston and Hairston 1997; de Roos *et al.* 2003).

However, the degree to which top predator ontogeny influences trophic dynamics is likely mediated by other factors, such as the complexity of the particular food web (Hairston and Hairston 1997; Hildrew *et al.* 2007b). Changes in top predator consumption rates are far more likely to have straightforward cascading effects in a simple tri-trophic food chain like the (dominant) chain in the Appledore rock pools than they are in a more complex food web with many constituents and linkages. Indeed, *Trichocorixa* is capable of consuming a wider variety of resources than what is present and accessible in the rock pools (*e.g.*, filamentous algae, dipteran larvae; Kelts 1979). The higher food-web complexity found in other ecosystems *Trichocorixa* inhabits could alter the trophic influence of this species, and its ontogeny, on food-web structure and dynamics (Polis and Strong 1996; Hairston and Hairston 1997). For example, the presence of alternative resource types that supplement the diet of young *Trichocorixa* instars could help meet the high energetic demands of these stages, thereby reducing mortality rates, but may also induce a classic ontogenetic niche shift.

In addition to food-web complexity, population structure within other trophic levels may also modulate the trophic effect of ontogenetic changes in the top predator. For example, many species at lower trophic levels also grow considerably over their lifetimes, which likely has consequences for their trophic interactions as both resources and consumers. This is the case in the Appledore pools, as both *Moina* and *Daphnia* grow considerably during their own ontogeny (Anderson *et al.* 1937; Martínez-Jerónimo and Gutierrez-Valdivia 1991), which likely influences both their vulnerability to predators and their grazing rates (Murdoch and

Scott 1984; Knoechel and Holtby 1986). Although it is currently unknown how selective or efficient *Trichocorixa* is when preying upon cladocerans of different sizes within the same species, many other predatory aquatic insects show strong selection for, and higher predation rates on, smaller prey size classes (*e.g.*, Thompson 1975; Pastorok 1981; Murdoch and Scott 1984; Ranta and Espo 1989). Indeed, *Trichocorixa* is negatively size selective when preying upon *Artemia* brine shrimp (Wurtsbaugh 1992), which corresponds to the preference for the smaller cladoceran species (*Moina* over *Daphnia*) shown in the present study (Figure 2.3) and suggests a general preference for smaller prey items. Considering that the rates at which cladocerans graze on phytoplankton is also strongly size-dependent (Knoechel and Holtby 1986; Kooijman 1993; DeMott *et al.* 2010), selection by *Trichocorixa* for specific size classes of cladocerans may have cascading effects on phytoplankton densities and dynamics. Such size-specific interactions have the potential to alter the dynamics of tri-trophic food webs qualitatively by introducing Allee effects or stabilizing population cycles (de Roos *et al.* 2003). It is therefore likely that the complete picture of the food-web consequences caused by ontogenetically variable predators such as *Trichocorixa* results from a combination of predator and prey population size structures.

Despite potential confounding factors, such as prey size distributions, increased predation by older *Trichocorixa* did appear to cause a large reduction in *Moina* populations *in situ* (Figures 2.5, 2.7). All three pools had *Trichocorixa* populations, and therefore there was no control situation (pool without predation) for comparison, but these observed patterns were similar across pools (despite differences in timing of maturity among pools) and were consistent with those expected, based on the results of my lab and mesocosm experiments. In particular, *Moina* densities decreased substantially following the first *Trichocorixa* generation reaching adulthood. This strong reduction in prey densities had important consequences for the *Trichocorixa* populations and subsequently for the rest of the rock-pool food web. First, after reducing *Moina* to near-extinction, the adult *Trichocorixa* densities decreased, perhaps

driven by flighted emigration in response to low resource densities, an expectation for motile predators based on optimal foraging theory (Charnov 1976) which has been shown to occur in this system (adult *Trichocorixa* have higher emigration rates when *Moina* densities are lower; Simonis 2012). The reduced predation that resulted from the decrease in adults may have contributed to the persistence of the *Moina* populations in the pools, despite their reaching very low densities, and would therefore point to the role of predator dispersal in stabilizing locally unstable food webs at larger spatial scales (Murdoch and Stewart-Oaten 1989; Simonis 2012). The *Moina* populations did eventually rebound from the crashes, but not until after the second generation of *Trichocorixa* hatched and crashed (Figures 2.5-2.7). The period of low *Moina* densities may have been prolonged by predation following the hatching of the second generation, and also may have contributed to the mass mortality seen in the early instars of the second generation (*ca.* Julian Day 200; Figures 2.5, 2.6), as these young stages have high energetic demands (see daily specific consumption in Table 2.2) that may not have been met by the low densities of prey present at the time. This high juvenile mortality resulted in generally low recruitment of the second *Trichocorixa* generation in these populations (Figures 2.5A, 2.6), which could promote longer term persistence of the local *Moina* populations.

Ontogenetic shifts in feeding ecology, such as those shown here for *Trichocorixa*, are widespread among animal taxa and can strongly influence the structure and dynamics of food webs (Peters 1983; Werner and Gilliam 1984; Werner 1988; Polis and Strong 1996; Persson *et al.* 1998; Rudolf and Lafferty 2011). Although most research has focused on the food-web effects of qualitative feeding shifts, many predators exhibit less extreme, but still important, quantitative changes in feeding rates with ontogeny (Peters 1983; Kooijman 1993). Here I have shown that an ontogenetic allometric increase in the *per capita* rate of predation by *Trichocorixa verticalis* on cladoceran zooplankton strengthened the trophic cascade to primary producers in freshwater rock pools. As a result, predation by adult *Trichocorixa* led to much stronger top-down control than did predation by juvenile *Trichocorixa*. Just as

among-taxa differences in predation rates and efficiencies may dictate the presence or strength of trophic cascades across ecosystems (Hairston and Hairston 1993; Polis 1999; Borer *et al.* 2005), ontogenetic variation in predation rates within top predator taxa may influence trophic dynamics within ecosystems. As a result, the size-structure of predator populations may play an important role in dictating when or how strongly trophic cascades will appear within a particular ecosystem. These results indicate that quantitative ontogenetic changes in predator feeding may also have significant food-web consequences, and suggest that merging of population and food web ecology may be necessary to understand and predict field ecosystem dynamics more accurately (Alford 1989; Hairston and Hairston 1993; de Roos *et al.* 2003; Cohen *et al.* 2003, Hildrew *et al.* 2007a).

ACKNOWLEDGEMENTS

Many thanks to the staff of the Shoals Marine Laboratory (SML) for logistical assistance, in particular to SML director Dr. W. Bemis. Thanks also to Dr. J. Morin and E. Kuo for preliminary research on the rock-pool system and to the Hairston and Flecker lab groups for earlier discussions on this topic. This manuscript was improved by the comments of A. Agrawal, S. Ellner, A. Flecker, M. Booth, K. Capps, N. Hairston Jr., S. Simonis, and two anonymous reviewers. I. Hewson, L. Quevillon, and P. Thompson provided field assistance. This work was supported financially by the Shoals Marine Laboratory, Cornell University Biogeochemistry and Environmental Biocomplexity Program, and a National Science Foundation Graduate Research Fellowship awarded to JLS.

REFERENCES

Abramoff, M. D., P. J. Magelhaes, and S. J. Ram. 2004. Image processing with ImageJ.

Biophotonic International 11:36-42.

Alford R. A. 1989. Variation in predator phenology affects predator performance and prey community composition. Ecology 70:206-219.

Aljetlawi, A. A., E. Sparrevik, and K. Leonardsson. 2004. Prey-predator size-dependent functional response: derivation and rescaling to the real world. Journal of Animal Ecology 73:239-252.

Anderson, B. G., H. Lumer, and L. J. Zupancic Jr. 1937. Growth and variability in Daphnia pulex. Biological Bulletin 73:444-463.

Bolker, B. and R Development Core Team. 2001. bbmle: tools for general maximum likelihood estimation. R package version 0.9.7. http://CRAN.R-project.org/package=bbmle

Borer, E. T., E. W. Seabloom, J. B. Shurin, K. E. Anderson, C. A. Blanchette, B. Broitman, S. D. Cooper, and B. S. Halpern. 2005. What determines the strength of a trophic cascade? Ecology 86:528-537.

Brown, J. H., J. F. Gillooly, A. P. Allen, V. M. Savage, and G. B. West. 2004. Towards a metabolic theory of ecology. Ecology 85:1771-1789.

Byström, P. and J. Andersson. 2005. Size-dependent foraging capacities and intercohort competition in an ontogenetic omnivore (Arctic char). Oikos 110:523-536.

Charnov, E. L. 1976. Optimal foraging, the Marginal Value Theorem. Theoretical Population Biology 9:129-136.

Chesson, J. 1978. Measuring preference in selective predation. Ecology 59:211-215.

Chesson, J. 1983. The estimation and analysis of preference and its relationship to foraging models. Ecology 64:1297-1304.

Cohen, J. E., T. Jonsson, and S. R. Carpenter. 2003. Ecological community description using the food web, species abundance, and body size. Proceedings of the National Academy of Sciences 100:1781-1786.

de Roos, A. M., J. A. J. Metz, E. Evers, and A. Leipoldt. 1990. A size dependent predator-prey interaction: who pursues whom? Journal of Mathematical Biology 28: 609-643.

de Roos, A. M. and L. Persson. 2002. Size-dependent life-history traits promote catastrophic collapses of top predators. Proceedings of the National Academy of Sciences 99:12907-12912.

de Roos, A. M., L. Persson, and E. McCauley. 2003. The influence of size-dependent life-history traits on the structure and dynamics of populations and communities. Ecology Letters 6:473-487.

DeMott, W. R., E. N. McKinney, and A. J. Tessier. 2010. Ontogeny of digestion in *Daphnia*: implications for the effectiveness of algal defenses. Ecology 91:540-548.

Dillon, P. M. 1985. Chironomid larval size and case presence influence capture success achieved by dragonfly larvae. Freshwater Invertebrate Biology 4:22–29.

Ebenman, B. and L. Persson. 1988. Size-structured populations: ecology and evolution. Springer-Verlag, Berlin, Germany.

Gotelli, N. J. and Ellison A. M. 2004. A primer of ecological statistics. Sinaeur Associates, Sunderland, Massachusetts, USA.

Hairston, N. G., F. E. Smith, and L. B. Slobodkin. 1960. Community structure, population control, and competition. American Naturalist 94:421-425.

Hairston, N. G. Jr. and N. G. Hairston Sr. 1993. Cause-effect relationships in energy flow, trophic structure, and interspecific interactions. American Naturalist 142:379-411.

Hairston, N. G. Jr. and N. G. Hairston Sr. 1997 Does food web complexity eliminate trophic-level dynamics? American Naturalist 149:1001-1007.

Hambright, K. D., N. G. Hairston Jr., W. R. Schaffner, and R. W. Howarth. 2007. Grazer control of nitrogen fixation: phytoplankton taxonomic composition and ecosystem functioning. Fundamental and Applied Limnology 170:103-124.

Hildrew, A., D. Raffaelli, and R. Edmonds-Brown. 2007a. Body size: the structure and

function of aquatic ecosystems, Cambridge University Press, Cambridge, UK.

Hildrew, A., D. Raffaelli, and R. Edmonds-Brown. 2007b. Body size in aquatic ecology: important, but not the whole story. Pages 326-334 *in* A. Hildrew, D. Raffaelli, and R. Edmonds-Brown, eds. Body size: the structure and function of aquatic ecosystems, Cambridge University Press, Cambridge, UK.

Jansson, A. 1982. Notes on some Corixidae (Heteroptera) from New Guinea and New Caledonia. Pacific Insects 24:95-103.

Jones, J. I. and E. Jeppesen. 2007. Body size and trophic cascades in lakes. Pages 118-139 *in* A. Hildrew, D. Raffaelli, and R. Edmonds-Brown eds. Body size: the structure and function of aquatic ecosystems, Cambridge University Press, Cambridge, UK.

Kelts, L. J. 1979. Ecology of a tidal marsh corixid, *Trichocorixa verticalis* (Insecta, Hemiptera). Hydrobiologia 64:37-57.

Knoechel, R. and L. B. Holtby. 1986. Cladoceran feeding rate: body length relationships for bacterial and large algal particles. Limnology and Oceanography 31:195-200.

Kooijman, S. A. L. M. 1993. Dynamical energy budgets in biological systems. Cambridge University Press, Cambridge, UK.

Loder, T. C. III, B. Ganning, and J. A. Love. 1996. Ammonia nitrogen dynamics in coastal rockpools affected by gull guano. Journal of Experimental Marine Biology and Ecology 196:113-129.

Manly, B. F. J. 1974. A model for certain types of selection experiments. Biometrics 30: 281-294.

Martínez-Jerónimo, F. and A. Gutierrez-Valdivia. 1991. Fecundity, reproduction, and growth of *Moina macrocopa* fed different algae. Hydrobiologia 222:49-55.

Mittelbach, G. G. 1981. Foraging efficiency and body size: a study of optimal diet and habitat use by bluegills. Ecology 65:1370-1386.

McCauley, E. 1984. The estimation of the abundance and biomass of zooplankton in samples.

Pages 228-263 *in* J. A. Downing and F. H. Rigler, eds. A manual on methods for the assessment of secondary productivity in fresh waters. Press, Malden, Massachusetts, USA.

Murdoch, W. M. and M. A. Scott. 1984. Stability and extinction of laboratory populations of zooplankton preyed on by the backswimmer *Notonecta*. Ecology 65:1231-1248.

Murdoch, W. M. and A. Stewart-Oaten. 1989. Aggregation by parasitoids and predators: effects on equilibrium and stability. American Naturalist 134:288–310.

Nandini, S. and S. S. S. Sarma. 2000. Lifetable demography of four cladoceran species in relation to algal food (*Chlorella vulgaris*) density. Hydrobiologia 435:117-126.

Nusch, E .A. 1980. Comparison of different methods for chlorophyll and phaeopigment determination. Archiv fur Hydrobiologia 14:14–36.

Pace, M. L., J. J. Cole, S. R. Carpenter, and J. F. Kitchell. 1999. Trophic cascades revealed in diverse ecosystems. Trends in Ecology and Evolution 14:483-488.

Paine, R. T. 1980. Food webs: linkage, interaction strength, and community infrastructure. Journal of Animal Ecology 49:666-685.

Pajunen, V. I. and I. Pajunen. 1991. Oviposition and Egg Cannibalism in Rock-Pool Corixids (Hemiptera: Corixidae). Oikos 60:83-90.

Pastorok, R. A. 1981. Prey vulnerability and size selection by *Chaoborus* larvae. Ecology 62:1311-1324.

Persson, L. 1987. The effects of resource availability and distribution on size class interactions in perch, *Perca fluviatilis*. Oikos 48:148-160.

Persson, L., K. Leonardsson, A. M.d Roos, M. Gyllenber, and B. Christensen. 1998. Ontogenetic scaling of foraging rates and the dynamics of a size-structured consumer-resource model. Theoretical Population Biology 54:270-293.

Peters, R. H. 1983. The ecological implications of body size. Cambridge University Press, Cambridge, UK.

Polis, G. A. and D. R. Strong. 1996. Food web complexity and community dynamics. American Naturalist 147:813-846.

Polis, G. A. 1999. Why are parts of the world green? Multiple factors control productivity and the distribution of biomass. Oikos 86:3-15.

R Development Core Team. 2011. R: a language and environment for statistical computing. R Foundation for Statistical Computing, Vienna, Austria.

Ranta, E. and J. Espo. 1989. Predation by the rock-pool insects *Arctocorisa carinata*, *Callieorixa producta* (Het. Corixidae) and *Potamonectes griseostriatus* (Col. Dytiscidae). Annales Zoologici Fennici 26:53-60.

Rogers, D. J. 1972. Random search and insect population models. Journal of Animal Ecology 41:369-383.

Rudolf, V. H. W. 2007. The interaction of cannibalism and omnivory: consequences for community dynamics. Ecology 88:2697–2705.

Rudolf, V. H. W. and K. D. Lafferty. 2011. Stage structure alters how complexity affects stability of ecological networks. Ecology Letters 14:75-79.

Sala, J. and D. Boix. 2005. Presence of the Nearctic water boatman *Trichocorixa verticalis verticalis* (Fieber, 1851) (Heteroptera, Corixidae) in the Algarve region (S Portugal). Graellsia 61:31-36.

Schmitz, O. J., P. A. Hambäck, and A. P. Beckerman. 2000. Trophic cascades in terrestrial systems: a review of the effects of carnivore removal on plants. American Naturalist 155:141-153.

Shine, R. 1991. Why do larger snakes eat larger prey items? Functional Ecology 5:493-502.

Shurin, J. B., E. T. Borer, E. W. Seabloom, K. Anderson, C. A. Blanchette, B. Broitman, S. D. Cooper, and B. S. Halpern. 2002. A cross-ecosystem comparison of the strength of trophic cascades. Ecology Letters 5:785-791.

Simonis, J. L. 2012. Prey (*Moina macrocopa*) population density drives emigration rate of its

predator (*Trichocorixa verticalis*) in a rock-pool metacommunity. Hydrobiologia DOI 10.1007/s10750-012-1268-9.

Strong, D. R. 1992. Are all trophic cascades wet? Differentiation and donor-control in speciose ecosystems. Ecology 73:747-754.

Sze, P. 1981. Observations on microalgae in supralittoral rockpools in New England (USA). Botanica Marina 24:337-341.

Thompson, D. J. 1975. Towards a predator-prey model incorporating age structure: the effects of predator and prey size on the predation of *Daphnia magna* by *Ischnura elegans*. Journal of Animal Ecology 44:907-916.

Tones, P. I. and U. T. Hammer. 1975. Osmoregulation in *Trichocorixa verticalis interiores* Sailer (Hemiptera, Corixidae) – an inhabitant of Saskatchewan saline lakes, Canada. Canadian Journal of Zoology 53:1207-1212.

Tones, P. I. 1977. The life cycle of *Trichocorixa verticalis interiors* Sailer (Hempitera, Corixidae) with special reference to diapause. Freshwater Biology 7:31-36.

van de Meutter, F., H. Trekels, and A. J. Green. 2010. The impact of the North American waterbug *Trichocorixa verticalis* (Fieber) on aquatic macroinvertebrate communities in southern Europe. Fundamental and Applied Limnology 177:283-292.

Werner, E. E. and J. F. Gilliam. 1984. The ontogenetic niche and species interactions in size-structured populations. Annual Review of Ecology and Systematics 15:393-425.

Werner, E. E. 1988. Size, scaling, and the evolution of complex life cycles. Pages 60-81 *in* B. Ebenman and L. Persson, eds. Size-structured populations: ecology and evolution. Springer-Verlag, Berlin, Germany.

Wetzel, R. G. and G. E. Likens. 2000. Limnological analyses. Springer, Berlin, Germany.

Woodward, G. and A. G. Hildrew. 2002. Body-size determinants of niche overlap and intraguild predation within a complex food web. Journal of Animal Ecology 71:1063-1074.

Wurtsbaugh, W. A. and T. S. Berry. 1990. Cascading effects of decreased salinity on the plankton, chemistry, and physics of the Great Salt Lake (Utah). Canadian Journal of Fisheries and Aquatic Sciences 47:100-109.

Wurtsbaugh, W. A. 1992. Food-web modification by an invertebrate predator in the Great Salt Lake (USA). Oecologia 89:168-175.

CHAPTER 3

BATHING BIRDS BIAS BETA-DIVERSITY: FREQUENT DISPERSAL BY GULLS HOMOGENIZES FAUNA IN A ROCK-POOL METACOMMUNITY[1]

[1] A manuscript in preparation with Dr. Julie C. Ellis.

ABSTRACT

Metacommunity theory predicts that regional dispersal of organisms among local habitat patches will influence spatial patterns of species diversity. In particular, increased dispersal rates are generally expected to increase local (α) diversity, yet homogenize local communities across the region (decrease β–diversity), resulting in no change in regional (γ) diversity. These predictions have met with mixed experimental results, and remain poorly tested in field metacommunities, where other ecological factors may also influence species diversity. Here, we use a system of freshwater rock pools on Appledore Island, Maine, USA to test the effects of dispersal rate on species diversity in metacommunities. The pools exist in clusters (metacommunities) that experience different levels of dispersal imposed by gulls (*Larus* spp.), which we show to be frequent passive dispersers of rock-pool invertebrates. Although previous research suggests that waterbirds may disperse aquatic invertebrates, our study is the first to quantify the rate at which such dispersal occurs and determine its effects on species diversity. In accordance with metacommunity theory, we found that metacommunities experiencing higher dispersal rates had significantly more homogeneous local communities (reduced β–diversity) and that γ–diversity was not influenced by dispersal rate. However, α–diversity in the rock pools was not significantly influenced by dispersal, as predicted by metacommunity theory. Rather, local diversity was significantly positively related to local habitat size. These results indicate that regional dispersal and local factors (here, habitat size) can interact to produce patterns of species diversity in metacommunities that are counterintuitive until their effects are disarticulated.

INTRODUCTION

A principal goal of metacommunity ecology is to elucidate how processes occurring

locally (within patches of habitat) and regionally (among habitat patches) combine to dictate observed patterns of species diversity across spatial scales (Leibold *et al.* 2004; Holyoak *et al.* 2005). Dispersal, the movement of organisms between distinct patches of habitat, is a fundamental ecological process that determines the spatial distribution of individual species and therefore likely influences patterns of species diversity (Hanski 1999; Clobert *et al.* 2001). While models vary in their specific predictions (Chave and Leigh 2002; Mouquet *et al.* 2002; Mouquet and Loreau 2003; Chase *et al.* 2005), metacommunity theory generally predicts a positive relationship between local species diversity (α–diversity) and dispersal rate, as increasing dispersal allows additional species to colonize patches (Figure 3.1). At the same time, this increased colonization is expected to homogenize the composition of species among habitat patches, thereby reducing among-patch variation (β–diversity) with increasing dispersal rates (Chave and Leigh 2002; Mouquet and Loreau 2003; Figure 3.1). As a result of the increase in α–diversity and decrease in β–diversity, regional species diversity (γ-diversity) is expected not to change with increasing dispersal (Mouquet and Loreau 2003; Chase *et al.* 2005; Figure 3.1). In some metacommunities, however, dispersal rates may become high enough for species to not be limited by colonization, at which point local ecological processes or factors (*e.g.*, competitive exclusion, keystone predation) are expected to determine species diversity both locally and regionally. Above this threshold dispersal rate, β–diversity is predicted to remain constant near 0 (communities are homogenized by high dispersal) and α–diversity is expected to decrease (due to, *e.g.*, competitively superior species dominating across the region), causing γ-diversity to decrease (Mouquet and Loreau 2003; Chase *et al.* 2005; Figure 3.1). These theoretical predictions have been tested experimentally, but a recent meta-analysis by Cadotte (2006) has indicated that the current body of experimental research is inconclusive regarding the effects of dispersal rate on species diversity in metacommunities. Further, metacommunity theory has seldom been applied to explain observed patterns of species diversity in field systems, where other factors such as habitat size

and resource density may also strongly influence species diversity (Rosenzweig 1995; Post *et al.* 2000; Driscoll and Lindenmayer 2009).

Here, we use a field ecosystem of freshwater rock pools on Appledore Island, Maine, USA (hereafter Appledore; Figure 3.2) to test the predictions of metacommunity theory regarding the influence of dispersal on species diversity. Approximately 1,500 rain-filled freshwater rock pools are patchily distributed on Appledore above the high-tide line, housing a community of 16 invertebrate taxa including rotifers, insects, and crustaceans (Table 3.1). For their inhabitants, the rock pools represent habitat "islands" embedded in an uninhabitable

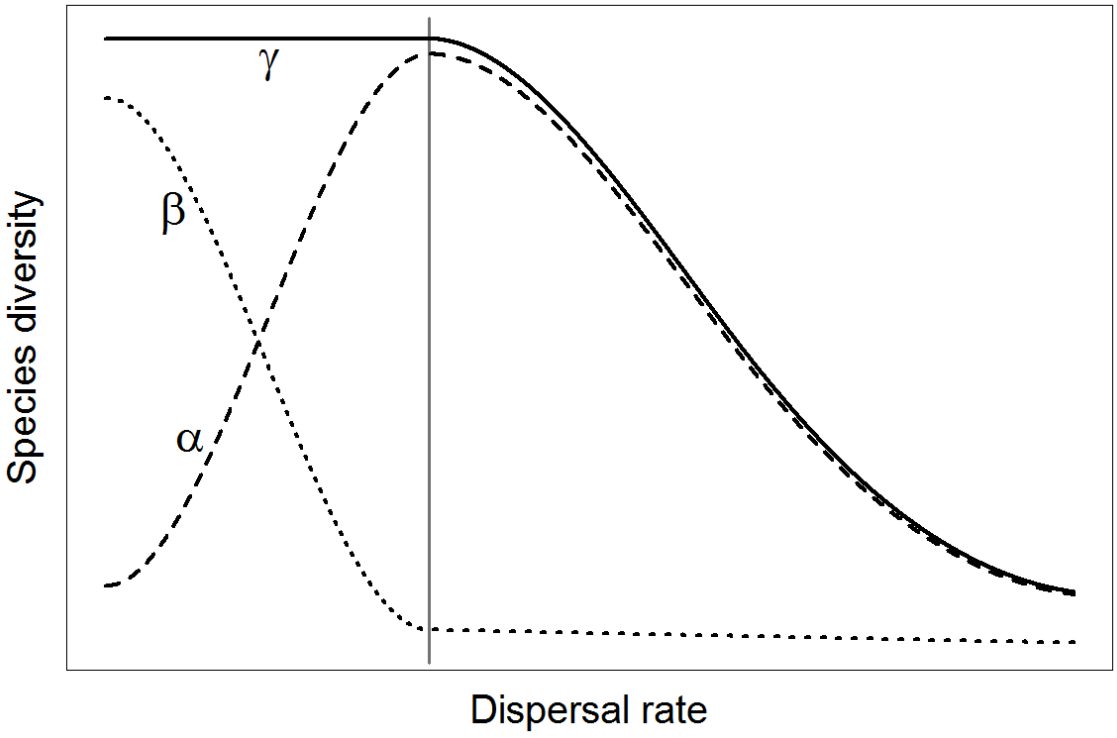

Figure 3.1. General theoretical predictions for the effect of dispersal on α–, β–, and γ–diversity (dashed, dotted, and solid black lines, respectively) in metacommunities (modified from Mouquet and Loreau 2003; Chase et al 2005; as well as references therein). The vertical solid grey line indicates the threshold level of dispersal above which local processes are expected to determine species diversity patterns.

Figure 3.2. A: Appledore Island, Maine, USA (white star), as part of the Isles of Shoals Archipelago, in relation to coast of New Hampshire and Maine, USA. Portsmouth, NH is depicted by the black arrow. B: Locations of observations for gull visitations (red circles), sampling points for diversity survey (blue triangles), and the central pond (orange star). C: An area of rock pools (shaded and numbered) on the eastern side of Appledore, as represented by the black rectangle in (B). Not all pools in the aerial photo of (C) are shaded and marked. Photos courtesy of J. Morin.

A
B
200 m
C
20 m

Table 3.1. Fraction of gulls (*Larus* spp.) carrying rock-pool invertebrates, ordered from most to least dispersed invertebrates.

Taxon	Freq. of Occurr.	Exiting Pools (of 25)	Near Pools (of 25)	Central Pond (of 2)	Total (of 52)
Moina macrocopa (C)	0.42	5	1	1	7
Brachionus rubens (R)	0.77	5	0	0	5
Acanthocyclops vernalis (C)	0.49	3	1	1	5
Aedes sp. (I)	0.20	3	1	0	4
Trichocorixa verticalis (I)	0.86	3	0	0	3
Daphnia pulex (C)	0.22	1	0	1	2
Chironomidae sp. (I)	0.89	0	0	1	1
Ostracoda sp. (C)	0.67	0	1	0	1
Ephydra sp. (I)	0.04	1	0	0	1
Dytiscidae sp. (I)	0	1	0	0	1
Chydorus sphaericus (C)	0.11	0	0	0	0
Harpacticoida sp. (C)	0.02	0	0	0	0
Amphipoda sp. (C)	0.01	0	0	0	0
Epiphanes sp. (R)	0	0	0	0	0
Bosmina sp. (C)	0	0	0	0	0
Daphnia laevis (C)	0	0	0	0	0

Notes. The number of gulls carrying each taxon is listed for each of the three classes of gulls (exiting pools, near pools, in the central pond) and in total. Parenthetical letters indicate the larger taxonomic classification (C: crustacean, R: rotifer, I: insect). The five insects are the only taxa capable of actively dispersing between pools. Freq. of Occur. (frequency of occurrence) indicates how common each taxon was in the survey of 90 pools (see *Materials and Methods*); taxa observed in the rock pools at other times but not during this survey were included with frequency = 0.

matrix of exposed granite bedrock. Although the insect species present can actively disperse among pools by flying during specific periods in their life histories, the rest of the taxa must rely on external mechanisms (*e.g.*, wind, animals) to passively disperse among pools. One potential dispersal agent for rock-pool fauna are the large breeding populations of Herring Gulls and Great Black-Backed Gulls (*Larus argentatus* and *L. marinus*, respectively) on Appledore (Ellis and Good 2006). We have routinely observed gulls visiting the pools to drink, swim, or bathe (Figure 3.3). If the gulls carry any rock-pool invertebrates on them externally, such visits represent potential dispersal events and the existing variation in gull density among rock pool clusters on Appledore (Figure 3.4A) constitutes a gradient of dispersal imposed upon the metacommunities.

Following Darwin's clever experiment showing that ducks could passively disperse freshwater snails among isolated wetlands (Darwin 1859), many ecologists have reported observations of waterbirds dispersing aquatic invertebrates, including taxa otherwise lacking the capacity to disperse between habitats (Maguire 1963; Bilton *et al.* 2001; Figuerola and Green 2002; Bohonak and Jenkins 2003; Charalambidou and Santamaría 2005; Frisch *et al.* 2007; Green *et al.* 2008). These observations have established that waterbirds can act as dispersal agents for aquatic invertebrates, yet there is a lack of quantitative data regarding the frequency and efficacy of waterbird-mediated dispersal of aquatic invertebrates. As a result, the effects of such dispersal on the spatial distributions of species and patterns of species richness in aquatic communities remains speculative (Figuerola and Green 2002; Bohonak and Jenkins 2003). Therefore, the goals of this study were first to quantify rates of gull-mediated dispersal in the rock-pool system and then to examine how invertebrate α–, β–, and γ–diversity vary among clusters of rock pools (metacommunities) in response to increasing rates of passive dispersal by gulls.

To determine if *Larus* if could disperse rock-pool invertebrates, we captured 52 gulls in the field, placing each into a plastic tub containing filtered well water to assess if they were

Figure 3.3. Adult (A. B) and juvenile (C, D) gulls visiting Appledore rock pools.

B
D
A
C

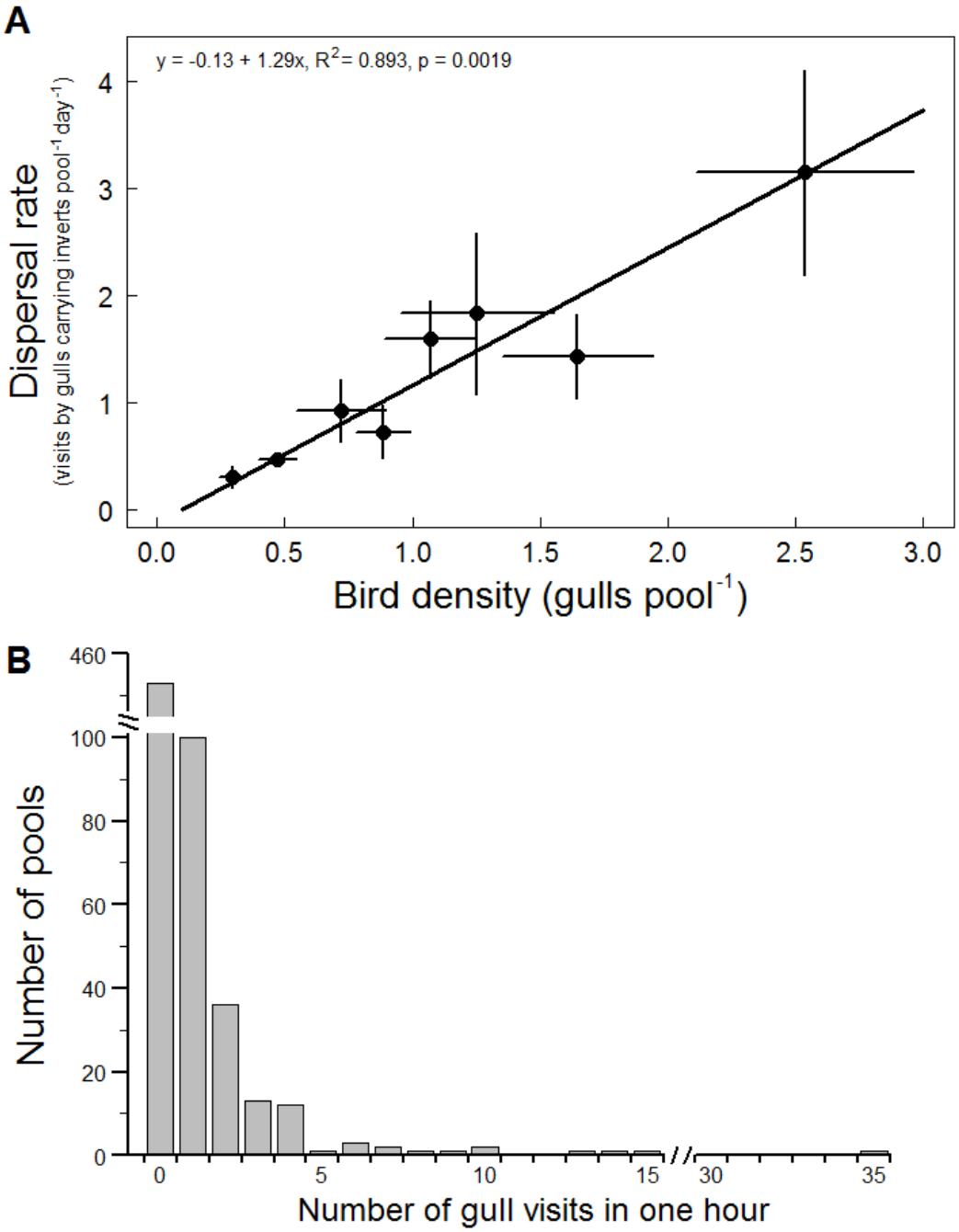

Figure 3.4. Gulls (*Larus* spp.) frequently visit rock pools on Appledore Island. A: Dispersal rate (visits by gulls carrying invertebrates pool^{-1} day^{-1}) increases significantly as a function of local gull density (gulls pool^{-1}). Data are seasonal averages (± SEM) for the eight observational areas (see Figure 3.2B), dispersal rates were estimated as described in *Materials and Methods*, and the line is the best-fit RMA regression using average values for both variables. B: Histogram of the frequency of visits by gulls pools across all eight sites and four time periods. Note the breaks in both axes.

carrying live animals (*Materials and Methods*). Twenty-five of the birds were intercepted as they exited pools, 25 were captured near pools but had not been in a pool for > 20 minutes, and the remaining two were captured from the central pond (Figure 3.2B). To scale up these results, we next quantified how frequently gulls visit the rock pools using modified scan sampling (Altmann 1974) at eight sites around Appledore that experienced varying gull densities (Figure 3.2N; *Materials and Methods*). We then used a Monte Carlo modeling approach and combined the transportation and visitation data sets to quantify the average rate at which gulls dispersed invertebrates among the rock pools and how this rate varied as a function of gull density within a metacommunity (*Materials and Methods*). Here we are focusing on external transport (on feathers, feet, *etc*.), as we have found no conclusive evidence that *Larus* disperses invertebrates internally (no viable invertebrates or eggs were found in 100 fresh fecal deposits; Simonis and Fetzer *unpub. data*).

Finally, we quantified the effects of this gull-mediated dispersal on rock-pool invertebrate diversity by sampling 90 pools in 10 clusters (metacommunities) around Appledore during July 2011 (7–10 pools per cluster; Figure 3.2B; *Materials and Methods*). For each pool we measured the total number of taxa present (α–diversity) and for each metacommunity we determined the taxonomic variation among pools (β–diversity; as multivariate dispersion using Sørensen's index of similarity; Sørensen 1948; Anderson *et al.* 2006; Anderson *et al.* 2011) and the total number of taxa present in the cluster (γ–diversity). The clusters varied in local bird density (range: 0 – 2.06 gulls $pool^{-1}$) and thus varied in the level of bird-mediated dispersal they experienced (Figure 3.4A). We also measured the volume and the chlorophyll-*a* concentration (proxy for resource density) of each rock pool, to test the effects of habitat size and resource density on species diversity (Rosenzweig 1995; Post *et al.* 2000). The significance of dispersal rate, pool volume, and resource density as predictors of α–, β–, and γ–diversity were tested using separate regressions for each diversity metric (*Materials and Methods*).

RESULTS AND DISCUSSION

Larus gulls are indeed capable of transporting aquatic invertebrates between rock pools on Appledore. In total, 20 of the 52 (38.5%) birds tested were found to be carrying at least one live invertebrate, with the maximum number of taxa being three (Table 3.2, average number of taxa on those 20 birds was 1.44) and the maximum number of invertebrates on any bird being 18 (17 *Brachionus* and one *Trichocorixa*). Birds exiting pools were significantly more likely to be carrying live animals than birds that had not recently visited pools (64% vs. 8%, $\chi^2_{df=1} = 17.01$, $P = 0.0005$). However, the fact that some birds not recently in pools harbored live aquatic invertebrates indicates the potential for rock-pool fauna to persist on gulls for an extended period of time outside of water (at least 20 minutes). These invertebrates likely persisted due to the gulls' dense feathers and preening oil (Gill 2007), which promote the creation of temporary aquatic microhabitats (J. L. Simonis *pers. obs.*). The length of time for which these microhabitats can harbor living aquatic organisms is unknown, but our data indicate that some remain habitable for 20 minutes or longer. The invertebrates found on the birds comprised the majority of rock-pool fauna (10 of 16 taxa, or 62.5%) and were generally also the most common taxa in the pools (Table 3.1). *Moina macrocopa*, one of the most abundant invertebrates in the pools, was found on seven gulls

Table 3.2. Number of invertebrate taxa found on gulls (*Larus* spp.)

Class	0 Taxa	1 Taxon	2 Taxa	3 Taxa
Recently exited pool	9	10	6	0
Near pool	23	1	0	1
Central Pond	0	1	0	1

Notes. For each class of gulls, the number of birds carrying 0 – 3 invertebrate taxa is listed.

(13.5% of total), the most of any taxon (Table 3.1).

Our field observations indicate that this gull-mediated dispersal of aquatic invertebrates occurs frequently in the Appledore system, as birds visited rock pools at an overall rate of 0.65 visits $pool^{-1}$ hr^{-1} (409 visits seen in 628 pool-hours of observation; SD: 2.04). However, visits were not evenly distributed among pools (Figure 3.4B): only 175 (27.9%) of the pools were visited during observations and the vast majority of those pools (92%, 161 of 175) were visited four or fewer times, yet one pool was visited 34 times in an hour. As a result, the distribution of visits was overdispered: the variance of visitation rates was 6.4 times higher than the mean visitation rate (4.16 and 0.65, respectively). The rate of visits by gulls also varied considerably among locations and months (range: 0 – 3.4 visits $pool^{-1}$ hr^{-1}, SD: 0.73) and a significant portion of this variation was predicted by the local density of gulls, such that pools were visited more frequently when there were more gulls in the area (Figure 3.5; ranged major axis [RMA] regression slope = 0.73, $R^2 = 0.43$, $P = 0.0003$). Of the observed visits, 10.3% (42 of 409) were by gulls going between multiple pools within 20 minutes, which represents a higher chance of transporting invertebrates, given the increased prevalence of invertebrates on gulls that have recently exited pools (Table 3.2).

The Monte Carlo combination of our experimental and observational data suggest that a typical pool is visited by gulls at a rate of 9.15 visits $pool^{-1}$ day^{-1} (range: 6.82 – 12.11, SD: 0.67) and 13.8% of those visits involved birds carrying viable invertebrates (range: 10.1% – 18.0%, SD: 1.0%), leading to an average rate of 1.26 visits by birds carrying invertebrates $pool^{-1}$ day^{-1} (range: 0.84 – 1.88, SD: 0.13). However, all pools are not equally likely to receive gulls carrying invertebrates, as there was large spatial variation in gull densities (seasonal averages within clusters, range: 0.30 – 2.54 gulls $pool^{-1}$, SD: 0.72). Indeed, the expected rate of gull-mediated dispersal (from the Monte Carlo analysis) increased significantly as a function of the density of gulls within the cluster (Figure 3.4A; ranged major axis [RMA] regression using seasonal averages of gull density and dispersal rate, slope =

1.29, $R^2 = 0.893$, $P = 0.0019$). It is important to note that these calculations did not include the ability of taxa to establish populations upon arriving, nor take into account that some taxa may already be present in the recipient pool. Nevertheless, our results demonstrate the high potential for *Larus* to be an important dispersal vector for invertebrates in the Appledore rock pools. In particular, gulls are likely the main mode of dispersal for the vast majority of rock-

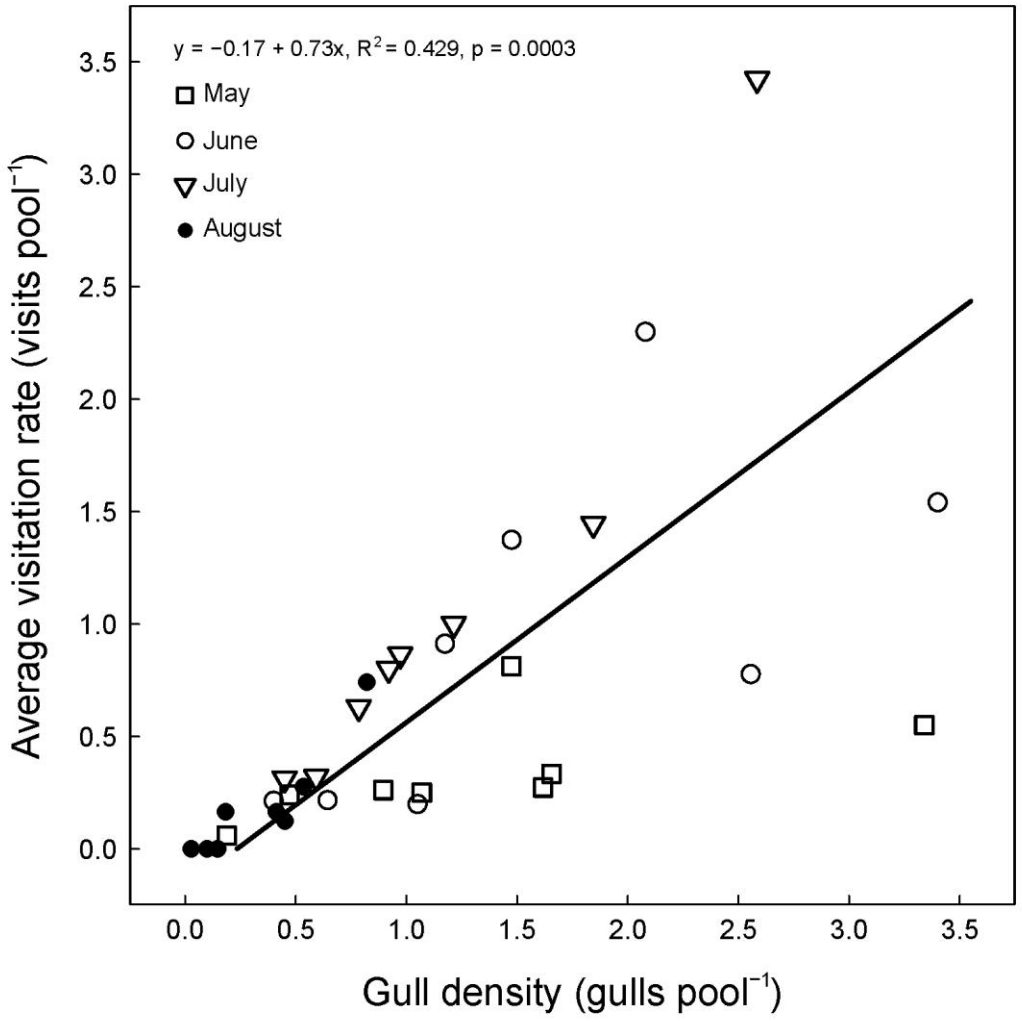

Figure 3.5. The rate of visits by gulls to pools significantly increases as a function of the local density of gulls (individuals $pool^{-1}$), across the four observation periods (denoted by different symbols). The line is the best-fit RMA regression.

pool taxa that cannot actively disperse between habitats (Table 3.1). Indeed, the rate of gull-mediated dispersal is much higher than the frequency of rain-induced overflows (average rate: 0.05 overflows $pool^{-1}$ day^{-1}), the other major vector of passive dispersal in the rock pools (K. E. Pellowe and J. L. Simonis, *unpub. data*).

Our survey of faunal diversity indicates that this frequent dispersal by *Larus* significantly influences spatial patterns of invertebrate species diversity in the Appledore rock pools (Figure 3.6). In particular, metacommunities experiencing higher levels of gull dispersal had significantly more similar local communities (lower β–diversity with increasing dispersal rate; Figure 3.6B; RMA regression, slope = -0.096, $R^2 = 0.60$, $P = 0.008$), as predicted by metacommunity theory (Chave and Leigh 2002; Mouquet and Loreau 2003; Figure 3.1). This result was not influenced by our using multivariate dispersion to quantify β–diversity: we obtained a similarly significant negative effect of dispersal on β–diversity if we used Whittaker's (Whittaker 1960) original equation, $\beta = \gamma/\alpha^*$ (where α^* is the average α–diversity for the cluster; RMA regression, slope = -0.272, $R^2 = 0.615$, $P = 0.004$), not surprising given the strong positive correlation between the two measures of β (Pearson correlation coefficient = 0.87, $P = 0.001$). Neither volume nor resource density was a significant predictor of β–diversity (using either the variance or average to summarize the values among pools within clusters).

Although metacommunity models predict that α–diversity should increase with dispersal rate up to a threshold (Mouquet *et al.* 2002; Mouquet and Loreau 2003; Figure 3.1), we found no significant relationship between dispersal rate and local taxonomic richness (α–diversity did increase with dispersal, but not significantly so, $P = 0.48$; Figure 3.6A). That is, clusters of pools experiencing higher rates of gull-mediated dispersal tended to have more similar local communities, but those pools did not have higher local taxon richness. α–diversity was also not affected by local resource density, but was significantly higher in larger pools (Poisson mixed-model regression, slope = 0.12, deviance explained = 9.8%, $P = 0.037$).

Figure 3.6. Effect of gull-mediated dispersal rate (estimated based on local gull density, see Figure 3.4B) on rock-pool taxon diversity (A: α–diversity, B: β–diversity, and C: γ–diversity). Points are the mean (± SEM) for α– and β–diversity, numbers next to the points indicate the sample size (number of pools sampled in the cluster), and the line in each panel represents the best-fit RMA regression between dispersal rate and diversity (fit using mean values for α– and β –diversities). Only the relationship for β–diversity was significant, but the best-fit lines for α– and γ–diversity were included (dashed and grayed) to show trends. β–diversity was measured as multivariate dispersion using Sørensen's index of similarity (Sørensen 1948; Anderson *et al.* 2006; Anderson et al 2011) and the range of possible β–diversity values using this metric was 0 – 0.671.

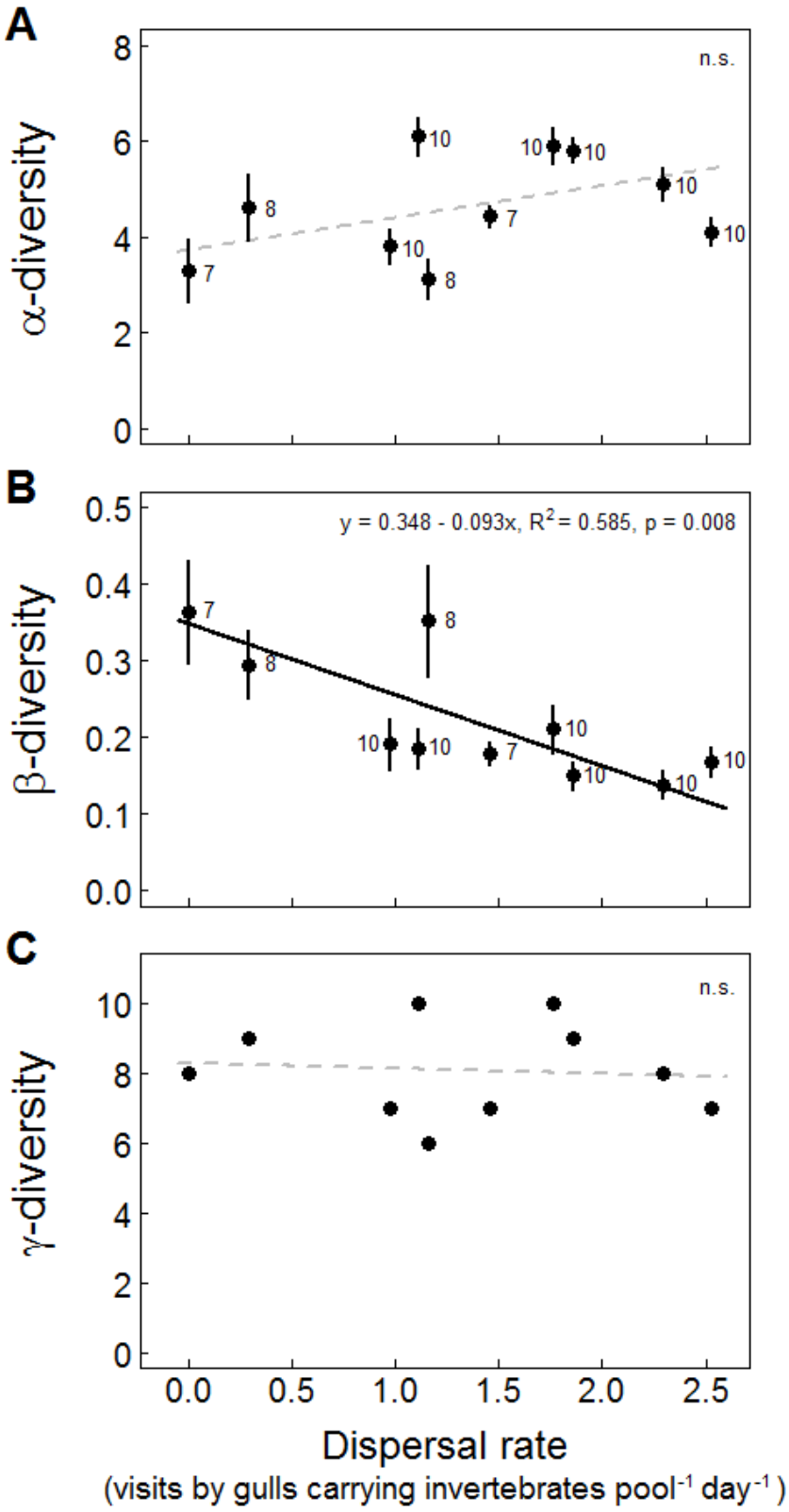
A
α-diversity
n.s.
B
β-diversity
y = 0.348 - 0.093x, R2 = 0.585, p = 0.008
C
γ-diversity
n.s.
Dispersal rate
(visits by gulls carrying invertebrates pool-1 day-1)

Metacommunity theory does predict that local factors will influence species diversity, but typically only after dispersal is high enough to fully homogenize local communities (*i.e.*, when dispersal is no longer limiting; Chave and Leigh 2002; Mouquet and Loreau 2003; Chase *et al.* 2005; Figure 3.1). In the Appledore system, however, habitat size significantly affected local diversity despite dispersal never being high enough to overcome limitation and fully homogenize local communities (β–diversity was always above 0 and still declining with increasing dispersal; Figure 3.6B). This result indicates that local factors may be important determinants of species diversity in metacommunities, even when dispersal rates are low.

As predicted by metacommunity theory (Mouquet and Loreau 2003; Chase *et al.* 2005; Figure 3.1), we found no significant relationship between γ–diversity and dispersal (gull density), indicating that transport by gulls did not contribute significantly to the number of species present in a cluster of pools ($P = 0.41$; Figure 3.6C). This result is also consistent with our observation that most pool visits are by gulls residing (nesting or roosting) nearby or within the cluster of pools, not by gulls coming from other parts of the island (J. L. Simonis, *pers. obs.*). While it is possible that gulls moving between different parts of Appledore may introduce taxa into clusters where they were previously absent, our data suggest that this longer-distance dispersal is too infrequent to influence patterns of species diversity. γ–diversity was also not significantly predicted by pool volume or resource density (using average values for the clusters). The lack of a relationship between γ–diversity and dispersal rate is predicted for low to moderate dispersal rates in metacommunity models, but in particular resulting from a balance between increased α–diversity and decreased β–diversity (Mouquet and Loreau 2003; Chase *et al.* 2005; Figure 3.1). Although we did observe an increase in β–diversity with dispersal rate, α–diversity did not change significantly along this axis. This seemingly paradoxical finding (significant change in β–, but not α– or γ–diversity, with dispersal) appears to result from the high amount of variance in α–diversity that was unexplained by dispersal (the R^2 for the RMA regression of α–diversity against dispersal =

0.144). As predicted by theory (Chave and Leigh 2002; Mouquet and Loreau 2003; Chase *et al.* 2005; Figure 3.1), the relationship between α–diversity and dispersal rate was indeed positive (estimated slope = 0.671; Figure 3.6A), albeit not statistically significantly so, perhaps due to the influence of rock-pool volume on local species richness. These results indicate that processes and factors occurring at different spatial scales (here, regional dispersal and local habitat size) can combine to create counterintuitive patterns of species diversity in metacommunities and highlight the importance of studying the influence of dispersal in field settings, where other processes and factors are also at play.

As has been observed in other systems (Maguire 1963; Bilton *et al.* 2001; Figuerola and Green 2002; Bohonak and Jenkins 2003; Charalambidou and Santamaría 2005; Frisch *et al.* 2007; Green *et al.* 2008), waterbirds (here *Larus*) have the ability to disperse invertebrates among local habitat patches. However, we have gone further than previous work to quantify both the rate of gull-mediated dispersal and its effects on the taxonomic diversity of the Appledore rock-pool metacommunity. Our results demonstrate that where dispersal of aquatic invertebrates by waterbirds occurs frequently, it can have significant consequences for spatial patterns of species diversity. However, species diversity in the rock-pool metacommunity was not influenced by just dispersal: α–diversity increased with habitat volume (c.f. Post *et al.* 2000), indicating that both local and regional processes interact to determine spatial patterns of aquatic faunal diversity. The relative significance of waterbird-mediated dispersal for species diversity in larger aquatic ecosystems (*e.g.*, lakes) remains to be tested, but once again, Darwin's keen insights (Darwin 1859) have been borne out.

MATERIALS AND METHODS

Quantifying Gull-Mediated Dispersal

We used juvenile gulls for the capture experiment, as they commonly visit the pools (juveniles accounted for 42% of observed visits, despite being only 25% of the observed population), could not escape our capture by flying, and are considerably easier to handle than adults. Of the 52 birds, 25 were intercepted as they were exiting rock pools, 25 were captured from near pools (< 5 m from a pool) but had not been in a pool for at least 20 minutes, and the remaining two were captured from the central pond on Appledore (Figure 3.2B). For the 25 gulls exiting pools, we observed the birds enter the pool, recorded the lengths of their visits, and captured them as they exited the pools of their own volition. The time the bird spent in the pool did not significantly affect whether it was carrying invertebrates (logistic regression, $P > 0.2$). Upon capture, each bird was placed into a tub (40 L Rubbermaid Roughneck™ Tote) containing 20 L of filtered well water for up to five minutes or until it actively attempted to exit the tub, at which point it was released (for animal care considerations). The time a gull spent in the tub did not affect whether invertebrates were found (logistic regression, $P > 0.6$). After each trial, we filtered the water through a 30-µm sieve, and put everything retained into a 250 mL bottle, which we placed on ice until we could examine the sample under a dissecting microscope (< 2 hr later).

We documented the frequency of gulls visiting pools at eight sites around Appledore that varied in local gull density (Figures 3.4B, 3.2A). Observations were made within a three-day window and were repeated in May, June, July, and August 2010 to account for temporal variation in visitation rates across the summer (the period of the year when gulls nest on Appledore). We haphazardly shuffled the observation order and time-of-day for each area across months to incorporate any variation in visitation behavior due to time of day or weather. Each observation session was preceded by an acclimation period of 15 minutes and lasted for one hour. The observation pools were defined as being at least 10 m from the observer (J.L.S.) yet still within a clear line of sight (by naked eye). The modified scan sampling (Altmann 1974) regimen involved constantly scanning all pools in the observation

area and noting when gulls entered which pools and for how long they stayed. Individual gulls were also tracked (using, *e.g.*, age, band, and spatial location), allowing us to determine whether any individuals entered multiple pools and the duration of any breaks between visits. We determined the local density of gulls by counting the number of individuals present at fifteen-minute intervals during the hour of observation (starting at time 0), averaging the five counts, and dividing by the number of pools in the cluster.

We used a Monte Carlo permutation approach to combine the data on gulls transporting invertebrates with those on gulls visiting pools and determine the overall gull-mediated dispersal rate. Each run of the permutation model determined how many times a typical pool was visited by gulls in total, and in particular by gulls carrying live invertebrates, during the summer. Conservatively, we assumed that gulls only visited pools during daylight hours, because we have no observations during nighttime. We calculated the total number of daylight hours for each of the four months by using sunrise-sunset data from NOAA for Appledore Island. Within each month, we determined the number of times the pool was visited by gulls (in total) by randomly drawing from the distributions of visits per hour. We then used binomial distributions to determine the fraction of those gulls that were carrying invertebrates. For each visit, we first determined whether or not that bird had recently been in another pool using our field observation rates (probability of recent visit = 0.103), and then determined whether or not that gull was carrying an invertebrate using our experimental data (if the gull was recently in another pool, the probability of it carrying an invertebrate = 0.64; if not, probability = 0.08). We permuted this model 10,000 times in total, using R (R Development Core Team 2011). Note that by drawing randomly from the observational data on visitation rates, we assumed that there was nothing about a pool that made it inherently attractive to gulls and that the pools we selected for our observations represented an unbiased sample.

To quantify the effect of local gull density on the gull-mediated dispersal rate

experienced by metacommunities, we conducted a similar Monte Carlo analysis separately for each of the eight clusters (Figure 3.2B) during each of the four months. We determined the distributions of visitation rates for each of the 32 cluster × month combinations and used these in place of the full distribution (which included all data) in the methods outlined above to calculate the average rate of gull-mediated dispersal experienced by a typical pool in that metacommunity at that time. All other aspects of the Monte Carlo approach remained the same. We then determined the (across-season) average dispersal rate experienced by each metacommunity and regressed this against the (across-season) average local gull density using RMA regression.

Effects of Dispersal on Taxonomic Diversity

At each of the 10 clusters (metacommunities), we determined the local gull density following identical methods to those used in the 2010 observational study, and converted this value to an expected gull-mediated dispersal rate for the metacommunity, given the regression shown in Figure 3.4A. One cluster had no gulls present, for which the regression predicted a slightly negative dispersal rate; we set the dispersal rate of this metacommunity to zero. We then sampled 7–10 representative pools within the metacommunity by collecting 250–2000 mL of water (*ca.* 5% of the volume of each pool) haphazardly from throughout the pool using a large-bulb aquatic pipette (*i.e.*, turkey baster). The volume was filtered through a 30-μm sieve and everything retained was preserved in 95% ethanol. We identified all individuals present to taxon (as presented in Table 3.1) and used the taxa present to calculate taxonomic diversities. For each pool we quantified the total number of taxa present (α–diversity) and for each metacommunity we determined the taxonomic variation among pools (β–diversity) and the total number of taxa present in the metacommunity (γ –diversity). For each pool, we also determined chlorophyll-*a* concentration (Nusch 1980; as a proxy for the density of algal

resources) and pool volume (assuming an inverted cone shape, c.f. Pajunen and Pajunen 2007) to test alternative drivers of faunal diversity.

We conducted a separate regression analysis for each of the three diversity metrics (α, β, γ). Ideally, we would have used RMA regressions for each analysis because all three predictor variables (dispersal rate, producer biomass, and pool volume) were estimated and thus likely contained significant variation (Anderson et al 2011; Legendre 2011). However, RMA regression does not allow for multiple predictor variables, random effects, weights, or non-normal response variables, which are also present in these analyses. Therefore, we used a combination of different regression methods to analyze the diversity data. For all three diversity metrics, the initial multiple regression models included the three predictor variables and all possible interactions, and model simplification proceeded through stepwise term deletion based on AIC scores. We used a Poisson mixed-model regression to test the effects of all three predictor variables on α–diversity, as the data were grouped by metacommunity (*i.e.*, pool cluster, a random effect) and discretely distributed (counts of taxa). For β–diversity, the initial multiple regression showed that only bird density was a significant predictor, and so we conducted the final analysis using RMA regression. We used a weighted Poisson regression to test the effects of the predictors on γ–diversity, where the response variable (total taxa within the metacommunity) was weighted by the number of pools sampled in each cluster. All analyses were conducted in R (R Development Core Team 2011) using the lmodel2 (Legendre 2011), vegan (Oksanen *et al.* 2011), and lme4 (Bates *et al.* 2011) packages.

ACKNOWLEDGEMENTS

This research was supported financially by Shoals Marine Laboratory, the A.W. Mellon Foundation, the Cornell Program in Biogeochemistry and Environmental

Biocomplexity, the National Science Foundation (NSF, DEB-1110545), and the Cornell University Graduate School. D. Bonter, W. Fetzer, J. Heiser, J. Hewitt, N. Koskal, L. Quevillion, M. Rosen, J. Stillwell, P. Thompson, and C. Wilkinson provided field assistance. The Hairston and Flecker lab groups, A. Agrawal, S. Ellner, and S. Simonis gave feedback on the manuscript. This research was conducted under the Cornell University IACUC (permit no. 2009-0112 to J. L. Simonis).

REFERENCES

Altmann, J. 1974. Observational study of behavior: sampling methods. Behaviour 49:227-267.

Anderson, M. J., K. E. Ellingsen, and B. H. McArdle. 2006. Multivariate dispersion as a measure of beta diversity. Ecology Letters 9:683-693.

Anderson, M. J., T. O. Crist, J. M. Chase, M. Vellends, B. D. Inouye, A. L. Freestone, N. J. Sanders, H. V. Cornell, L. S. Comita, K. F. Davies, S. P. Harrison, N. J. B. Kraft, J. C. Stegen, and N. G. Swensen. 2011. Navigating the multiple meanings of β diversity: a roadmap for the practicing ecologist. Ecology Letters 14:19-28.

Bates, D., M. Maechler, and B. Bolker. 2011. lme4: Linear mixed-effects models using S4 classes. R package version 0.999375-42. http://CRAN.R-project.org/package=lme4.

Bilton, D. T., J. R. Freeland, and B. Okamura. 2001 Dispersal in freshwater invertebrates. Annual Review of Ecology and Systematics 32:159-181.

Bohonak, A. J. and D. G. Jenkins. 2003. Ecological and evolutionary significance of dispersal by freshwater invertebrates. Ecology Letters 6:783-796.

Cadotte, M. W. 2006. Dispersal and species diversity: a meta-analysis. American Naturalist 167:913-924.

Charalambidou, I and L. Santamaría. 2005. Field evidence for the potential of waterbirds as

dispersers of aquatic organisms. Wetlands 25:252-258.

Chase, J. M., P. Amarasekare, K. Cottenie, A. Gonzalez, R. D. Holt, M. Holyoak, M. F. Hoopes, M. A. Leibold, M. Loreau, N. Mouquet, J. B. Shurin, and D. Tilman. 2005. Competing theories for competitive metacommunities. Pages 335-354 *in* M. Holyoak, M. A. Leibold, and R. D. Holt, eds. Metacommunities: Spatial Dynamics and Ecological Communities. University of Chicago Press.

Chave, J. and E. G. Leigh Jr. 2002 A spatially explicit neutral model of β-diversity in tropical forests. Theoretical Population Biology 62:153-168.

Clobert, J., E. Danchin, A. A. Dhondt, and J. D. Nichols. 2001. Dispersal. Oxford University Press, New York.

Darwin, C. 1859. On the Origin of Species by Means of Natural Selection, or the Preservation of Favoured Races in the Struggle for Life. John Murray, London.

Driscoll, D.A., D. B. Lindenmayer. 2009. Empirical tests of metacommunity theory using an isolation gradient. Ecological Monographs 79:485-501.

Ellis, J. C. and T. P. Good. 2006. Nest attributes, aggression, and breeding success of gulls in single and mixed species subcolonies. Condor 108:211-219.

Figuerola, J. and A. J. Green. 2002. Dispersal of aquatic organisms by waterbirds: a review of past research and priorities for future studies. Freshwater Biology 47:483-494.

Frisch D., A. J. Green, J. Figuerola. 2007. High dispersal capacity of a broad spectrum of aquatic invertebrates via waterbirds. Aquatic Sciences 69:568-574.

Gill, F. B. 2007. Ornithology, 3rd Edition. Freeman and Company, New York.

Green, A.J., K. M. Jenkins, D. Bell, P. J. Morris, and R. T. Kingsford. 2008 The potential role of waterbirds in dispersing invertebrates and plants in arid Australia. Freshwater Biology 53:380-392.

Hanski, I. 1999. Metapopulation Ecology. Oxford Univ Press, New York.

Holyoak, M., M. A. Leibold, and R. D. Holt. 2005. Metacommunities: Spatial Dynamics and

Ecological Communities. University of Chicago Press, Chicago.

Legendre, P. 2011. lmodel2: model II regression. R package version 1.7-0. http://CRAN.R-project.org/package=lmodel2.

Leibold, M. A., M. Holyoak, N. Mouquet, P. Amarasekare, J. M. Chase, M. F. Hoopes, R. D. Holt, J. B. Shurin, R. Law, D. Tilman, M. Loreau, and A. Gonzalez. The metacommunity concept: a framework for multi-scale community ecology. Ecology Letters 7:601-613.

Maguire, B. Jr. 1963. The passive dispersal of small aquatic organisms and their colonization of isolated bodies of water. Ecological Monographs 33:161-185.

Mouquet, N. and M. Loreau. 2003. Community patterns in source-sink metacommunities. American Naturalist 162:544-557.

Mouquet, N., J. L. Moore, and M. Loreau. 2002. Plant species richness and community productivity: why the mechanism that promotes coexistence matters. Ecology Letters 5:56-65.

Nusch, E. A. 1980. Comparison of different methods for chlorophyll and phaeopigment determination. Archiv fur Hydrobiologia 14:14–36.

Oksanen, J. F. G. Blanchet, R. Kindt, P. Legendre, P. Minchin, R. B. O'Hara, G. L. Simpson, P. Solymos, M. H. H. Stevens, and H. Wagner. 2011. vegan: community ecology package. R package version 2.0-0. http://CRAN.R-project.org/package=vegan.

Pajunen, V. I. and I. Pajunen. 2007. Habitat characteristics contributing to local occupancy and habitat use in rock pool Daphnia metapopulations. Hydrobiologia 592:291-302.

Post D. M., M. L. Pace, N. G. Hairston Jr. 2000 Ecosystem size determines food-chain length in lakes. Nature 405:1047-1049.

R Development Core Team. 2011. R: a language and environment for statistical computing. R Foundation for Statistical Computing, Vienna, Austria. ISBN 3-900051-07-0, URL http://www.R-project.org/.

Rosenzweig, M. L. 1995. Species Diversity in Space and Time. Cambridge University Press.

Simonis, J. L. 2012. Prey (*Moina macrocopa*) population density drives emigration rate of its predator (*Trichocorixa verticalis*) in a rock-pool metacommunity. Hydrobiologia DOI 10.1007/s10750-012-1268-9.

Sørensen, T. A. 1948. A method of establishing groups of equal amplitude in plant sociology based on similarity of species content, and its application to analyses of the vegetation on Danish commons. Biologiske Skrifter 5:1–34.

Whittaker, R. 1960. Vegetation of the Siskiyou Mountains, Oregon and California. Ecological Monographs 30:279-338.

CHAPTER 4

COMBINING DEMOGRAPHIC AND GENETIC APPROACHES TO STUDY THE COMPLEX STRUCTURE OF AN APEX-PREDATOR METAPOPULATION

ABSTRACT

In spatially structured landscapes, dispersal connects local populations at larger spatial scales, often creating complex population dynamics. When the dispersing species is also a strong interactor (*e.g.*, apex predator) its dispersal likely also has consequences for spatial food-web and ecosystem dynamics. Here I study the dispersal and spatial population dynamics of *Trichocorixa verticalis*, a mobile and voracious apex predator in a system of freshwater rock pools on Appledore Island (Maine, USA). A field experiment shows that dispersal by *T. verticalis* is frequent (average rate: 0.18 immigrants $pool^{-1}$ day^{-1}) and that individuals can fly at least 50 m, far enough to colonize any pool on Appledore. Yet seemingly paradoxically, local populations experience high turnover and *T. verticalis* is absent from ~ 50% of suitable pools at any time, indicating that their high dispersal is not able to prevent local extinctions or promote immediate recolonization of patches following extinctions. In the same metapopulation, mitochondrial genetic diversity is shown to be very high within local populations and relatively small among populations, especially at increasing distance. These results indicate that the combination of high dispersal and turnover generate complex demographic and genetic consequences in metapopulations.

INTRODUCTION

Dispersal is a fundamental biological process by which individuals moving between locations connect local populations at larger, regional spatial scales (Hanski 1999; Clobert *et al.* 2001). At the very least, dispersal of individuals promotes gene flow and alters local population sizes, but it may also prevent local extinction in "sink" patches and promote colonization of available but empty habitat (Mayr 1963; MacArthur and Wilson 1967; Brown and Kodric-Brown 1977; Hanski 1999). Because dispersing individuals are also engaged in

within-patch ecological processes, such as trophic interactions and nutrient recycling, dispersal also has the potential to connect food webs and ecosystems at larger spatial scales (Loreau *et al.* 2003; Holyoak *et al.* 2005; McCann *et al.* 2005). Indeed, many dispersive species have large impacts on both the distribution of resources and the rate of ecosystem processes occurring within food webs (Kneitel and Miller 2003; Holyoak *et al.* 2005; Van de Koppel *et al.* 2005; Flecker *et al.* 2010). In particular, mobile species that are strong interactors (*e.g.*, apex predators, dominant competitors, key nutrient recyclers) may act as process subsidies (*sensu* Flecker *et al.* 2010) whose spatial distributions and movements determine the rates of important ecosystem processes across the landscape (Loreau et al 2003; McCann *et al.* 2005). In such cases where mobile species are strong interactors, understanding their spatial population dynamics becomes crucial to determining how they influence food-web and ecosystem dynamics across space. However, populations are often influenced by multiple ecological factors that vary across space and time, causing complex spatial dynamics that may be difficult to characterize (Harrison 1991; Hill *et al.* 1996; Harrison and Taylor 1997; Sutcliffe *et al.* 1997; Dunham and Rieman 1999; Hanski 1999; Clobert *et al.* 2001; Driscoll 2007). In such situations, it is valuable to collect multiple types of data (*e.g.*, demographic and genetic) on the same species and combine them to understand their spatial dynamics (Gaggiotti 2004; Hulsmans *et al.* 2007).

Metapopulation theory offers a useful framework for understanding how dispersal influences the spatial distribution and dynamics of populations (Levins 1970; Harrison 1991; Hanski 1999), and predicting its accompanying influences on food webs and ecosystems (Loreau *et al.* 2003; Leibold and Miller 2004). Theoretical studies suggest that the key parameters driving spatial population dynamics are the *per capita* rate of dispersal (and how it decays with distance) and the variability in local population size (Harrison 1991; Hanski 1999). At very low dispersal rates, local extinctions occur more frequently than can be countered by colonization, and the entire metapopulation is at risk of extinction. As dispersal

rates increase, the frequency of colonization events will eventually approximate the frequency of local extinctions, generating a classic "Levins metapopulation" (Levins 1970), where local populations are still extinction-prone, but the metapopulation persists regionally through a balance of colonizations and extinctions (*i.e.*, turnover). The high rate of population turnover in Levins metapopulations is generally expected to generate local populations that are low in genetic diversity and genetically distinct from each other (Wade and McCauley 1988; Whitlock and McCauley 1990; Harrison and Hastings 1996). With further increase in dispersal rates, local extinctions are expected to be rare and local population dynamics should be strongly influenced by dispersing individuals, effectively collapsing the metapopulation structure into a single, genetically panmictic population that is unaffected by the patchiness of the landscape (Slatkin 1985; Hanski 1999; Jansen 1999; Simonis 2012a). In intermediate cases, however, dispersal may be high enough to influence local population abundances, but not high enough to prevent local extinctions (Sutcliffe *et al.* 1997; Hanski 1999).

In addition to *per capita* dispersal rates, variation in local population size among habitat patches is also theorized to influence metapopulation dynamics by determining both the number of potential dispersers and the probability of local population extinction (Harrison 1991; Hanski 1999). Among-patch differences in local population abundance may result from variation in the quality or size of habitat patches (Pulliam 1988). When large, variation in local population sizes can create "source-sink" dynamics, where "source" patches support large and genetically diverse populations with little risk of extinction that supply re-colonizers to genetically depauperate, small populations existing in extinction-prone "sink" patches (Boorman and Levitt 1973; Frankham 1997). However, it is often the case that no patches are true "sources" completely safe from extinction, but rather that all experience some level of extinction risk, which varies as a function of local population size (Hanksi 1999).

Resulting from the combination of dispersal and population-size effects on colonization and extinction rates, many species inhabiting fragmented landscapes exhibit

complex spatial population dynamics that may not be captured well by simple metapopulation models, such as the Levins model. These metapopulations have been termed "mixed-structure" by Harrison (1991) to encompass the fact that they display components of many classic metapopulation models. Mixed-structure metapopulations are presumed to be prevalent, especially among motile consumers in highly fragmented landscapes (Driscoll 2007), and therefore could play an important role in driving food-web and ecosystem dynamics across spatial scales (McCann *et al.* 2005). However, mixed-structure metapopulations remain poorly documented empirically (Sutcliffe *et al.* 1997; Driscoll 2007), limiting current understanding of the influence of mobile consumers on spatial food-web and ecosystem dynamics (McCann *et al.* 2005).

A major difficulty in empirically studying spatially structured populations, and mixed-structure metapopulations in particular, is directly measuring dispersal and extinction rates, as well as describing how they affect population dynamics. Indeed, dispersal is an inherently difficult ecological process to quantify directly, and is instead often inferred using indirect methods, such as stable isotopes or population genetics (Clobert *et al.* 2001). However, indirect methods rely on assumptions derived from simple metapopulation models regarding how dispersal influences spatial populations, and therefore can give spurious effects when used to measure dispersal rates from observed dynamics, particularly in mixed-structure metapopulations (Bohonak 1999). Ideally, metapopulation dynamics should be studied using a combination of methods (*e.g.*, experimental, demographic, and genetic approaches), thereby limiting the assumptions that need to be made in interpreting results (Gaggiotti 2004).

In the present study I quantify the effect of dispersal and variation in local population size on the spatial population dynamics of a strong interactor, the aquatic insect *Trichocorixa verticalis*. *T. verticalis* is the apex predator in a system of freshwater rock pools, yet is the only taxon in the food chain capable of actively dispersing among pools. This system affords the opportunity to combine direct and indirect methods for studying dispersal and spatial

population dynamics in a trophically relevant species (Srivastava *et al.* 2004; Brendonck *et al.* 2008). Results from a combination of observational, experimental, and population-genetic studies indicate that *T. verticalis* disperses frequently among pools, albeit at a variable rate. At the same time, populations are absent from many suitable habitat patches and local populations exhibit high turnover rates. Local populations also show high levels of genetic diversity, yet there is differentiation among populations at far distances. These results indicate that high, yet variable, rates of dispersal and turnover may combine to generate complex metapopulation dynamics.

METHODS

Study System

The system of focus in this study is the metapopulation of *Trichocorixa verticalis* (Hempitera, Corixidae) inhabiting freshwater rock pools on Appledore Island, Isles of Shoals, Maine, USA (Figure 4.1). *T. verticalis* is a predatory aquatic insect native to saline and freshwater habitats across North America (Tones and Hammer 1975; Tones 1977; Kelts 1979; Wurtsbaugh and Berry 1990; Simonis 2012b) and has also invaded wetlands in Iberia, Africa, and New Caledonia (Jansson 1982, Sala and Boix 2005, Van de Meutter *et al.* 2010). Similar to other corixids, *T. verticalis* undergoes incomplete metamorphosis and has a life history consisting of eggs, five flightless juvenile stages, and a flight-capable adult stage (Kelts 1979; Simonis 2012b). *T. verticalis* overwinters as eggs and typically completes at least two generations each summer (J. L. Simonis, *unpub. data*; Tones 1977; Kelts 1979).

On Appledore, *T. verticalis* is commonly found inhabiting the *ca*. 1,500 fishless freshwater pools that exist above the high-tide line (Simonis 2012b). The pools contain a relatively simple food web, where *T. verticalis* is the apex predator, voraciously preying upon

Figure 4.1. A: The Isles of Shoals Archipelago, in relation to coast of New Hampshire and Maine, USA. Portsmouth, NH, is depicted by the black arrow, Appledore Island by the large black star and White Island (location of the weather data) by the small white star. B: Locations of clusters of pools sampled on Appledore for genetic analyses. C: An area of rock pools (shaded and numbered) on the eastern side of Appledore near pool 350 (as marked in b). Note not all pools present in (C) are numbered and shaded. All photos courtesy of J. Morin.

A
B
200s
350
400s
30s
1s
795
560s
200 m
C
20 m

the cladoceran *Moina macrocopa*, the dominant grazer zooplankter. A single adult *T. verticalis* can consume over 50 *M. macrocopa* per day (Simonis 2012b), a rate high enough to reduce the density of *M. macrocopa* and indirectly increase phytoplankton biomass via a trophic cascade (J. L. Simonis, *in prep*). Given their strong influence on within-pool trophic dynamics, dispersal by *T. verticalis* constitutes an important process subsidy (*sensu* Flecker *et al.* 2010) to local food webs that could have trophic consequences at multiple spatial scales (Loreau *et al.* 2003; McCann *et al.* 2005; Simonis 2012b).

Previous research on this metapopulation indicates that adult *T. verticalis* are indeed highly dispersive fliers (average *per capita* emigration rate: 0.207 d^{-1}), but also that their dispersal rate is significantly affected by environmental conditions (Simonis 2012b). In that experiment, the *per capita* rate of *T. verticalis* emigration was negatively related to local prey density (as expected for an optimal forager; Charnov 1976) and positively related to temperature. These results, combined with the fact that only the adult life-history stage of *T. verticalis* can fly, suggest that although this species is highly mobile, its dispersal rate is not likely to be constant across space or time, a situation which may generate complex spatial population dynamics (Harrison 1991; Hill *et al.* 1996; Hanksi 1999).

Field Measures of Immigration

The first goal of this study was to quantify the rate and spatial extent of flight-based dispersal among pools by *T. verticalis*. To do this, I conducted a field immigration experiment using 40 L Rubbermaid Roughneck™ totes (hereafter "mesocosms") as faux rock pools. In May 2010, I distributed 20 mesocosms on the exposed rock among the pools around Appledore, such that each was within 20 m of the closest pool (average distance: 3.39 m, range: 0.1 m – 19.5 m), and within 55 m of the closest population of *T. verticalis* (average distance: 9.45 m, range: 0.1 m – 53.3 m). I filled the mesocosms with 30 L of filtered well

water, added two small dowels for perches for immigrants, and introduced an inoculum of zooplankton and phytoplankton. The plankton inoculum was made by combining live plankton samples from six pools around Appledore, and was devoid of any *T. verticalis*. I then covered each mesocosm with 3.5 cm × 3.5 cm hex chicken wire to prevent water birds (*i.e.*, *Larus* gulls) from entering, while still allowing dispersal of *T. verticalis* (Simonis 2012b). I checked the mesocosms every 2 – 4 days from May 21 until August 31 (29 total sample dates), removing and enumerating all immigrants. On each sample date, I also noted if the immigrants had laid eggs, and removed them to prevent population establishment. Throughout the summer I maintained the overall water level in each mesocosm by adding filtered well water as necessary.

I also collected data on metapopulation, environmental, and temporal factors that could influence immigration rates for use in a predictive model. Every week, I measured the straight-line distance to the closest population for each mesocosm and estimated the abundance of potential immigrants in the metapopulation by determining the number of *T. verticalis* adults (*i.e.*, the potential dispersers) in five representative rock pools. At each of the five pools, I sampled 2 L of water haphazardly from throughout the water column using a large-bulb pipette (turkey baster; *ca*. 1.5 cm diameter opening), filtered that volume through a 30 µm mesh, counted the number of adult *T. verticalis* present, then immediately returned all sampled plankton to the pool. Because *T. verticalis* dispersal is positively related to temperature (Kelts 1979; Simonis 2012b) and may be related to other weather phenomena, I also obtained local weather data from NOAA Station IOSN3, located on nearby White Island (Figure 4.1A; *ca.* 2 km SSW of Appledore). For each sample date, I determined the minimum, maximum, mean, and coefficient of variation (cv) for temperature, wind, pressure, and dew point during the interval since the previous sampling date. The immigration data showed a striking periodic trend where peaks in immigration appeared to align with the new moon (see *Results*), and so I also determined the cosine of the moon phase (describes the

intensity of moonlight) for each sample date.

I modeled immigration using a generalized linear mixed model, where the response variable was the number of immigrants (Poisson-distributed) into each mesocosm on each sample date, weighted by the number of days since the last sample to account for the irregular sampling intervals. I blocked the data by including individual mesocosm as a random variable. To simplify the model, I first determined which, if any, summary statistic for each of the four weather variables best predicted immigration in a single-term model. No summary of either atmospheric pressure or dew point significantly predicted immigration, and so they were not included in the model. The best predictor for temperature was the interval maximum and for wind was the interval cv. I also included calendar date as a predictor to account for any seasonal trends not attributable to other terms. Thus, the full model included distance to the closest population (on a natural log scale), number of adults in the focal pools, maximum temperature, cv of wind, cosine of moon phase (intensity of moonlight, barring cloud cover), and Julian date as fixed predictors, mesocosm as a random effect, and the weighting term, with no interactions. Interactions were not necessarily of interest and so were left out of the model to facilitate fitting. I fit the model using the glmer function in the lme4 package in R (Bates *et al.* 2011; R Development Core Team 2012).

Metapopulation Demography

I used data from a three-year field survey of the Appledore metapopulation to elucidate the effects of *T. verticalis* dispersal and variation in local population size on their spatial dynamics. In particular, I was interested in quantifying the spatial and temporal patterns in the fraction of pools occupied by *T. verticalis* and the frequencies of extinctions and colonizations. In August of 2008 and June and August of 2009 and 2010, I visited 107 representative pools spread around the periphery of Appledore and determined whether there

was a local population of *T. verticalis* present using a combination of water-column and direct observational sampling. Water-column sampling occurred as described for the survey of the pools in the dispersal study, but I did not enumerate individuals. Because of the possibility of not capturing *T. verticalis* if they were at low densities using this method (false absence), I also visually assessed the presence of *T. verticalis* in each pool by walking around its entire perimeter, gently tapping a meter stick on the benthos. Changes in light intensity (due to my shading the pool) and vibrations in the water cause non-moving *T. verticalis* to begin to swim, allowing me to determine if individuals were present. Additionally, I estimated the volume of each pool in 2009 and 2010 (assuming basins were shaped as inverted cones, following Pajunen and Pajunen 2007) and used a logistic regression to determine if occupancy was predicted by average pool volume (on a $\log_{10}(x + 0.01)$ scale). I determined the spatial location of each pool using a handheld GPS instrument (Garmin GPSmap 62s) and checked the coordinates of each pool against high resolution aerial imagery (Google Earth). The farthest distance between any two pools in this data set was 868.5 m (*ca*. 90% of the maximum length of Appledore; Figure 4.1A).

I determined the spatial autocorrelation in patterns of *T. verticalis* occupancy among pools to characterize the effect of dispersal on population presence and absence. I quantified spatial autocorrelation among (volume-corrected) occupancy patterns using a multivariate extension of Moran's *I* statistic (Moran 1950; Bertorelle and Barbujani 1995), where each pool had five data, one for each time point. To quantify the overall pattern of spatial autocorrelation in occupancy, I weighted pairs of pools by the natural log of the distance between them, standardized such that the pair of pools the maximum distance apart had a weight of 0 and pools immediately adjacent to each other had a weight approaching 1.0 (weight = 1 - log(distance + 0.1)/log(868.5 + 0.1), where 868.5 m was the maximum distance between pools in this data set) and calculated Moran's *I*. I determined the statistical significance of this *I* value with 10,000 Monte Carlo permutations, where I randomized the

occupancy patterns among pools, keeping the five data together (*i.e.*, not randomizing separately within sample points). To determine the relevant spatial scale of the autocorrelation, I then used a distance-class approach, where I included all pairs of pools closer than the distance class (weight = 1) and excluded any more distant pairs (weight = 0), calculated *I*, and determined the significance of I via permutation. For this analysis, I used distance classes ranging from 1 m to 850 m (1, 2, 5, 10 and 20 m, then 50 to 850 m in 50 m increments). These analyses were conducted in R (R Core Development Team 2012) using custom-written scripts.

I used Hanski's (1999) Incidence Function Model (IFM) to estimate colonization and extinction rates of pools in this survey. In particular, I fit the observed incidence data using a Markov Chain Monte Carlo (MCMC) method of implicit statistical inference, as described by Moilanen (1999), which allowed me to fit all five time points together (and included the irregular interval between sample dates). A key component of this model is the measure of each pool's connectivity, *S*, which determines (once rescaled) how likely that pool is to be colonized:

$$S_i = \sum \left(\frac{1}{6} p_j V_j^{\beta} e^{-\alpha d_{ij}} \right) \quad \text{for } j \neq i \qquad (4.1)$$

The total connectivity of pool *i* is described as the sum of its connectivities to all other pools ($j \neq i$), which is a function of the distance between the pools (d_{ij}, influenced by the distance decay parameter α), the observed occurrences of a population in the other pool (p_j), and the expected number of dispersers in that pool, if a population exists ($1/6V_j^{\beta}$). Total population size scales with habitat volume *V* (on a $\log_{10}$ scale) via the exponential parameter β and is then converted to the number of flight-capable adults by the 1/6 multiplier (the average fraction of the population that is adults; J. L. Simonis *unpub. data*). These connectivity values are then converted to pool-specific colonization rates (C_i) by the scaling parameter *y*:

$$C_i = \frac{{S_i}^2}{{S_i}^2+y}. \qquad (4.2)$$

Pool-specific extinction rates are determined by the volume of the pool, V_i and two parameters x and z:

$$E_i = \frac{z}{{V_i}^x} \qquad \text{for } V_i \geq V_0 = z^{1/x} \qquad (4.3)$$

where V_0 is the volume below which the extinction rate equals 1.0. And finally, the predicted incidence (*i.e.*, probability of occurrence in that pool, given the parameters) is calculated:

$$J_i = \frac{C_i}{C_i+E_i-C_iE_i}. \qquad (4.4)$$

Thus, the IFM can be applied to observed metapopulation incidence data with five parameters (α, β, x, y, z) that describe two processes: colonization and extinction. Following Hanski (1999), I estimated α and β independently of the incidence data and included those parameter values in the IFM, which I fit with observed incidence data to estimate x, y, and z and calculate C and E.

I estimated α (the specific effect of distance on dispersal) from the immigration study by holding all other parameters at their median values to recalculate the intercept of the Poisson regression model. I used data from an independent survey of 136 pools in June 2008 to quantify the relationship between habitat volume and local population size (described by β). For this survey, I followed the aforementioned methods to measure pool volume and population density, converted density to population size (via multiplication), and estimated the relationship between population size and habitat volume (on a $\log_{10}(x + 0.01)$ scale) by fitting the data with a non-linear least squares regression model using the nls function in R (R Development Core Team 2012). I then fit the MCMC version of the IFM model to the

observed incidence data with these empirically derived estimates for α and β. The maximum likelihood estimates for the remaining parameters (which describe how colonization scales with connectivity and how extinction scales with local population size; Hanksi 1999) were determined using a custom-written script (following Moilanen 1999), which was optimized via the mle2 function in the bbmle package in R (Bolker and R Core Development Team 2012). I used the resulting model fit to calculate extinction and colonization rates for each pool, and to estimate the pool volume below which the extinction rate is 1.0 (V_0).

Mitochondrial DNA Population Genetic Structure

I used a population-genetic approach to elucidate the effects of *T. verticalis* dispersal and turnover on the genetic connectivity among pools and genetic diversity within pools. In May 2011, I collected juvenile *T. verticalis* from 20 rock pools distributed in seven clusters (1-5 pools sampled per cluster) spread around the periphery of Appledore (Table 4.1, Figure 4.1B). All sampled *T. verticalis* were juveniles to assure that individuals had not recently flown in from another location. I froze all samples at -20° C (while on Appledore) and then -80° C (in Ithaca, NY) until they were processed. I determined the location of each pool using the same methods as for the demographic survey. For each pool, I measured the density of *T. verticalis* and the volume of the pool (both as previously described), the number of other populations within a 5 m radius, and the distance to the closest *T. verticalis* population.

I extracted and isolated total genomic DNA from 8 – 12 individuals from each pool (220 in total) using DNeasy^{TM} kits (QIAGEN). For each individual, I then amplified and sequenced a 1347-bp fragment of the COI gene and the adjacent tRNA-leucine region of mitochondrial DNA (mtDNA) using the primers CI-J-1718 and TL2-N-3014 (Simon *et al.* 1995) in a polymerase chain reaction (PCR). This fragment spanned the final 1320 bp of the 3' end of the Cytochrome Oxidase I (COI) gene and the first 27 bp of the 5' end of the

Table 4.1. Clusters, locations (UTM 19), demographic, and habitat variables of the 20 populations of *T. verticalis* sampled in the genetic survey.

Pool	Cluster	Easting (0368...)	Northing (476….)	Volume (log_{10} L)	Density (ind. L^{-1})	Pop. Size	Closest Pop. (m)
1	1s	155	0658	2.55	3	1059	1.31
2	1s	154	0661	2.67	1	465	1.31
30L	30s	180	1068	1.18	12	180	0.1
31	30s	180	1066	2.38	9	2165	0.5
32	30s	181	1064	2.33	17	3637	0.8
33	30s	187	1068	3.42	18	47538	0.5
34	30s	186	1071	1.09	26	319	3.2
200	200s	505	1166	4.37	7	162771	0.49
201	200s	509	1162	3.56	1.3	4894	1.7
203	200s	512	1175	2.31	56	11555	0.97
350	350	503	0940	3.63	39	165856	4.95
401	400s	702	0795	2.51	0.7	217	1.68
403	400s	703	0791	2.48	3	912	1.68
410	400s	696	0779	2.77	20	11736	0.8
411	400s	697	0777	2.49	8	2458	0.8
566	560s	515	0436	2.29	44	8608	0.95
567	560s	514	0439	2.46	1	290	0.95
569	560s	509	0437	1.77	15	879	0.18
570	560s	504	0434	2.70	28	13958	0.18
795	795	125	0610	2.64	22	9527	18.25

Note. For cluster locations see Figure 4.1B.

adjacent tRNA-leucine. Each PCR was 10 µL total reaction volume, containing 1 µL DNA, 6.9 µL ddH_2O, 1 µL 10X buffer, 0.4 µL 50 mM $MgCl_2$, 0.2 µL 10 mM dNTPs, 0.1 µL *Taq* polymerase, and 0.2 µL of each 10 µM primer, and covered with a drop of mineral oil. The PCR sequence consisted of 35 cycles of 94° C for 50 s, 50° C for 45 s, and 72° C for 2 min and was conducted on a PXE 0.2 Thermal Cycler. I purified the PCR products by adding 0.1 µL Antarctic Phosphotase (New England Biolabs), 0.1 µL Exonuclease I (New England Biolabs), 0.2 µL 10X buffer, and 1.6 µL ddH_2O directly to the PCR plate, and incubating at 37° C for 45 min, then 90° C for 15 min. As most PCR products were robust, I added an additional 10 µL ddH_2O to each well post-incubation.

I sequenced each PCR product in both the forward and reverse directions by adding 2.1 µL ddH_2O, 0.75 µL 5X buffer, 0.5 µL Big Dye v. 3.1 (Applied Biosystems), and 0.15 µL of the respective primer (forward or reverse) to 1.5 µL of the diluted PCR product. The sequencing reaction consisted of 35 cycles of 94° C for 50 s, 50° C for 20 s, and 60° C for 4 min and was conducted on a PXE 0.2 Thermal Cycler. I purified the sequencing reactions products using Agencourt CleanSEQ beads and sent the resulting pure, labeled mtDNA to the Cornell University Life Sciences Core Laboratory Center, where it was sequenced on an ABI 3730xl capillary DNA sequencer. I aligned the forward and reverse sequences for each individual and created a consensus sequence using CodonCode Aligner (version 4.0.4; CodonCode Corporation), and trimmed the sequence down to the 1208-bp region for which all individuals had callable bases. On this mtDNA region, 93 bases were variable, with 28 being singletons and 65 being parsimony-informative.

I used DnaSP (v5, Librado and Rozas 2009) and Arlequin (v3.5.1.3, Excoffier and Lischer 2010) to summarize the genetic data within and among populations. Using DnaSP, I calculated haplotype abundance and diversity, nucleotide diversity (Jukes and Cantor 1969), and the average number of nucleotide differences between pairs of individuals; all analyses were conducted for each population separately and for the whole dataset. I used simple linear

regressions to determine if within-pool haplotype diversity was significantly predicted by local population size, pool volume, the distance to the closest other *T. verticalis* population, or the density of *T. verticalis* populations within 5 m. With an AMOVA in Arlequin, I then assessed the spatial hierarchical structure of genetic variation with three grouping levels: individuals within populations, populations within clusters, and among clusters. The significance of this variation structure was tested using 10,000 permutations.

To more directly examine the influence of dispersal on the population-genetic data, I then employed a combination of methods to analyze the explicit spatial structure of the genetic data. First, I determined the spatial autocorrelation of the genetic data using a similar approach to that which I used for the population occurrence data, but with the focal data being the sequence of each individual (Bertorelle and Barbujani 1995) and assuming that individuals within the same pool were separated by a geographic distance of 0.0 m. I reduced the data to just the 93 polymorphic sites in the sequence, but because some sites had more than two nucleotide states, I turned each base into a composite variable comprising four binary data (Bertorelle and Barbujani 1995), resulting in each individual having a data string of 372 bits. I quantified the spatial autocorrelation across the whole dataset using standardized distances (the maximum distance between pools in this data set was 741 m) on a natural log scale, and then conducted a distance-class analysis using classes ranging from 0 m to 700 m (0 2, 5, 10, and 20 m, then 50 to 700 m in 50 m increments). I also used classic measures of isolation by distance (Wright 1943) by calculating the between-population F_{ST} for each pair of pools (Tamura and Nei 1993) in Arlequin, then regressing the pairwise population genetic distances [F_{ST} / (1-F_{ST})] against the natural logarithm of the straight-line Euclidian distances between the pools (Rousset 1997). For this analysis, I used a ranged major axis regression, implemented via the lmodel2 package in R (Legendre 2011). Finally, I determined the spatial scale at which populations were statistically significantly differentiated by calculating the *P*-value of the pairwise F_{ST}'s using randomization (10,000 permutations) in

Arlequin, correcting the *P* -values using the False Discovery Rate (Benjamini and Hochberg 1995), and plotting the corrected *P* -values against geographic distance between populations.

RESULTS

Immigration Rates

In total, 359 *T. verticalis* immigrated into the 20 mesocosms over the 101-day sample period, producing an average rate of 0.18 immigrants mesocosm^{-1} d^{-1}, or an expected waiting time of 5.6 days between immigration events. However, there was substantial temporal variation in *T. verticalis* immigration rates (min.: 0.00, max.: 1.08 immigrants mesocosm^{-1} day^{-1}; Figure 4.2A) as well as variation among mesocosms (min.: 0.00, max.: 0.62 immigrants mesocosm^{-1} day^{-1}). Only one mesocosm was not colonized at all during the entire study. Of the 19 mesocosms that were colonized, eggs were found in 15 mesocosms on at least one sample date, indicating that dispersing adults are capable of starting new populations upon arrival into a vacant pool. Typically fewer than five individuals arrived between sample dates (91.5% of the time when immigrants were found, it was fewer than five), yet there were two sample dates where more than 20 immigrants were observed in a mesocosm (different mesocosms in each instance). The variation in the number of immigrants received by mesocosms was significantly affected by all parameters in the model (Table 4.2).

Most relevant for this study, immigration rate decreased as a function of the distance from the closest population (slope: -0.728, on a natural log scale, $P < 0.0001$; Figure 4.2B; Table 4.2). Mesocosms that were within 10 m of the closest population experienced an average rate of 0.192 immigrants mesocosm^{-1} day^{-1}, and mesocosms further than this distance received 0.130 immigrants mesocosm^{-1} day^{-1}. However, dispersal did occur at far distances, as mesocosms that were 50 m or more from the closest population still experienced

Figure 4.2. A: Rate of immigration (immigrants mesocosm^{-1} day^{-1}) by *Trichocorixa* to mesocosms over the course of Summer 2010. Data are the mean (± SEM) immigration rates for the 20 mesocosms and the solid line is the prediction of the fitted Poisson regression based on immigration to individual mesocosms. Both the data and the predicted line were converted to rates (divided the number of immigrants by the days between samples) for graphical representation. Circles along the x-axis represent new and full moons (filled and open circles, respectively) and the dotted line marks the average immigration rate (0.18 immigrants mesocosm^{-1} day^{-1}). B: Rate of *Trichocorixa* immigration as a function of distance to the closest population (on a natural logarithmic scale). The asterisks indicate that both the data and predicted line have been corrected for the influence of the other variables influencing immigration (Table 4.2) by holding all other model parameters at their median values. Note that this correction can generate negative immigration rates. The data were converted to immigration rates by dividing by the number of days since the previous sample and the prediction line was converted to a rate by dividing by the mean number of days since the previous sample (3.48 days). The data were jittered slightly along both axes for presentation and note the break in the y-axis to display the extreme immigration rate of 6.44 immigrants mesocosm^{-1} day^{-1} (distance 0.4 m).

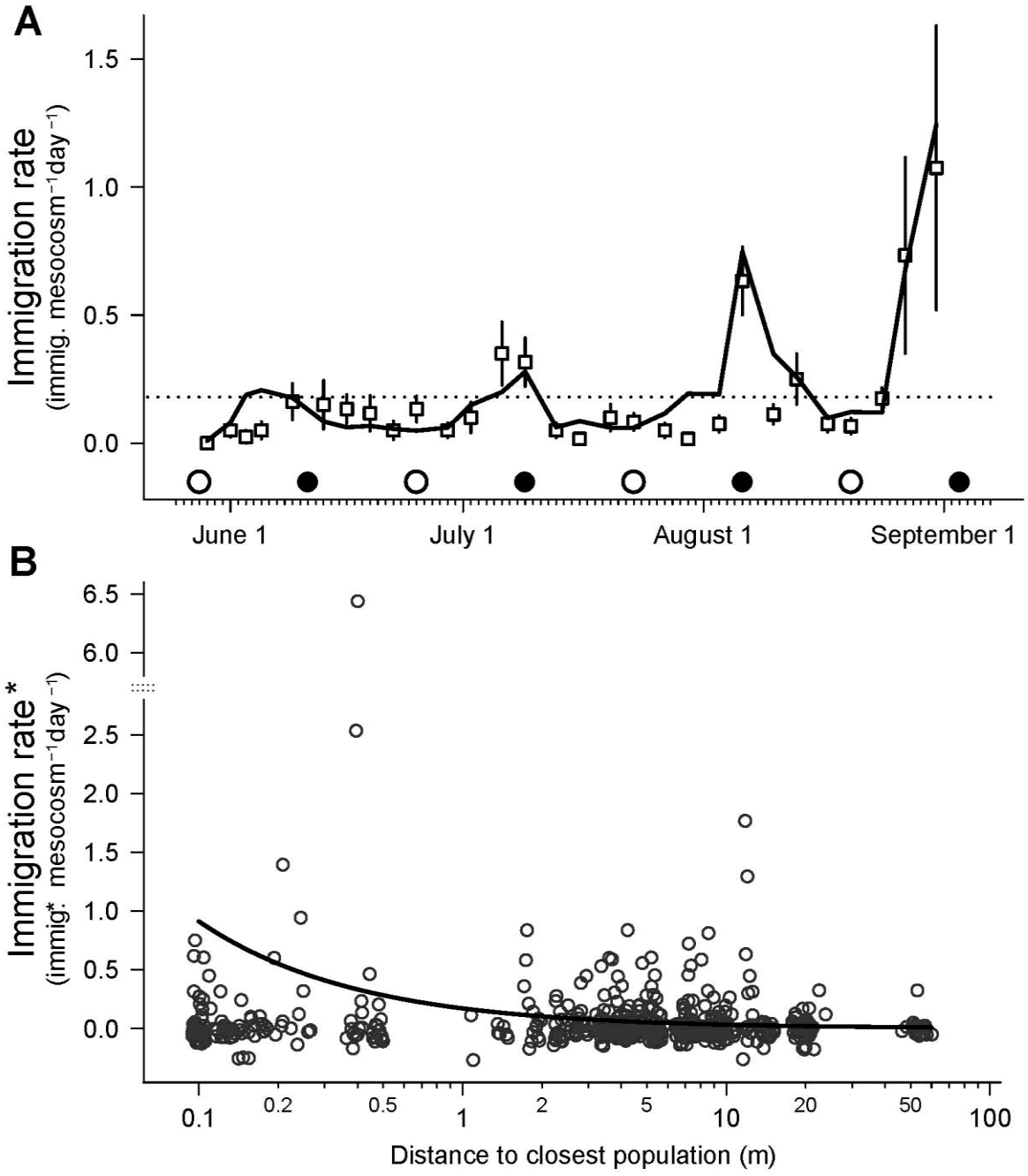
A
Immigration rate
(immig. mesocosm^{-1}day^{-1})
1.5
1.0
0.5
0.0
June 1
July 1
August 1
September 1
B
Immigration rate*
(immig.* mesocosm^{-1}day^{-1})
6.5
6.0
2.5
2.0
1.5
1.0
0.5
0.0
0.1
0.2
0.5
1
2
5
10
20
50
100
Distance to closest population (m)

moderately high immigration rates (0.144 immigrants mesocosm^{-1} day^{-1}). In addition to the effect of distance, the immigration rate was also higher when there were more adults in the focal populations (slope: 0.032, $P < 0.0001$), when maximum temperatures were higher (slope: 0.067, $P < 0.0001$), when winds were less variable (slope: -0.925, $P = 0.045$), when there was less moonlight (slope: 0.733 as a function of cosine of moon phase, $P < 0.0001$), and later in the summer (slope: 0.016, $P < 0.0001$). In combination, these six terms explained 38.7% of the deviance in the individual mesocosm-level data and were able to capture the seasonal patterns observed in immigration quite well (Figure 4.2A; normalized root mean squared error on daily immigration totals = 7.53%). Accounting for the other measured factors, this study estimated that the decrease in immigration as a function of distance was best described by $\alpha = -0.522 - 0.728 \times \log(d_{ij})$.

Metapopulation Demography

Despite the high rate of dispersal, *T. verticalis* populations were, on average, found in only 49.7% of pools at any one time (min.: 40.2%, max.: 64.5%; Table 4.3). Not surprisingly, larger pools were far more likely to have *T. verticalis* populations present than smaller pools (logistic regression; odds-ratio: 3.43, $P < 0.001$, 17% deviance explained; Figure 4.3A) and population size increased exponentially with habitat volume (on a $\log_{10}$ scale, estimated scaling parameter $\beta = 7.977$, $P < 0.0001$; Figure 4.3B). Further, *T. verticalis* occupancy patterns were significantly positively spatially autocorrelated overall ($I = 0.0411$, $P < 0.0001$), and this autocorrelation held to distances of 850 m (Figure 4.4A). The autocorrelation in occupancy was highest at 1 m and decreased almost monotonically as a function of distance (on a natural log scale) until converging to the expected value at 850 m, which included 99.8% of distances. Pool volume was not significantly spatially autocorrelated (using similar methods to the occupancy analysis; $I = 0.013$, $P > 0.1$), however, suggesting that the spatial

pattern in occupancy was not driven by a spatial pattern in habitat volume.

The best-fit IFM parameter estimates were $x = 2.468$, $y = e^{14.581}$, and $z = 0.671$ (all $P < 0.0001$). These values of x and z combine to predict that populations in pools with volumes less than ~ 7.1 L are doomed to extinction ($V_0 = 10^{0.851}$). Of the 12 pools in the survey (11.2%) that had volumes below this fitted V_0 value, only five had *T. verticalis* populations present on any sample date, but one such pool was occupied on four of five sample dates

Table 4.2. Parameters in the immigration statistical model

Parameter	Range	Med.	SD	Estimate	SE(est)	*P*
Intercept				-5.41	0.636	< 0.001
Distance from Closest Pop. (log scale, m)	-2.30 – 4.07	1.66	1.72	-0.728	0.043	< 0.001
Adults in Metapop.	0 – 16	34	8.35	0.032	0.007	< 0.001
Maximum Temperature (°C)	16.5 – 30.3	26.50	3.47	0.067	0.011	< 0.001
Wind (cv, raw: m s^{-1})	0.25 – 0.66	0.45	0.09	-0.925	0.461	0.045
Moon Phase (cosine)	-0.98 – 0.98	0	0.69	0.733	0.062	< 0.001
Julian Date	149 – 243	194	28.55	0.016	0.001	< 0.001

Notes. All parameters were fit using a weighted generalized linear mixed model, where there response data were counts of immigrants between intervals (weighted by interval length) and modeled using a Poisson distribution. Range, Med. (median), and SD (standard deviation) refer to the values of the predictor variable, where Estimate, SE(est) (*i.e.*, the standard error of the estimate) and *P* refer to the model fit. Wind data were measured in meters per second, but since the coefficient of variation was used as the summary statistic, the predictor was technically unit-less.

(Figure 4.3A). These 12 extinction-prone pools contributed strongly to the average rate of extinction rate being higher than the average colonization rate (average extinction rate with all 107 pools: 0.291 mo.$^{-1}$ compared to 0.201 mo.$^{-1}$ without the 12 extinction-prone pools; average colonization rate: 0.243 mo.$^{-1}$; Table 4.3). In contrast, twelve large pools were predicted to experience extinction rates below 0.05 mo.$^{-1}$, but no pool was safe from extinction (min. E_i: 0.019 mo.$^{-1}$). As a result of variation in spatial occupancy patterns, IFM-estimated colonization rates varied widely among pools (time averages, min.: 0.187 mo.$^{-1}$, max.: 0.820 mo.$^{-1}$) and across time (among-pool means, min.: 0.185 mo.$^{-1}$, max.: 0.297 mo.$^{-1}$).

Table 4.3. Observed occupancy and IFM-predicted colonization and extinction rates.

		2008	2009		2010	
		August	June	August	June	August
Occupancy		0.626	0.409	0.645	0.402	0.411
C_i (mo.$^{-1}$)	mean:	0.187	0.285	0.185	0.297	0.262
	min.:	0.021	0.043	0.017	0.047	0.042
	max.:	0.804	0.816	0.801	0.820	0.816
E_i (mo.$^{-1}$)	mean:	0.291	…	…	…	…
	min.:	0.019	…	…	…	…
	max.:	1.000	…	…	…	…

Notes. Occupancy is shown as the fraction of pools occupied (out of 107). Values for C_i and E_i were predicted for all pools using equations (4.2) and (4.3), respectively. E_i is constant for pools across time and so is only shown for the first date.

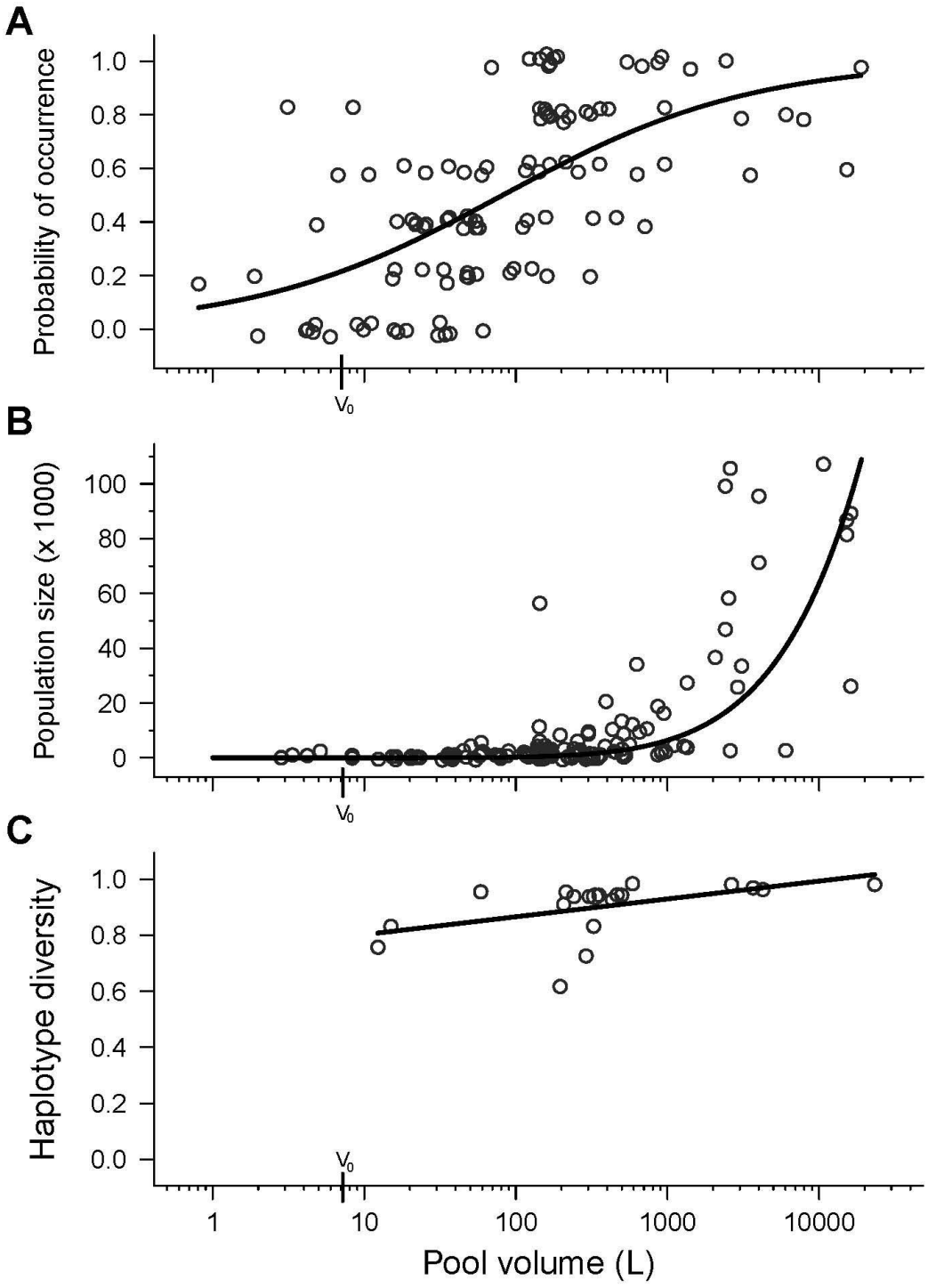

Figure 4.3. Effect of habitat volume (on a $\log_{10}$ scale) on the occurrence (A), size (B), and genetic diversity (C) of local *T. verticalis* populations. Data were jittered slightly in the y-direction for presentation in (A) and (B), but all regressions were fit with the raw data. The volume below which the IFM predicts an extinction probability of 1.0 ($V_0 = 10^{0.851}$ L) is noted along each x-axis.

Figure 4.4. Spatial autocorrelation in *T. verticalis* population occupancy (A) and mitochondrial DNA variation (B) as a function of distance between pools (on a natural log scale). In both panels, the open circles represent data that are significantly different from the expected value (dashed line) and filled circles represent data that are not significantly different from the expected value (determined by Monte Carlo permutations). The open square in (B) at distance 0 m corresponds to individuals within populations. The horizontal boxes just above the x-axis in (B) depict the distributions of between-pool distances within clusters (white box) and between clusters (grey box); the lines are means, the boxes are means ± one standard deviation, and the whiskers are 95% CI.

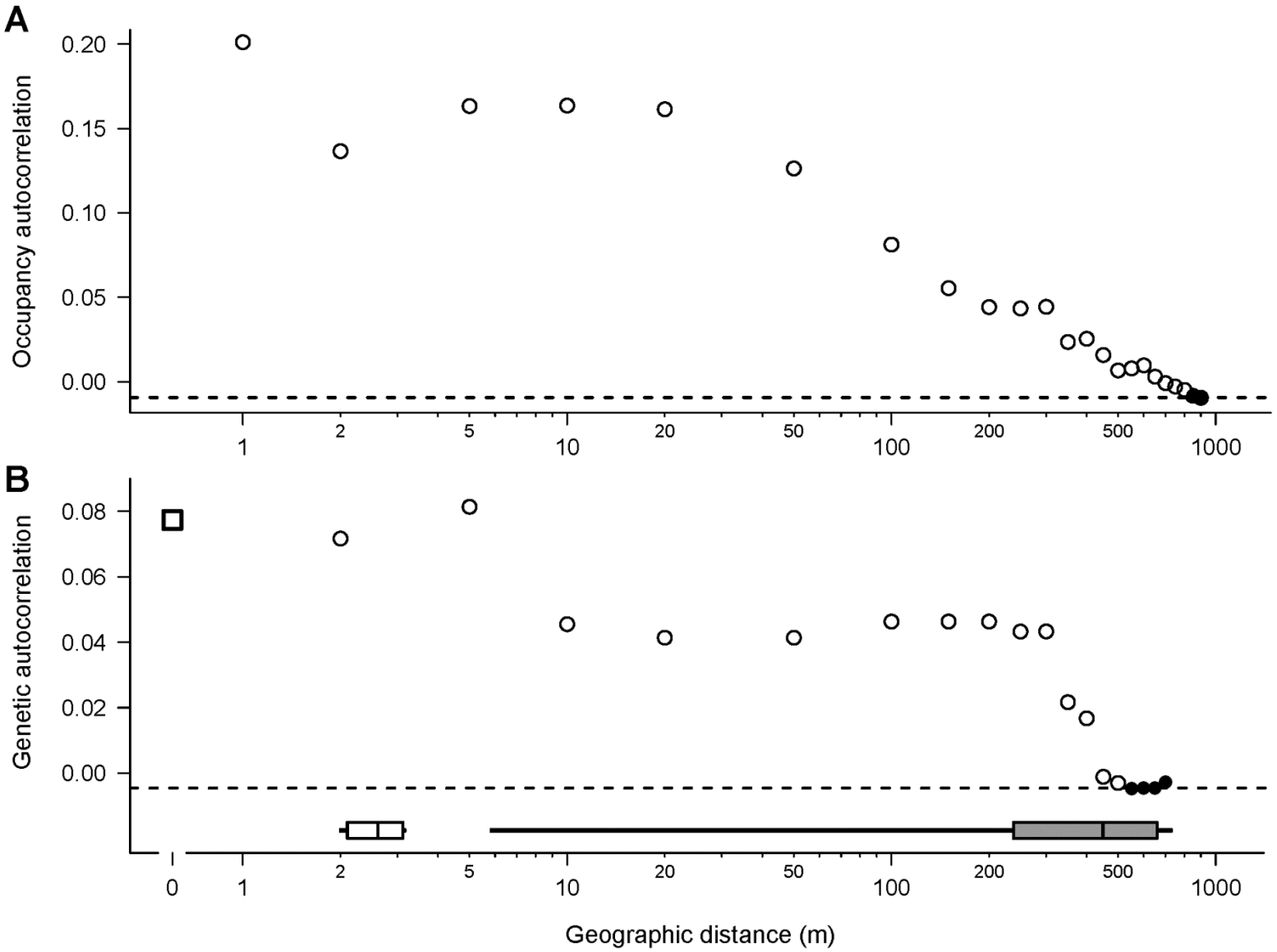
A
Occupancy autocorrelation
0.20
0.15
0.10
0.05
0.00
1
2
5
10
20
50
100
200
500
1000
B
Genetic autocorrelation
0.08
0.06
0.04
0.02
0.00
0
1
2
5
10
20
50
100
200
500
1000
Geographic distance (m)

Spatial Genetic Structure

Mitochondrial genetic diversity was very high in the Appledore *T. verticalis* metapopulation, both among and within populations (Table 4.4). Fifty-nine haplotypes were present among the 220 individuals sampled across all pools (region-wide haplotype diversity: 0.954 ± 0.005, mean ± SD) and each of the 20 populations sampled had at least five different haplotypes, generating within-population haplotype diversities between 0.618 and 0.985 (mean: 0.903, SD: 0.099). The high genetic diversity within populations is evident in the AMOVA results, as well (Table 4.5), as 90.07% of observed genetic diversity occurred among individuals within populations ($F = 0.093$, $P < 0.0001$). Minor, yet significant, genetic variation was nevertheless present among populations within clusters (3.98% variation, $F = 0.042$, $P = 0.019$) and among clusters (5.32% variation, $F = 0.053$, $P = 0.016$). In agreement with the population persistence data, within-population genetic diversity was significantly higher in larger pools (Figure 4.3C; slope = 0.06, $P = 0.027$, $R^2 = 0.202$). However, within-population diversity was not affected by local population size, the distance to the closest population, or the number of pools within 5 m (all $P > 0.1$).

Similar to the occupancy data, the genetic data were overall positively spatially autocorrelated ($I = 0.0344$, $P < 0.0001$) and this pattern held up to 450 m (Figure 4.4B). However, the genetic data showed a different pattern of decay in the spatial autocorrelation as a function of distance than did the occupancy data (Figure 4.4). As expected, the genetic data were most autocorrelated within pools (distance class 0 m). The autocorrelation remained high and was relatively unaffected by distance within clusters of pools (see white horizontal box in Figure 4.4B), then decreased markedly between 5 and 10 m and again remained

Table 4.4. Genetic data on the 20 populations of *T. verticalis* sampled in the genetic survey.

Pool	Cluster	N	Variable Sites	Haplotype Diversity	Nucleotide Diversity	Avg. Nucleotide Difference
1	1s	9	30	0.944 ± 0.070	0.0100 ± 0.001	12.06
2	1s	11	32	0.945 ± 0.054	0.0099 ± 0.001	12.00
30L	30s	12	34	0.833 ± 0.100	0.0076 ± 0.002	9.15
31	30s	12	32	0.939 ± 0.048	0.0076 ± 0.001	9.18
32	30s	12	39	0.955 ± 0.057	0.0085 ± 0.001	10.23
33	30s	11	33	0.982 ± 0.046	0.0088 ± 0.001	10.62
34	30s	12	27	0.758 ± 0.093	0.0071 ± 0.002	8.56
200	200s	11	38	0.982 ± 0.046	0.0100 ± 0.001	12.07
201	200s	12	33	0.970 ± 0.044	0.0090 ± 0.001	10.85
203	200s	10	28	0.911 ± 0.077	0.0088 ± 0.001	10.58
350	350	8	28	0.964 ± 0.077	0.0070 ± 0.002	8.43
401	400s	12	33	0.833 ± 0.100	0.0068 ± 0.002	8.26
403	400s	12	35	0.939 ± 0.058	0.0075 ± 0.001	9.06
410	400s	12	37	0.985 ± 0.040	0.0081 ± 0.001	9.74
411	400s	12	32	0.939 ± 0.058	0.0076 ± 0.001	9.18
566	560s	11	19	0.618 ± 0.164	0.0069 ± 0.001	8.36
567	560s	11	22	0.727 ± 0.144	0.0073 ± 0.001	8.80
569	560s	10	32	0.956 ± 0.059	0.0069 ± 0.001	8.30
570	560s	9	32	0.944 ± 0.070	0.0085 ± 0.002	10.20
795	795	11	34	0.927 ± 0.066	0.0100 ± 0.001	12.04

Notes. See Table 4.1. for location, demographic, and habitat variables. Diversity values are means ± SD. N = sample size.

relatively constant until decreasing rapidly at 300 m and converging to the expected value at 450 m. This positive genetic spatial autocorrelation over much of the range of distances between pools matches the weak, yet significant pattern of genetic isolation by geographic distance (RMA regression: slope = 0.0125, $P = 0.044$, $R^2 = 0.02$, Figure 4.5A) and the observation that populations were not significantly differentiated until they were at least 400 m apart (Figure 4.5B).

DISCUSSION

The combination of metapopulation demography and genetic data presented here indicate that *T. verticalis* exists in a mixed-structure metapopulation (*sensu* Harrison 1991) in the Appledore rock pools where high but variable dispersal rates and high turnover combine to cause complex spatial dynamics. Dispersal by *T. verticalis* occurs frequently enough that pools are, on average, expected to receive an immigrant every 5.6 days. Despite the high dispersal, however, *T. verticalis* is absent from approximately half of the available habitat

Table 4.5. Analysis of Molecular Variance for the *T. verticalis* Appledore metapopulation.

Source	d.f.	SS	V	%	*F*	*P*
Among clusters	6	96.00	0.293	5.32	0.053	0.016
Among populations within clusters	13	96.80	0.219	3.98	0.042	0.019
Within populations	200	997.94	4.990	90.07	0.093	< 0.0001
Total	219	1190.74	5.502			

Notes. V = variance component, % = percentage variation explained, *F* = relevant F-statistic, *P* = significance (based on 10,100 permutations).

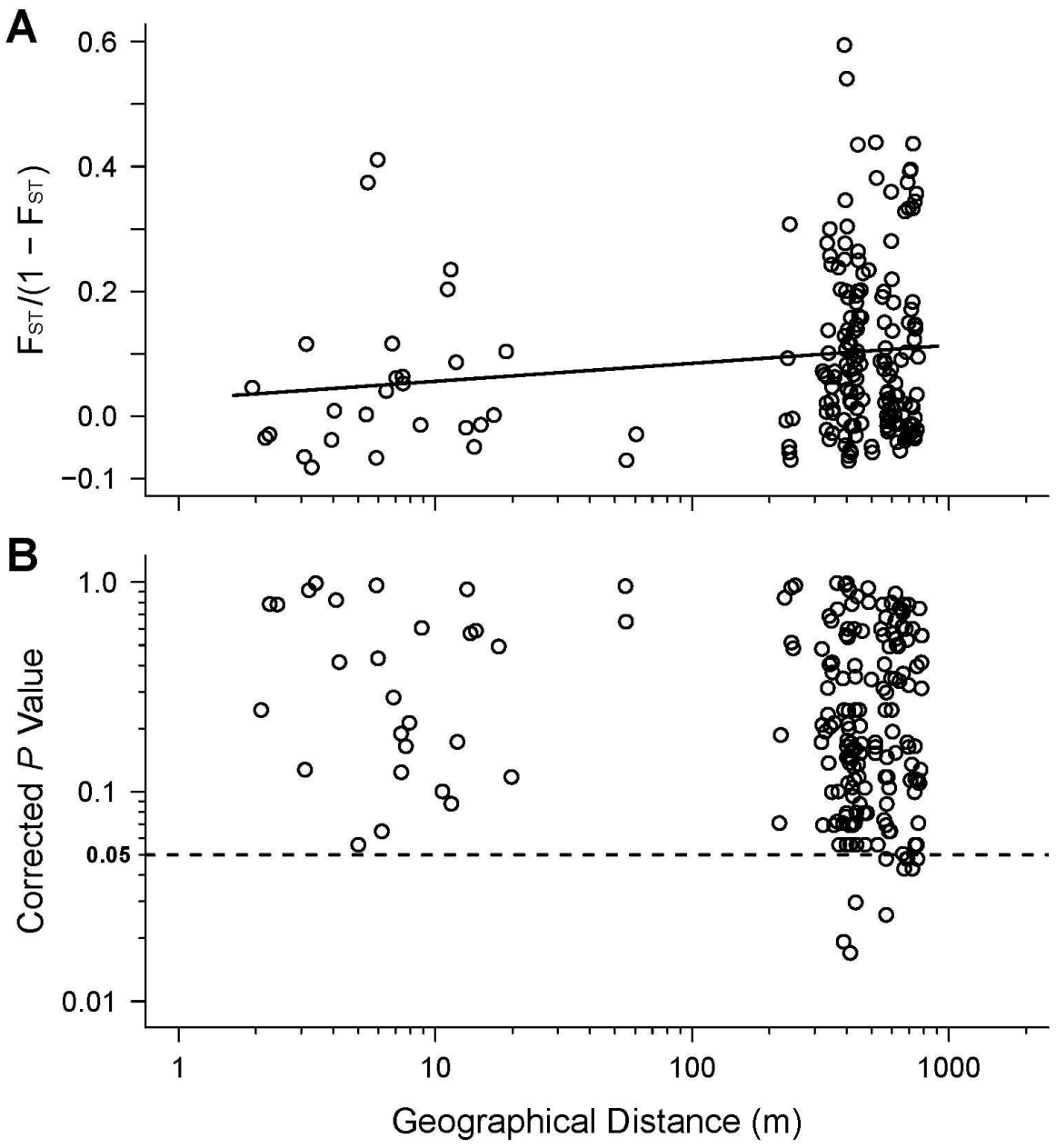

Figure 4.5. Isolation by (Euclidian) distance among *T. verticalis* populations on Appledore Island. A: Pairwise genetic distances as a function of geographical distance, with line from the fitted RMA regression. B: Statistical significance of pairwise F_{ST} comparisons as a function of geographical distance. *P* values were corrected using the FDR and are graphed using a natural logarithmic axis. For both (A) and (B), distance is plotted on a natural logarithmic axis and the data have been slightly jittered along the x-axis to show overlapping points.

patches, local populations experience frequent extinctions, and colonization and extinction rates are near-equal. As predicted for metapopulations with high dispersal (Slatkin 1985; Harrison 1991), genetic diversity within local *T. verticalis* populations is high and populations are only genetically differentiated at distances approaching the size of Appledore (Figure 4.5B). Significant genetic differentiation among populations is expected when turnover rates are high, as seen here, but the absolute level of among-population differentiation was generally small and only significant at far distances, which may be expected for species that also have high dispersal rates (Slatkin 1985; Harrison and Hasting 1996; Hanski 1999). These results indicate that, indeed, *T. verticalis* individuals are moving among pools and reproducing frequently upon immigration. This matches the observation of common egg laying by recent immigrants in the dispersal experiment. However, it is unknown if female immigrants are arriving with already fertilized eggs or are mating after they arrive.

Intriguingly, the distance to which *T. verticalis* populations exhibit spatial autocorrelation in occupancy is similar to the distance to which there was positive autocorrelation in genetic variation, although the two data sets show somewhat different patterns of decay in autocorrelation with distance (Figure 4.4). This result suggests that dispersal influences the occupancy and genetics of *T. verticalis* similarly at spatial scales approaching the size of the island, despite the difference in patterns of occupancy and genetics. Given the widespread dispersal, local extinctions are likely a major factor causing the absence of *T. verticalis* from such a high fraction of suitable pools. Indeed, local extinctions are frequent, but not uniformly likely across pools, as populations in large pools tend to be more persistent and have higher genetic diversity (Boorman and Levitt 1973; Pulliam 1988; Frankham 1997). However, the *T. verticalis* metapopulation does not exhibit true "source-sink" dynamics, where local populations are exclusively sources or sinks, given that populations in large pools are still extinction-prone and there is high genetic diversity in populations inhabiting small pools.

These findings parallel other motile animals in fragmented landscapes, where dispersal had complex consequences that could only be described by a combination of metapopulation models (Hill *et al.* 1996; Sutcliffe *et al.* 1997; Dunham and Rieman 1999). This is not to say that all motile animals in fragmented landscapes inhabit mixed-structure metapopulations, but that mixed-structure metapopulations and complex spatial population dynamics may be common among animals that are able to persist in fragmented landscapes where turnover rates are high (Harrison and Taylor 1997; Hanski 1999; Driscoll 2007). This could have large ramifications for how dispersal affects ecosystems at larger spatial scales, as motile animals are often also strong interactors that act as spatial process subsidies (*sensu* Flecker *et al.* 2010) and therefore have large impacts on other species or key nutrients (McCann *et al.* 2005; Van de Koppel *et al.* 2005; McIntyre *et al.* 2007). It is therefore important to elucidate what causes metapopulations to exhibit complex spatial dynamics, so that these dynamics can be better captured in models of spatial populations and food webs.

One likely contributor to the complex structure of the *T. verticalis* metapopulation is the large variation in observed dispersal (Figure 4.2A). Although the overall rate of immigration was 0.18 immigrants mesocosm^{-1} d^{-1}, the rates varied between 0 and 1.08 immigrants mesocosm^{-1} d^{-1}, and nearly 75% (427 of 580) of observations resulted in no *T. verticalis* being found (*i.e.*, a proximate immigration rate of 0 for that mesocosm on that day). This variation was driven by a combination of metapopulation structure (distance to closest population, population size and age structure), environmental conditions (temperature and wind), and temporal effects (seasonal trends, moon phase). Although not studied explicitly here, *T. verticalis* dispersal rates are also influenced by the local availability of prey, such that emigration rates increase as local prey density decreases (Simonis 2012b). Negative resource density-dependent dispersal is common among consumers, and may have profound effects on spatial food-web dynamics (Charnov 1976; Bowler and Benton 2005; Simonis 2012; Hanski 1999). Indeed, dispersal is influenced by a myriad of physiological, ecological, genetic,

environmental, and temporal factors (Clobert *et al.* 2001), resulting in observed dispersal rates that vary widely across space and time. Significant temporal variation in dispersal rates can cause populations to fluctuate between conditions where colonization is less frequent than local extinction (putting the entire metapopulation is at extinction risk), approximately equally frequent to local extinction (Levins metapopulation), and more frequent than local extinction (creating a homogenized population) (Hill *et al.* 1996). This was observed in the *T. verticalis* metapopulation, as the average pool-specific colonization rate fluctuated above and below the average pool-specific extinction rate throughout the metapopulation survey (Table 4.3).

In addition to deterministic factors causing variation in dispersal rates, dispersal is a demographic process, and thus is also subject to intrinsic variation caused by demographic stochasticity (May 1973; Chesson 1978; Simonis 2012a). Demographic stochasticity introduces random variation in the waiting time until the next demographic event occurs (*e.g.*, until the next immigrant arrives), such that even if the expected dispersal rate were fixed (not influenced by deterministic factors), there would be random variation in realized dispersal rates. For example, at the mean *T. verticalis* dispersal rate of 0.18 immigrants $pool^{-1}$ d^{-1}, 83.5% of pools would be expected to receive no immigrants on a given day and 16.4% of pools would be expected to receive no immigrants within a given 10-day window (Figure 4.6). This inherent, demographic variation in realized dispersal is expected to cause local populations to be less connected than deterministically predicted, even when dispersal rates are high enough to expect a well-mixed metapopulation with synchronized local population dynamics (Chesson 1978; Ovaskainen and Hanski 2004; Simonis 2012a).

In combination, deterministic factors and inherent demographic stochasticity will cause realized dispersal to deviate from the average expected value. If this deviation is small, a constant dispersal rate may be an appropriate approximation, as assumed by most metapopulation models. However, if realized dispersal varies widely from the average expected value, as was seen here for *T. verticalis*, the spatial dynamics of the population may

not be well captured by a model that assumes a fixed dispersal rate. The interactive effects of deterministic variation and demographic stochasticity in dispersal on spatial population dynamics are currently not well understood (Chesson 1978; Simonis 2012a), but my study suggests that variation in realized dispersal rate is a major factor contributing to complex spatial population dynamics. This variation could explain the absence of *T. verticalis* populations in approximately half the available pools on Appledore despite the high average rate of dispersal.

Metapopulation dynamics are often also influenced by variation among local

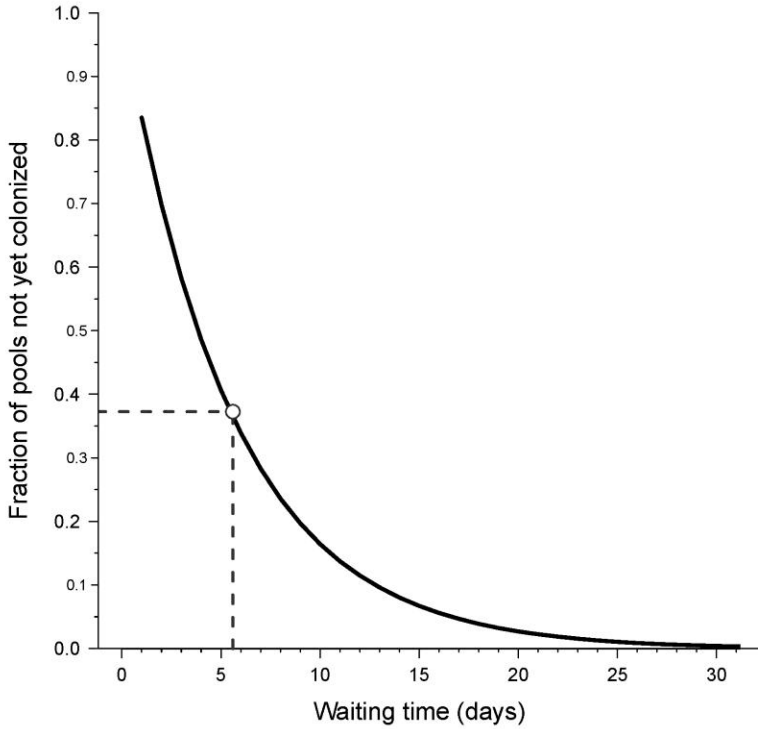

Figure 4.6. The fraction of pools that have not yet received a *Trichocorixa* immigrant as a function of time, given a fixed immigration rate of 0.18 individuals pool^{-1} day^{-1}. This relationship is described by an exponential distribution, which corresponds to waiting times between events of a Poisson process. The open circle and dashed lines represent the fraction of pools still uncolonized at time equals 5.6 days (*i.e.*, the average waiting time; = 0.18^{-1}), *ca*. 37%.

population sizes, which is regulated by habitat size and determines local extinction rates (Harrison 1991; Driscoll 2007). In many systems, all local populations are not equally likely to go extinct, due to variation in population size. As a result, some populations may act as "sources" that consistently provide immigrants to extinction-prone "sink" populations (Boorman and Levitt 1973; Pulliam 1988). This was the case in the *T. verticalis* system, as not all populations exhibited the same probability of extinction (Table 4.3), and larger pools were more likely to have persistent populations with higher genetic diversity (Figure 4.3). This effect of pool volume on extinction risk is likely driven by the relationship between population size and pool volume as well as the relationship between pool volume and the probability of a catastrophic drying event (Hulsmans *et al.* 2008). Indeed, smaller pools are much more likely to dry entirely during the middle of the summer on Appledore (J. L. Simonis, *pers. obs*.). However, pool volume was not a perfect predictor of persistence, as even the largest pools had a modest (10-20%) chance of a local extinction during the three years of my study, and the second largest pool in the survey had a population present on only three of the five sampling dates (Figure 4.3A). *T. verticalis* extinctions in larger pools could have occurred due to catastrophic events, such as inundation with salt water during intense storm events (J. L. Simonis, *pers. obs.*), or local ecological factors, such as low prey density driving mass emigration (Simonis 2012b).

Given the propensity for local extinctions in this system, it is likely that the 14% of *T. verticalis* populations that persisted through the (relatively short) duration of the metapopulation survey will go extinct sometime in the near future. However, these pools did generally have below-average extinction rates (average E_i: 0.076^{-1}) and temporally-averaged colonization rates that were about equal to the mean colonization rate for all pools across all sample dates (average C_i of persistent pools: 0.245 $mo.^{-1}$, average C_i for all pools: 0.243^{-1}), suggesting that they are comparatively buffered from extinction. This type of metapopulation, where all local populations are extinction-prone but to varying degrees and

local extinctions are caused by a variety of factors, is likely common (Harrison 1991; Harrison and Taylor 1997). However, the dynamical consequences of variable local extinction risk in metapopulations are not well understood (Harrison 1991; Hanski 1999). It is likely that the persistence and dynamics of many spatially fragmented populations, including the *T. verticalis* metapopulation, result from a complex interaction between regional dispersal and local extinction-promoting processes (Harrison 1991; Hill *et al.* 1996), both of which are variable in space and time.

Dispersal of strong interactor species, like the apex predator *T. verticalis* in the Appledore rock pools, not only influences their population, but also affects the spatial dynamics of the food webs and ecosystems of which they are constituents (Holyoak *et al.* 2005; McCann *et al.* 2005; Van de Koppel *et al.* 2005; Flecker *et al.* 2010). Indeed, consumption of zooplankton grazers by *T. verticalis* is strong enough to generate a top-down trophic cascade within pools (J. L. Simonis, *unpub. data*). Furthermore, *T. verticalis* is the only species in this food chain capable of actively dispersing among the pools. The prediction in such a situation, where the apex predator is also the most dispersive, is that dispersal by the predator will link local food webs at the regional scale, perhaps generating complex dynamics such as spatial apparent competition among prey populations (Van de Koppel *et al.* 2005; Simonis 2012a). This expectation is based on the notion that highly dispersive consumers will exhibit spatially synchronized population dynamics. As shown here with *T. verticalis*, however, highly dispersive apex predators can exhibit complex spatial population dynamics that are described best as mixed-structure metapopulations. For example, despite being dispersive enough to link local populations, *T. verticalis* is frequently absent from suitable pools, perhaps providing refuges for prey populations (Huffaker and Kennett 1956; Murdoch and Stewart-Oaten 1989; Simonis 2012b). As a result, predator dispersal may connect local food webs in a manner that is more complex than previously thought. Considering the prevalence of mixed-structure metapopulations among motile animals (Hill *et al.* 1996;

Sutcliffe *et al.* 1997; Dunham and Rieman 1999), the consequences of complex metapopulation dynamics for food webs and ecosystems deserve further study, both theoretically and empirically.

ACKNOWLEDGEMENTS

I am incredibly grateful to the staff of the Shoals Marine Lab (SML), especially director W. Bemis, for logistical assistance and to J. Morin (and multiple undergraduate interns) for preliminary research on the rock-pool system. This research would not have been possible without field assistance from S. Collins and K. Pellowe, laboratory guidance and support of S. Bogdanowicz (Cornell Evolutionary Genetics Core Facility) and E. Larson, nor the brainstorming and suggestions on data analysis of N. Hairston, B. Dalziel, and S. Ellner. A. Agrawal, S. Ellner, A. Flecker, and N. Hairston provided incredible feedback on an earlier version of this manuscript. This work was supported financially by SML, the Cornell University Biogeochemistry and Environmental Biocomplexity Program, the Andrew W. Mellon Foundation, the National Science Foundation (NSF, DEB-1110545), and an NSF Graduate Research Fellowship awarded to JLS.

REFERENCES

Bates, D., M. Maechler, and B. Bolker. 2011. lme4: Linear mixed-effects models using S4 classes. R package version 0.999375-42. http://CRAN.R-project.org/package=lme4.

Bertorelle, G. and G. Barbujani. 1995. Analysis of DNA diversity by spatial autocorrelation. Genetics 140:811-819.

Benjamini, Y. and Y. Hochberg. 1995. Controlling the false discovery rate: a practical and powerful approach to multiple testing. *Journal of the Royal Statistical Society Series*

B, 57:289-300.

Bohonak, A. 1999. Dispersal, gene flow, and population structure. The Quarterly Review of Biology 74:21-45.

Bolker, B. and R Development Core Team. 20120. bbmle: tools for general maximum likelihood estimation. R package version 1.0.4.1. http://CRAN.R-project.org/package=bbmle.

Boorman, S. A. and P. R. Levitt. 1973. Group selection on the boundary of a stable population. Theoretical Population Biology 4:85-128.

Bowler, D. E. and T. G. Benton. 2005. Causes and consequences of animal dispersal strategies: relating individual behavior to spatial dynamics. Biological Reviews 80:205–225.

Brendonck, L., M. Jocque, A. Hulsmans and B. Vanschoenwinkel. 2008. Pools 'on the rocks': freshwater rock pools as model system in ecological and evolutionary research. Limnetica 29:25-40.

Brown, J. H. and A. Kodric-Brown. 1977. Turnover rates in insular biogeography: effect of immigration on extinction. Ecology 58:445-449.

Charnov, E. L. 1976. Optimal foraging, the Marginal Value Theorem. Theoretical Population Biology 9:129–136.

Chesson, P. 1978. Predator–prey theory and variability. Annual Review of Ecology and Systematics 9:323–347.

Clobert, J., E. Danchin, A. A. Dhondt and J. D. Nichols. 2001. Dispersal. Oxford University Press, New York.

Driscoll, D. A. 2007. How to find a metapopulation. Canadian Journal of Zoology 85:1031-1048.

Dunham, J. B. and B. E. Rieman. 1999. Metapopulation structure of bull trout: influences of physical, biotic, and geometrical landscape characteristics. Ecological Applications

9:642-655.

Excoffier, L. and H. E. L. Lischer. 2010. Arlequin suite ver. 3.5: A new series of programs to perform population genetics analyses under Linux and Windows. Molecular Ecology Resources. 10:564-567.

Flecker, A. S. 1996. Ecosystem engineering by a dominant detritivore in a diverse tropical stream. Ecology 77:1845-1854.

Flecker, A. S., P. B. McIntyre, J. W. Moore, J. T. Anderson, B. W. Taylor and R. O. Hall, Jr. 2010. Migratory fishes as material and process subsidies in riverine ecosystems. American Fisheries Society Symposium 73:559-592.

Frankham, R. 1997. Do island populations have less genetic variation than mainland populations? Heredity 78:311-327.

Gaggiotti, O. E. 2004. Multilocus genotype methods for the study of metapopulation processes. Pages 133-150 *in* I. A. Hanski and O. E. Gaggiotti, eds. Ecology, Genetics, and Evolution of Metapopulations. Elsevier Press, New York.

Hanski, I. 1999. Metapopulation ecology. Oxford University Press, New York.

Harrison, S. 1991. Local extinction in a metapopulation context: an empirical evaluation. Biological Journal of the Linnaean Society 42:73-88.

Harrison, S. and A. Hastings. 1996. Genetic and evolutionary consequences of metapopulation structure. Trends in Ecology and Evolution 11:180-183.

Harrison, S. and A. D. Taylor. 1997. Empirical evidence for metapopulation dynamics. Pages 27-42 *in* I. A. Hanski and M. G. Gilpin, eds. Metapopulation Biology: Ecology, Genetics, and Evolution. Academic Press, New York.

Hill, J. K., C. D. Thomas and O. T. Lewis. Effects of habitat patch size and isolation on dispersal by *Hesperia comma* butterflies: implications for metapopulation structure. Journal of Animal Ecology 65:725-735.

Holyoak, M., M. A. Leibold and R. D. Holt. 2005. Metacommunities: spatial dynamics and

ecological communities. Chicago University Press, Chicago.

Huffaker, C. B. and C. E. Kennett. 1956. Experimental studies on predation. I. Predation and cyclamen mite populations on strawberries in California. Hilgardia 26:191-222.

Hulsmans, A., K. Moreau, L. De Meester, B. Riddoch, and L. Brendonck. 2007. Direct and indirect measures of dispersal in the fairy shrimp Branchipodopsis wolfi indicate a small-scale isolation-by-distance pattern. Limnology and Oceanography 52:676-684.

Hulsmans, A., B. Vanschoenwinkel, C. Pyke, B. Riddoch, and L. Brendonck. 2008. Quantifying the hydroregime of a temporary pool habitat: A modelling approach for ephemeral rock pools in SE Botswana. Ecosystems 11:89-100.

Jansen, V. A. A. 1999. Phase locking: another cause of synchronicity in predator–prey systems. Trends in Ecology and Evolution 14:278–279.

Jukes, T. and C. Cantor. 1969 Evolution of protein molecules. Pages 21-132 *in* H. N. Munro, ed. Mammalian Protein Metabolism. Academic Press, New York.

Kelts, L. J. 1979. Ecology of a tidal marsh corixid, *Trichocorixa verticalis* (Insecta, Hemiptera). Hydrobiologia 64:37-57.

Kneitel, J. M. and T. E. Miller. 2003. Dispersal rates affect species composition in metacommunities of *Sarracenia purpurea* inquilines. The American Naturalist 162:165-171.

Legendre, P. 2011. lmodel2: model II regression. R package version 1.7-0. http://CRAN.R-project.org/package=lmodel2.

Leibold, M. and T. E. Miller. 2004. From metapopulations to metacommunities. Pages 133-150 *in* I. A. Hanski and O. E. Gaggiotti, eds. Ecology, Genetics, and Evolution of Metapopulations. Elsevier Press, New York.

Levins, R. 1970. Extinction. Pages 77-107 *in* M. Gerstenhaber, ed. Some Mathematical Questions in Biology. Lectures on Mathematics in Life Sciences 2. American Mathematical Society, Providence RI.

Librado, P. and J. Rozas. 2009. DnaSP v5: A software for comprehensive analysis of DNA polymorphism data. Bioinformatics 25:1451-1452.

Loreau, M., N. Mouquet and R. D. Holt. 2003. Meta-ecosystems: a theoretical framework for a spatial ecosystem ecology. Ecology Letters 6:673–679.

MacArthur, R. H. and E. O. Wilson. 1967. The Theory of Island Biogeography. Princeton University Press.

May, R. M. 1973. Stability and complexity in model ecosystems. Princeton University Press, Princeton, NJ.

Mayr, E. 1963. Animal species and evolution. Harvard University Press.

McCann, K. S., J. B. Rasmussen and J. Umbanhowar. 2005. The dynamics of spatially coupled food webs. Ecology Letters 8:513-523.

McIntyre, P., L. E. Jones, A. S. Flecker and M. J. Vanni. 2007. Fish extinctions threaten nutrient cycling in tropical freshwaters. Proceedings of the National Academy of Sciences 104:4461-4466.

Moilanen, A. 1999. Patch occupancy models of metapopulation dynamics: efficient parameter estimation using implicit statistical inference. Ecology 80:1031-1043.

Moran, P. A. P. 1950. Notes on continuous stochastic phenomena. Biometrika 37:17-33.

Murdoch, W. W. and A. Stewart-Oaten. 1989. Aggregation by parasitoids and predators: effects on equilibrium and stability. The American Naturalist 134:288–310.

Ovaskainen, O. and I Hanski. 2004. From individual behavior to metapopulation dynamics: unifying the patchy population and classic metapopulation models. The American Naturalist 164:364-377.

Paine, R. T. 1974. Intertidal community structure: experimental studies on the relationship between a dominant competitor and its principal predator. Oecologia 15:93-120.

Pajunen, V. I. and I. Pajunen. 2007. Habitat characteristics contributing to local occupancy and habitat use in rock pool Daphnia metapopulations. Hydrobiologia 592:291–302.

Pulliam H. R. 1988. Sources, sinks, and population regulation. The American Naturalist 132:652-661.

R Core Development Team. 2012. R: A Language and Environment for Statistical Computing. R Foundation for Statistical Computing, Vienna, Austria. ISBN 3-900051-07-0, URL http://www.R-project.org/

Rousset, F. 1997. Genetic differentiation and estimation of gene flow from *F*-statistics under isolation by distance. Genetics 145:1219-1228.

Sala, J. and D. Boix. 2005. Presence of the Nearctic water boatman *Trichocorixa verticalis verticalis* (Fieber, 1851) (Heteroptera, Corixidae) in the Algarve region (S Portugal). Graellsia 61:31-36.

Simon, C., F. Frati, A. Beckenbach, B. Crespi, H. Liu, and P. Flook. 1994. Evolution, weighting, and phylogenetic utility of mitochondrial gene sequences and a compilation of conserved PCR primers. Annals Entomological Society of America 87:651-701.

Simonis, J. L. 2012a. Demographic stochasticity reduces the synchronizing effect of dispersal in predator-prey metapopulations. Ecology 93:1517-1524

Simonis, J. L. 2012b. Prey (*Moina macrocopa*) population density drives emigration rate of its predator (*Trichocorixa verticalis*) in a rock-pool metacommunity. Hydrobiologia.

Slatkin, M. 1985. Gene flow in natural populations. Annual Review of Ecology and Systematics 16:393-430.

Srivastava, D. S., J. Kolasa, J. Bengtsson, A. Gonzalez, S. P. Lawler, T. E. Miller, P. Munguia, T. Romanuk, D. C. Schneider and M. K. Trzcinski. 2004. Are natural microcosms useful model systems for ecology? Trends in Ecology and Evolution 19:379-384.

Sutcliffe, O. L., C. D. Thomas and D. Peggie. 1997. Area-dependent migration by ringlet butterflies generates a mixture of patchy population and metapopulation attributes. Oecologia 109:229-234.

Tamura, K. and M. Nei. 1993. Estimation of the number of nucleotide substitutions in the control region of mitochondrial DNA in humans and chimpanzees. Molecular Biology and Evolution 10:512-526.

Tones, P. I. and U. T. Hammer. 1975. Osmoregulation in *Trichocorixa verticalis interiores* Sailer (Hemiptera, Corixidae) – an inhabitant of Saskatchewan saline lakes, Canada. Canadian Journal of Zoology 53:1207-1212.

Tones, P. I. 1977. The life cycle of *Trichocorixa verticalis interiors* Sailer (Hempitera, Corixidae) with special reference to diapauses. Freshwater Biology 7:31-36.

Van de Koppel, J., R. D. Bardgett, J. Bengtsson, C. Rodriguez-Barrueco, M. Rietkerk, M. J. Wassen, and V. Wolters. 2005. The effects of spatial scale on trophic interactions. Ecosystems 8:801-807.

Van de Meutter, F., H. Trekels and A. J. Green. 2010 The impact of the North American waterbug *Trichocorixa verticalis* (Fieber) on aquatic macroinvertebrate communities in southern Europe. Fundamental and Applied Limnology 177:283-292.

Wade, M. J. and D. E. McCauley 1988. Extinction and colonization: their effects on the genetic differentiation of local populations. Evolution 42:995-1005.

Whitlock, M. C. and D. E. McCauley. 1990. Some population genetic consequences of colony formation and extinction: Genetic correlations within founding groups. Evolution 44:1717-1724.

Wright, S. 1943. Isolation by distance. Genetics 28:114-138.

Wurtsbaugh, W. A. and T. S. Berry. 1990. Cascading effects of decreased salinity on the plankton, chemistry, and physics of the Great Salt Lake (Utah). Canadian Journal of Fisheries and Aquatic Science 47:100-109.

CHAPTER 5

PREY (*MOINA MACROCOPA*) POPULATION DENSITY DRIVES EMIGRATION RATE OF ITS PREDATOR (*TRICHOCORIXA VERTICALIS*) IN A ROCK-POOL METACOMMUNITY[1]

[1] Published as: Joseph L. Simonis. 2012. Prey (*Moina macrocopa*) population density drives emigration rate of its predator (*Trichocorixa verticalis*) in a rock-pool metacommunity. *Hydrobiologia*. DOI 10.1007/s10750-012-1268-9.

ABSTRACT

Dispersal connects spatially separated local food webs at a larger, metacommunity scale, and as a result, dispersal may both influence and be influenced by local food-web dynamics. Here, I focused on a rock-pool metacommunity and used a combination of observational, experimental, and theoretical approaches to explore the role of local prey (*Moina macrocopa*) density on the rate of emigration by their predator (*Trichocorixa verticalis*) and in turn, the effect of predator emigration on the *per capita* predation rate experienced by local prey populations. A lab feeding experiment quantified predation rates, demonstrating that indeed adult *T. verticalis* are voracious predators of *M. macrocopa*. *M. macrocopa* densities vary over five orders of magnitude across both space and time in rock pools, and a mesocosm experiment showed that this variation significantly influences *T. verticalis* emigration: predators emigrated more rapidly when prey were in lower densities. Finally, computer simulations demonstrated that this pattern of dispersal by *T. verticalis* has the potential to relieve local *M. macrocopa* populations from predation when the prey are at low densities, thereby reducing the likelihood that local *M. macrocopa* populations will be driven extinct by predation from *T. verticalis*.

INTRODUCTION

Dispersal, the movement of organisms from one area to another, is a fundamental biological process that has potential ecological consequences for individuals, populations, food webs, and ecosystems (Ives *et al.* 1993; Hanski 1999; Clobert *et al.* 2001; Holyoak *et al.* 2005). Dispersing individuals connect otherwise separated local populations at larger spatial scales in what is known as a metapopulation (Hanski 1999). However, local populations of potentially dispersing organisms are also embedded in food webs and engage in local trophic

interactions with predators, competitors, and resources. Dispersal therefore also links food webs across space in a metacommunity and has the potential to influence both local and regional food-web dynamics (Holyoak *et al.* 2005; McCann *et al.* 2005).

Simultaneously, aspects of the local food web can drive dispersal, setting up a feedback between local (trophic) and regional (dispersal) processes (French and Travis 2001; Hauzy *et al.* 2010). At the very least, local population sizes, and thus the number of possible dispersers, are often dictated by local trophic interactions (Morin 1999). Furthermore, many factors that influence dispersal are directly related to local food-web interactions, such as predator avoidance and resource acquisition (Charnov 1976; Clobert *et al.* 2001; Bowler and Benton 2005). As a result, dispersal may both influence and be influenced by local food-web dynamics (Hauzy *et al.* 2010).

For example, the dispersal rates of many consumers depend on the availability of local food resources. Although some consumers disperse more frequently when resources are more abundant (forays, *e.g.*, Bennetts and Kitchens 2000), most consumers emigrate away from areas more frequently when resources are less dense (Bernstein 1984; Ives *et al.* 1993; Kuussaari *et al.* 1996; French and Travis 2001; Kennedy and Hard 2003; Bowler and Benton 2005; Hauzy *et al.* 2007). Such negative resource-density-dependent (NRDD) dispersal is predicted by Optimal Foraging Theory (Charnov 1976) and could lead to consumers aggregating in areas of abundant resources (Readshaw 1973). Indeed, even individually weak, negative responses of consumer dispersal rate to resource density can cause significant spatial aggregation of consumers at the metapopulation level (Ives *et al.* 1993). Aggregation of predators may strongly influence the local predation risk experienced by prey individuals, and could even permit locally unstable consumer-resource interactions to persist regionally (Murdoch and Stewart-Oaten 1989). Despite the pervasiveness of NRDD dispersal (Bowler and Benton 2005), its effects on metacommunity and food-web dynamics remain poorly understood, primarily because most metacommunity studies assume dispersal is density-

independent (Hauzy *et al.* 2007; Hauzy *et al.* 2010).

The present study uses a metacommunity system of freshwater rock pools to elucidate the influence of prey density on predator dispersal and the resulting effect on the local predation risk experienced by the prey. The rock pools are found on Appledore Island, Maine, USA and contain a relatively simple three-level food chain (linear food web) consisting of the predatory water boatman *Trichocorixa verticalis* (Hemiptera, Corixidae), which consumes the herbivorous cladoceran *Moina macrocopa* (Daphniidae), which in turn grazes on phytoplankton (primarily chlorophyte algae) (J. G. Morin and J. L. Simonis, *unpub. data*). *T. verticalis* is a voracious zooplanktivore (Wurtsbaugh 1992; see also *Results*) that consumes enough *M. macrocopa* to cause a strong local top-down trophic cascade within the rock pools (J. L. Simonis, *unpub. data*). Additionally, although *T. verticalis* individuals are aquatic throughout their lives, they are able to fly as adults (Kelts 1979), and thus may connect food chains among rock pools through active dispersal (*sensu* Clobert *et al.* 2001). By comparison, both *M. macrocopa* and chlorophyte algae are not able to actively disperse among rock pools. Rather, they must rely on external agents, such as birds (in particular *Larus* gulls) or overflowing water (during rain events), to passively disperse among pools (Bohonak and Jenkins 2003).

Currently, the factors influencing the dispersal of *T. verticalis* are unknown, as are the consequences of *T. verticalis* dispersal for *M. macrocopa*. Specifically, it is unclear if *T. verticalis* dispersal is related to the density of its prey, *M. macrocopa*. Thus, the goals of the current study were to determine if the emigration rate of *T. verticalis* (predator) is dependent upon *M. macrocopa* (prey) density and to quantify the effect of *T. verticalis* dispersal on the predation risk experienced by *M. macrocopa*. An important component of this second goal is quantifying the rate at which *T. verticalis* preys upon *M. macrocopa*.

METHODS

Study System

Appledore Island (38.5 ha) is the largest island in the Isles of Shoals archipelago (Gulf of Maine, USA) and home to the Shoals Marine Laboratory (SML). Approximately 1,500 freshwater rock pools, ranging in size from *ca*. 1.0 to 30,000 L, are patchily distributed above the high-tide line around the perimeter of Appledore (J. L. Simonis, *unpub. data*). These pools contain a relatively simple food web that consists primarily of the chlorophyte-*M. macrocopa*-*T. verticalis* food chain outlined in the Introduction. Although other species of aquatic invertebrates are found in the pools (*e.g.*, *Daphnia pulex*, chironomids, ostracods, and cyclopoid copepods), *M. macrocopa* is by far the most abundant prey for *T. verticalis*: average densities of *M. macrocopa* are *ca.* 2,000 ind L^{-1}, whereas all other potential prey typically have densities under 100 ind L^{-1} (see *Results*). Similar to other corixids, *T. verticalis* undergoes incomplete metamorphosis and has a life history consisting of eggs, five juvenile stages, and adults (Kelts 1979). Only the adult stage of *T. verticalis* has wings, and thus the ability to actively disperse among pools. Further, adult *T. verticalis* are voracious predators of *M. macrocopa* (see *Results*) and additional field experiments have shown that consumption of *M. macrocopa* by adult *T. verticalis* is strong enough to induce a top-down trophic cascade in the rock pools (J. L. Simonis, *unpub. data*).

Surveys of M. macrocopa *Densities in Rock Pools*

In order to determine the relevant range of *M. macrocopa* densities experienced by *T. verticalis*, I conducted two field surveys. In early June 2008, I sampled 82 rock pools distributed around the entirety of Appledore to quantify spatial variation in *M. macrocopa* densities. I selected the pools to be representative of biotic and abiotic environmental

variation present among pools. At each pool, I collected duplicate samples of water (250 mL – 10 L each, depending on the volume of the pool) haphazardly from throughout the water column using a large-bulb pipette. I processed the duplicate samples independently, but combined the data for presentation and analyses. *M. macrocopa* and other invertebrates were removed from the water via a 75 µm mesh sieve and preserved in 95% ethanol until they were enumerated under a dissecting microscope. When *M. macrocopa* was present in high densities, I counted representative subsamples. I conducted the second survey to determine the temporal variation in *M. macrocopa* density within pools, by sampling a single (typical) pool every two-to-four days from May 22 to August 15, 2009 (29 total samples). On each date, duplicate samples of 500 mL were taken and processed following protocols as outlined above. The volume of this pool averaged 300 L (range: 250 – 425 L), thus each sampling removed only *ca*. 0.3% of the *M. macrocopa* present in the pool at that time.

Predation by Adult T. verticalis *on* M. macrocopa

I used a standard functional response experiment to quantify the rate of predation by adult *T. verticalis* on *M. macrocopa*. Single adult *T. verticalis* were placed into glass jars containing 100 mL of filtered (0.45 µm) well water and non-gravid, adult female *M. macrocopa* as prey. I collected all prey and predators for this experiment from *ca.* 10 rock pools, and kept them separately in the lab in 20 L containers with excess food (*M. macrocopa* was fed rock-pool algae and *T. verticalis* was fed *M. macrocopa*) for up to one week before they were used. To standardize hunger levels among predators, I starved all *T. verticalis* individuals for the 24 hours preceding the start of a feeding trial. Prey abundances used were 1, 2, 4, 8, 10, 12, 15, 20, 25, 30, 40, 50, 75, and 100 individuals per jar, giving densities between 10 and 1,000 prey L^{-1}, which covers most of the range seen in the Appledore rock pools (see *Results*). I ran duplicate trials for each of the 14 prey densities. Experimental jars

were placed in a temperature-stable room (mean: 18 °C, range: 16-20 °C) with fluorescent lamps ("plant and aquarium", Phillips 40W) on a 12:12 light:dark cycle. After 24 hours, I removed the predators from the jars and enumerated the remaining prey. Prey were not replaced during the trials and I triplicated all initial and final prey counts to ensure accuracy. I fit the data using the Rogers Random Predator Equation (Rogers 1972), which is the standard Type-II functional response adapted to account for depletion of prey during the experiment, using maximum likelihood methods and the mle2 function in the R package bbmle (Bolker and R Core Development Team 2011).

Effect of M. macrocopa *Density on the Emigration Rate of* T. verticalis

To determine if *M. macrocopa* density influenced the rate of emigration by adult *T. verticalis* from rock pools, I conducted a field experiment using 35 L mesocosms (Rubbermaid™ totes). I varied the prey density within each mesocosm between 0 and 1,000 *M. macrocopa* L^{-1} (covering most of the range of prey densities measured in the field surveys, see Figure 5.1). I structured the experiment as a duplicated regression design with two mesocosms at each of 20 prey density levels (0, 0.15, 0.25, 0.5, 1, 2, 3, 5, 7, 10, 15, 25, 35, 50, 75, 100, 175, 275, 500, 1,000 *M. macrocopa* L^{-1}), for 40 total experimental units. I collected all prey and predators for this experiment from *ca.* 20 rock pools, and kept them separately in the lab in 80 L containers with excess food (*M. macrocopa* was fed rock-pool algae and *T. verticalis* was fed *M. macrocopa*) for up to one week before they were used. Due to logistical constraints, I conducted the experiment in eight temporal blocks of five mesocosms each. The five prey densities used in each block were determined randomly and the temporal blocks were initiated every other day.

I filled each mesocosm with 20 L of filtered (0.45 μm) well water and added the appropriate number of *M. macrocopa* to achieve the desired prey density. For prey densities

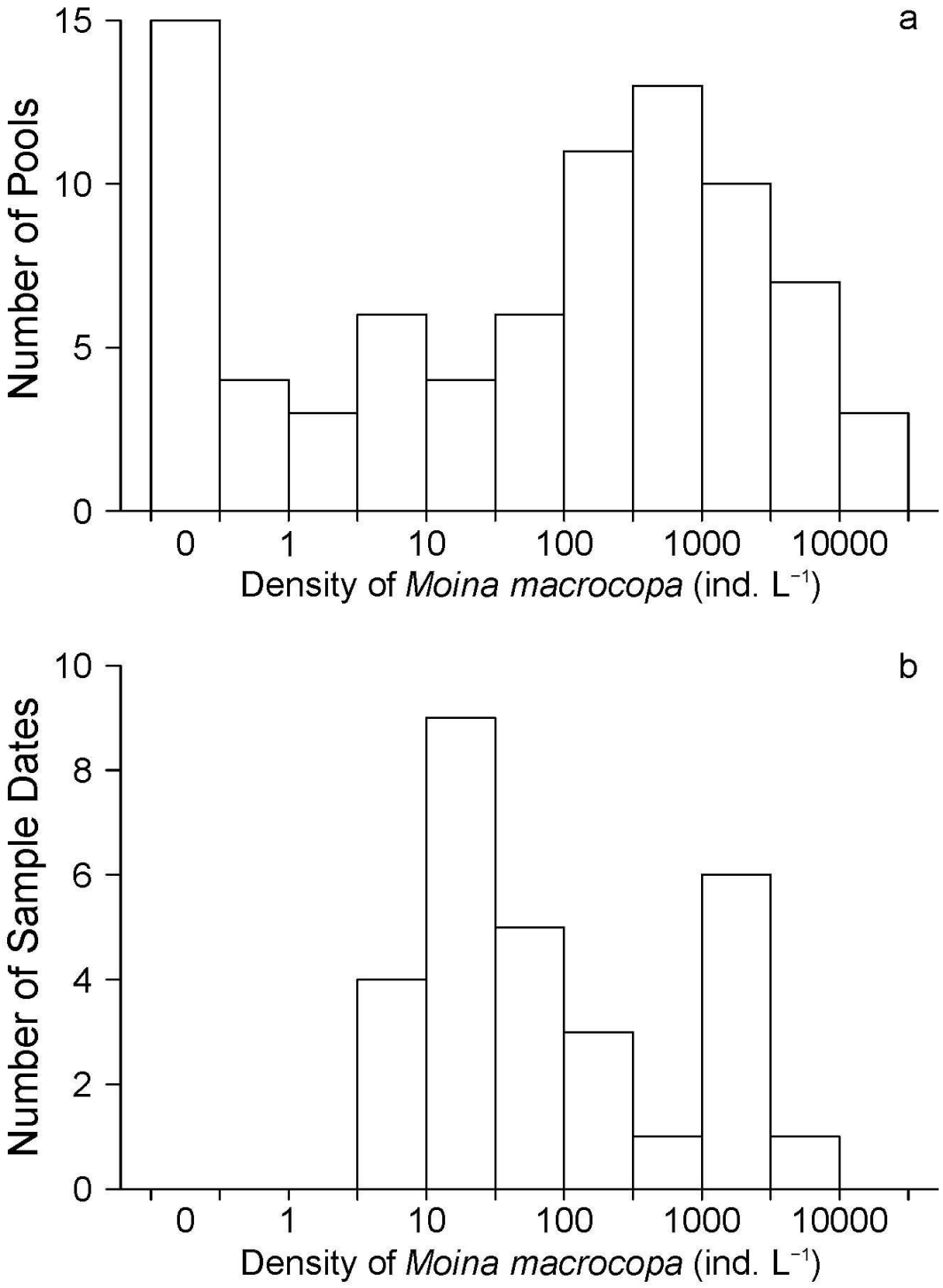

Figure 5.1. Variation in density of *M. macrocopa* across space (a) (multiple pools sampled in June 2008) and time (b) (multiple samples of the same pool during May-August 2009). Note the x-axis is on a $\log_{10}$ scale.

above 25 individuals L^{-1}, which were too high to count the exact number of individuals needed, I prepared a temporary "dense stock" of *M. macrocopa* and counted five replicate subsamples to determine how much of the "dense stock" was needed to achieve the desired density. This volume was sieved to remove excess water prior to adding to the mesocosm. I then added 10 adult *T. verticalis* to each mesocosm, along with four perches (30 cm bamboo sticks). Mesocosms were covered with 13 mm hex chicken wire to prevent birds from entering them. The five mesocosms were placed on a flat lawn on the SML campus and at least 200 m away from the closest source of potential immigrants (*i.e.*, the closest rock pool with a *T. verticalis* population). The mesocosms were also placed at least 5 m from each other to minimize possible movement of *T. verticalis* among them. Because I could not mark individual *T. verticalis*, it is impossible to be certain that there was no movement among mesocosms or immigration from other sources. However, in all of the runs of this experiment, not once were more than 10 *T. verticalis* found in a mesocosm, suggesting that immigration was minimal or nonexistent in this experiment.

All trials began in the early afternoon (1:00 p.m. EST) and ran for 24 hours. At the end of the trial, the number of remaining *T. verticalis* in each mesocosm was determined. Any dead predators were noted and removed from the analyses. Because *T. verticalis* dispersal is likely positively temperature-dependent (increased flying attempts in warmer conditions; Kelts 1979), I also recorded water temperature of each mesocosm three hours after beginning a trial. I analyzed the data with a mixed-model logistic regression in R using the glmer function in the lme4 package (Bates *et al.* 2011; R Development Core Team 2011). The response variable was the proportion of *T. verticalis* emigrating, with appropriate weights to account for trials with predator mortality. The full model included *M. macrocopa* density [$\log_{10}$(density + 0.1)] and water temperature as fixed continuous predictors and temporal block as a grouping ("random") factor, as well as all possible interaction terms. Model

simplification proceeded through stepwise term deletion and comparison of AICc scores and likelihood ratio tests (LRT) (Pinheiro and Bates 2000; Burnham and Anderson 2002).

Effect of Predator Dispersal on Per Capita *Predation Risk*

I then quantified the effect of dispersal by *T. verticalis* on the predation risk experienced by *M. macrocopa*. In particular, I determined the *per capita* predation risk to *M. macrocopa* as a function of prey density under three predator dispersal scenarios: no dispersal, prey-density-independent dispersal, and NRDD dispersal of *T. verticalis*. The third scenario is what occurs in this system (see *Results*), whereas the first and second are hypothetical scenarios for comparison. This exercise was conducted by computer simulation, with conditions identical for all three dispersal scenarios and mimicking the experiment: 20 L of water, prey densities ranging from 0 to 1,000 *M. macrocopa* L^{-1}, 10 predators, and 24 hours (note, however, that *per capita* predation rates are undefined when prey density is equal to 0.0).

In both dispersal-present scenarios, the proportion of predators emigrating was calculated for the median water temperature measured during the emigration experiments (27.85 °C, since temperature was a significant predictor of predator emigration, see Results). In the hypothetical prey-density-independent dispersal situation, the proportion of predators emigrating (20.4%) was determined by fitting a logistic regression to the emigration data, but with only temperature and block effects and no interactions. This model was similar to the best-fit model (see *Results*), except that it did not include prey density as a predictor term. Thus, the predicted proportion of predators emigrating was constant, regardless of prey density. By comparison, the proportion of predators emigrating was negatively related to prey density in the NRDD scenario, as described by the best-fit model detailed in *Results*.

For the purposes of these simulations, I made the simplifying assumption that

predators emigrated before consuming any prey. After accounting for emigration, the remaining *T. verticalis* consumed *M. macrocopa* according to the fitted functional response (see *Results*). The number of prey consumed was then divided by the total number of prey initially present (initial prey density × 20 L) to calculate *per capita* predation risk. The simulation results were then plotted as *per capita* predation risk as a function of initial prey density for each of the three dispersal scenarios for visual comparisons. All simulations were conducted in R (R Development Core Team 2011) and code is available from the author upon request.

RESULTS

Surveys of M. macrocopa *Densities in Rock Pools*

Population densities of *Moina macrocopa* varied over multiple orders of magnitude across both space and time (Figure 5.1). In June 2008, populations of *M. macrocopa* were detected in 67 of the 82 pools sampled (81.7%), with densities ranging from 0.7 to 25,470 individuals L^{-1} (median: 306.6; mean: 2,053; SD: 4,600.5 individuals L^{-1}). In comparison, *Daphnia pulex*, the other cladoceran zooplankter observed in the system, was only found in nine pools and in much lower densities (range: 0.5 – 465; median: 8.0 individuals L^{-1}). Chironomid larvae are another possible prey item for *T. verticalis* (Kelts 1979), and were found in many pools (74 of 82), although generally at low densities (range: 0.2 – 700; median: 13.6 individuals L^{-1}).

In 2009, the population density of *M. macrocopa* in the single pool sampled also varied substantially over time, although considerably less than seen among the pools in 2008. The population was detected in the pool on all 29 of the sample dates in 2009, with densities ranging from 4.0 to 3,367 individuals L^{-1} (median: 35.0; mean: 553.5; SD: 953.2 individuals

L^{-1}). *D. pulex* was only found on one date (1.0 individuals L^{-1}), but chironomid larvae were present on 27 of the 29 sampling dates (density range: 1 – 24; median: 6.0 individuals L^{-1}).

Predation by Adult T. verticalis *on* M. macrocopa

Adult *T. verticalis* were able to readily capture and consume *M. macrocopa* in the lab feeding experiments, with the maximum number of prey consumed by a single predator being 50 (Figure 5.2). The functional response had a saturating shape (Type-II), described by both attack rate (1.562 d^{-1}, standard error: 0.145, $P < 0.00001$) and handling time (0.011 d, standard error: 0.002, $P < 0.00001$). Overall, the functional response fit the data well (normalized root mean square error: 8.86%).

Effect of M. macrocopa *Density on the Emigration Rate of* T. verticalis

The best-fit statistical model describing the proportion of *T. verticalis* emigrating from the mesocosms included both the *M. macrocopa* density and temperature fixed effects as well as the blocking (random) effect. None of the possible interaction terms were useful predictors (all $P > 0.49$ by LRT) and were dropped from the model. There was a significant, negative effect of prey density [on a $\log_{10}(x + 0.1)$ scale] on the proportion of predators emigrating (Figure 5.3a, odds ratio: -0.42, $P = 0.0005$). The fitted relationship predicted that when there were no prey, 36.8% of the predators would emigrate within 24 hours; when the prey density was 1,000 individuals L^{-1}, the predicted proportion emigrating dropped to 9.7% (with temperature held at 27.85 °C, the median temperature measured during the experiment). There was also a significant positive effect of temperature on the proportion of *T. verticalis* emigrating (Figure 5.3b, odds ratio: 0.10, $P = 0.045$). However, the effect of prey density was much stronger and explained substantially more of the deviance in the response variable than

temperature did (magnitude of the prey density odds ratio is 4.2 times that of the temperature odds ratio; prey density explained 21.1% of the deviance, compared with 6.6% explained by temperature).

Effect of Predator Dispersal on Per Capita *Predation Risk*

In the computer simulations, dispersal by *T. verticalis* substantially reduced the *per capita* predation risk experienced by *M. macrocopa*, regardless of whether their dispersal was dependent on prey density (Figure 5.4). Under the hypothetical scenario of no predator dispersal, *per capita* predation risk decreased at an accelerating rate with the logarithm of

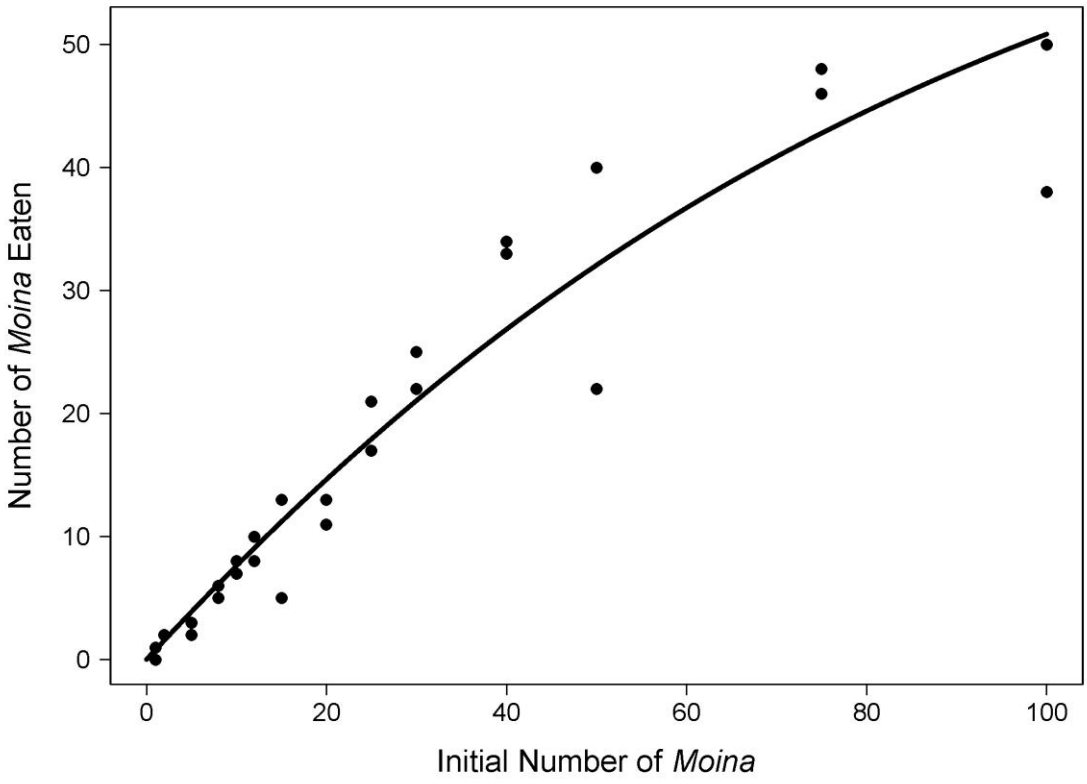

Figure 5.2. Functional response for adult *T. verticalis* feeding on *M. macrocopa*. The line depicts the functional response, which was fit using the Rogers Random Predator Equation.

prey density (dashed line, Figure 5.4), the expected pattern for a Type-II functional response as predators become increasingly satiated (Holling 1959). Density-independent predator dispersal (dotted line, Figure 5.4) reduced predator densities the same amount across all prey densities, causing a decrease in the intercept of the predation risk-prey density curve, without changing its overall shape from that of the no-dispersal scenario. In both of those hypothetical scenarios, the maximum *per capita predation* risk experienced by the prey occurs at the lowest prey density.

In contrast, NRDD dispersal qualitatively altered the form of the predation risk-prey density curve from monotonic to hump-shaped (solid line, Figure 5.4). Under this realistic scenario, the maximum predation risk occurs at an intermediate density (*ca*. 70 prey

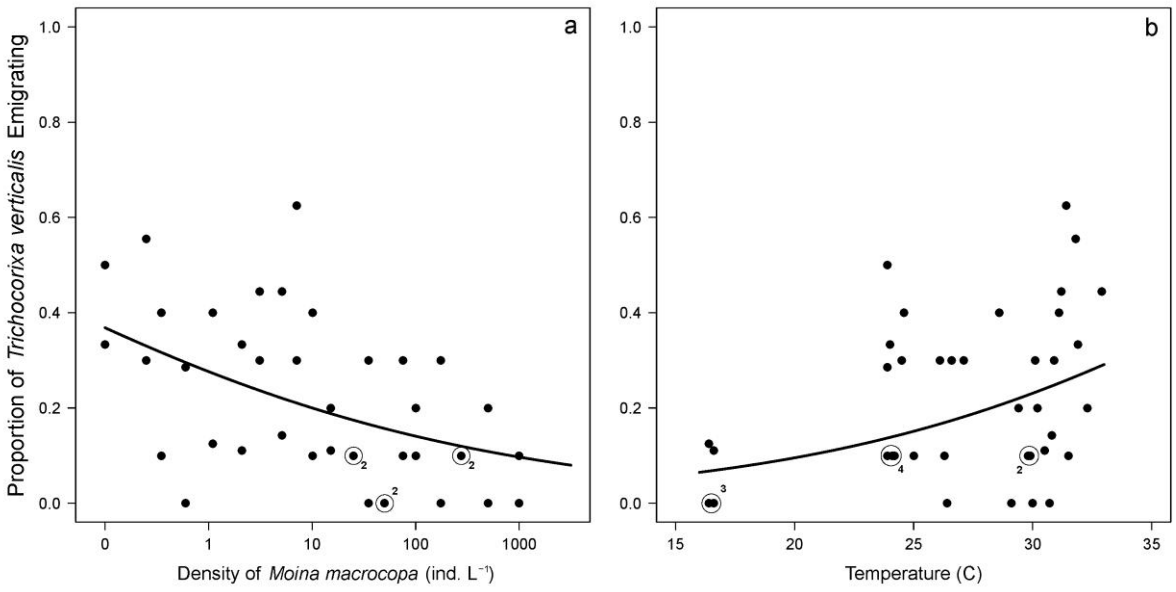

Figure 5.3. Emigration rate of *T. verticalis* as a function of both (a) *M. macrocopa* density (on a $\log_{10}$ scale) and (b) temperature. The solid lines are the predictions from the fitted mixed model logistic regression presented in text for each of the two main effects separately, with the other main effect held constant at the median value (a: temperature held at 27.85 °C; b: prey density held at 12.5 ind. L^{-1}). An open circle surrounding points denotes overlapping data (numeral indicates how many data are overlapping).

individuals L^{-1}). The decrease in predation risk at low prey densities is the result of predators emigrating more readily, thus relieving prey from predation more strongly, with decreasing prey density. The decrease causes the predation risk curves for the two dispersal-present scenarios to cross at a prey density of *ca*. 10 individuals L^{-1}, which corresponds to the predicted proportion of predators emigrating under the density-independent dispersal scenario (20.4%). At prey densities below this value, *M. macrocopa* is relieved from predation due to NRDD dispersal by *T. verticalis*. At densities above this value, *T. verticalis* disperses less frequently, and thus *M. macrocopa* experience an increase in predation risk, compared to the hypothetical situation where prey density does not influence predator dispersal. Because some predators disperse even when prey densities are extremely high (Figure 5.3), the

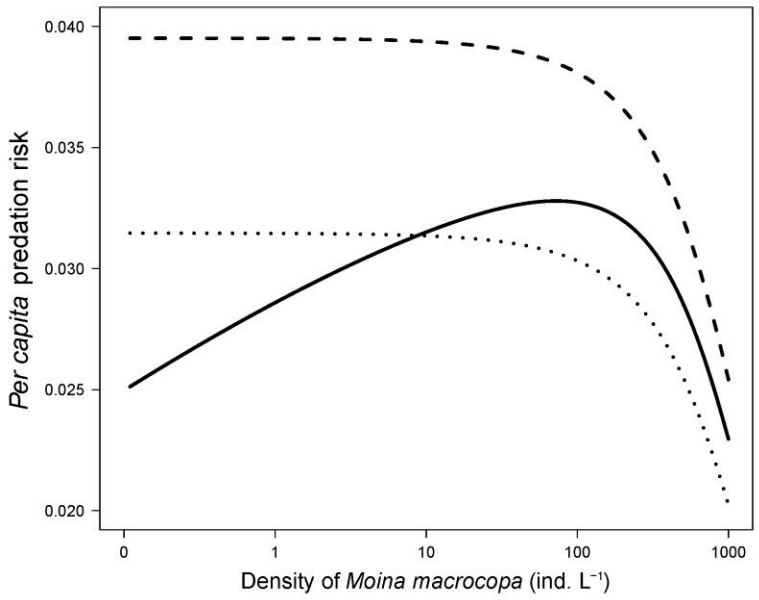

Figure 5.4. Effect of predator (*T. verticalis*) dispersal on *per capita* predation risk for *M. macrocopa*. The dashed line represents no dispersal, the solid line represents *M. macrocopa* density-dependent dispersal, and the dotted line represents hypothetical *M. macrocopa* density-independent dispersal (based on a logistic regression with only temperature and block effects). For both dispersal models, temperature was held constant at the median value recorded during experiments (27.85 °C). See text for details. Note the x-axis is on a $\log_{10}$ scale.

predation risk curve for the NRDD dispersal scenario lies intermediate to the relationships for the no-dispersal and density-independent dispersal scenarios at high prey densities.

DISCUSSION

Given the large spatial and temporal variation in the density of its most abundant prey (*Moina macrocopa*) observed in the Appledore rock pools (Figure 5.1), it is not surprising that *Trichocorixa verticalis* displayed a generally high dispersal propensity in the emigration experiments (*ca.* 20% of predators emigrated within 24 hours, regardless of prey density). Indeed, variable local resource density is one factor expected to select for dispersal as a life-history strategy (Clobert *et al.* 2001; Bowler and Benton 2005). However, the ultimate driver (or drivers) of dispersal by *T. verticalis* in the rock-pool system could be any combination of factors, including, *e.g.*, habitat persistence and inbreeding avoidance (Clobert *et al.* 2001; Bowler and Benton 2005). The current study cannot speak directly to the questions of the ultimate cause of dispersal by *T. verticalis*, but suggests that the availability of *M. macrocopa* as a food resource plays an important role in dictating *T. verticalis* dispersal among rock pools.

Whatever the ultimate causes of dispersal, when a species is able to actively disperse among patches, individual predators must still make decisions about whether or not to emigrate based on their current environments (Bowler and Benton 2005). By influencing the density of predators, these emigration decisions have consequences for the predation risk experienced locally by their prey. In this proximate sense, prey density strongly affected predator dispersal in the rock pools of Appledore Island, as *T. verticalis* displayed a negative relationship between emigration rate and *M. macrocopa* density (NRDD dispersal, Figure 5.3a). Indeed, prey density was a much stronger driver of predator dispersal than temperature was, another proximate factor that has been suggested to influence dispersal by *T. verticalis*

(Kelts 1979). This result of NRDD dispersal matches the general, intuitive predictions of classic Optimal Foraging Theory that consumer movement rates should be a negative function of resource density (Charnov 1976). It should be noted, however, that not all consumer species disperse more frequently at lower resource densities (*e.g.*, Nunes *et al.* 1997; Bennetts and Kitchens 2000).

This pattern of NRDD dispersal by *T. verticalis* in response to *M. macrocopa* density causes a local positive numerical response between the two trophic levels, through which predators are predicted to aggregate (increase in density over time) in rock pools with higher prey abundances (Readshaw 1973; Murdoch and Stewart-Oaten 1989). Because the local *T. verticalis—M. macrocopa* trophic interaction is described by a Type-II functional response (Figure 5.2), a positive numerical response introduces a refuge for prey from predation risk when prey are present at low densities (Figure 5.4) that would otherwise not exist. In the absence of NRDD dispersal by *T. verticalis* (if individuals did not disperse or dispersed independent of prey density), predation risk would remain high at low prey densities, and *T. verticalis* predation could drive local *M. macrocopa* populations extinct (Figure 5.4). Conversely, in the presence of NRDD dispersal, as predation by *T. verticalis* reduces local *M. macrocopa* population densities, it also indirectly increases the rate of *T. verticalis* emigration, thereby lessening the future impact of predation and reducing the likelihood of the local *M. macrocopa* population going extinct from predation. As a result, NRDD dispersal is predicted to convert an unstable local Type-II functional response into a stable Type-III functional response at the metacommunity scale (Murdoch and Stewart-Oaten 1989). However, this prediction remains to be explicitly tested.

For the rock- pool metacommunity on Appledore Island, the *per capita* predation risk curves for NRDD and density-independent dispersal are predicted to cross at approximately 10 *M. macrocopa* L^{-1} (Figure 5.4). At densities below this level, local *M. macrocopa* populations are predicted to experience lower *per capita* predation rates than they would if *T.*

verticalis dispersal were independent of local prey density, resulting in an increase in the potential persistence of local *M. macrocopa* populations (*i.e.*, a reduction in the likelihood of extinction due to predation). Although the majority of *M. macrocopa* population densities measured in the surveys were above 10 individuals L^{-1}, densities below 10 individuals L^{-1} were observed in both the one-time survey of 82 pools in 2008 [19.4% of pools with detectable populations (13 of 67)] and the repeated sampling of the single pool in 2009 [13.8% of sample dates (4 of 29)] (Figure 5.1), indicating that the decrease in the *per capita* predation rate at low prey densities is indeed relevant for populations in the field. Indeed, the *M. macrocopa* population that I repeatedly sampled exhibited positive growth rates following all of the four days when the population density had dropped below 10 individuals L^{-1} (mean growth rate = 0.23 d^{-1}), compared to only 41.7% (10 of 24) of growth rates being positive following days when the population was above 10 individuals L^{-1} (mean growth rate = -0.04 d^{-1} for all 24 days). However, without additional observational data and controlled experiments, it is unclear how important this release from predation at low prey densities is, relative to other factors (*e.g.*, increased *per capita* resource densities), for the persistence of local *M. macrocopa* populations.

Although *M. macrocopa* is the most abundant prey resource for *T. verticalis* in the rock pools, it is not the only potential prey item in this system. Indeed, *T. verticalis* may consume a range of food types including, *e.g.*, chironomid larvae (Kelts 1979), which are present and widely distributed in the rock pools. However, the chironomid larvae construct protective cases that likely restrict the ability of predators such as *T. verticalis* to prey upon them (Dillon 1985). Given the scant data on this predator, it is currently unknown if *T. verticalis* can use other potential food resources present in the rock pools, nor is it known if any single food resource (including *M. macrocopa*) provides all of the nutrients necessary for growth and development. If *T. verticalis* does consume other prey items, it may lessen the specific effect of local *M. macrocopa* density on *T. verticalis* emigration. If this were the

case, predator emigration would likely be a function local prey availability more generally.

The results from this study suggest that local (trophic) and regional (dispersal) processes are intimately linked in the Appledore Island rock-pool system in a way that could influence metacommunity dynamics, not just through altering local predator-prey dynamics, but also by increasing the persistence of local *M. macrocopa* populations. *M. macrocopa* is the both the dominant zooplankton grazer and the most abundant prey resource for *T. verticalis* in the rock pools, and thus is a key trophic link between algal production and *T. verticalis*. Furthermore, *M. macrocopa* is not able to actively disperse among rock pools, but rather must rely on external mechanisms, such as gulls wading through pools or overflowing water connecting pools during rain events, to passively recolonize pools following local extinctions (as has been found for zooplankton in other rock pool systems, *e.g.*, Vanschoenwinkel *et al.* 2008). Therefore, by increasing the persistence of local *M. macrocopa* populations, NRDD dispersal by *T. verticalis* has the potential to affect the structure and function of rock-pool food webs at both the local and metacommunity scales.

ACKNOWLEDGEMENTS

I am incredibly grateful to P. Spaak, M. Manca, N. Hairston, Jr. (NGH), the Orenstein Family, and the Cornell Ecology and Evolutionary Biology Department for the opportunity and funding to participate in this Symposium. I also thank the staff of the Shoals Marine Lab (SML), especially director W. Bemis, for logistical assistance with these studies and J. Morin for preliminary research on the rock-pool system. The NGH and A. Flecker lab groups provided helpful discussions on this topic and S. Collins, S. Simonis, and NGH gave helpful comments on an earlier version of this manuscript. This work was supported financially by SML, the Cornell University Biogeochemistry and Environmental Biocomplexity Program, the Andrew W. Mellon Foundation, the National Science Foundation (NSF, DEB-1110545),

and an NSF Graduate Research Fellowship awarded to JLS. This is contribution #161 from the Shoals Marine Laboratory.

REFERENCES

Bates, D., M. Maechler, and B. Bolker. 2011. lme4: Linear mixed-effects models using S4 classes. R package version 0.999375-42. http://CRAN.R-project.org/package=lme4.

Bernstein, C. 1984. Prey and predator emigration responses in the acarine system *Tetranychus urticae-Phytoseiulus persimilis*. Oecologia 61:134-142.

Bennetts, R. E. and W. M. Kitchens. 2000. Factors influencing movement probabilities of a nomadic food specialist: proximate foraging benefits or ultimate gains from exploration? Oikos 91:459-467.

Bolker, B. and R Development Core Team. 2011. bbmle: tools for general maximum likelihood estimation. R package version 0.9.7. http://CRAN.R-project.org/package=bbmle.

Bowler, D. E. and T. G. Benton. 2005. Causes and consequences of animal dispersal strategies: relating individual behavior to spatial dynamics. Biological Reviews 80:205-225.

Burnham, K. P. and D. R. Anderson. 2002. Model Selection and Mutimodel Inference: A Practical Information-Theoretic Approach. Springer-Verlag, New York.

Charnov, E. L. 1976. Optimal foraging, the Marginal Value Theorem. Theoretical Population Biology 9:129-136.

Clobert, J., E. Danchin, A. A. Dhondt, and J. D. Nichols. 2001. Dispersal. Oxford University Press.

Dillon, P. M. 1985. Chironomid larval size and case presence influence capture success achieved by dragonfly larvae. Freshwater Invertebrate Biology 4:22-29.

French, D. R. and J. M. J. Travis, 2001. Density-dependent dispersal in host-parasitoid assemblages. Oikos 95:125-135.

Hanski, I. 1999. Metapopulation ecology. Oxford University Press.

Hauzy, C., F. D. Hulot, A. Gins, and M. Loreau. 2007. Intra- and interspecific density-dependent dispersal in an aquatic prey-predator system. Journal of Animal Ecology 76:552-558.

Hauzy, C., M. Gauduchon, F. D. Hulot, and M. Loreau. 2010. Density-dependent dispersal and relative dispersal affect the stability of predator-prey metacommunities. Journal of Theoretical Biology 266:458-469.

Holling, C. S. 1959. The components of predation as revealed by a study of small mammal predation of the European pine sawfly. The Canadian Entomologist 91:293-320.

Holyoak, M., M. A. Leibold, and R. D. Holt. 2005. Metacommunities: spatial dynamics and ecological communities. Chicago University Press.

Ives, A. R., P. Kareiva, and R. Perry. 1993. Response of a predator to variation in prey density at three hierarchical scales: lady beetles feeding on aphids. Ecology 74:1929-1938.

Kelts, L. J.1979. Ecology of a tidal marsh corixid, *Trichocorixa verticalis* (Insecta, Hemiptera). Hydrobiologia 64:37-57.

Kennedy, P. L. and J. M. Ward. 2003. Effects of experimental food supplementation on movements of juvenile northern goshawks (*Accipiter gentilis atricapillus*). Oecologia 134:284-291.

Kuussaari, M., M. Nieminen, and I. Hanski. 1996. An experimental study of migration in the Glanville fritillary butterfly *Melitaea cinxia*. Journal of Animal Ecology 65:791-801.

McCann, K. S., J. B. Rasmussen, and J. Umbanhowar. 2005. The dynamics of spatially coupled food webs. Ecology Letters 8:513-523.

Morin, P. J. 1999. Community Ecology. Blackwell Publishing, Malden, MA, USA.

Murdoch, W. W. and A. Stewart-Oaten. 1989. Aggregation by parasitoids and predators:

effects on equilibrium and stability. American Naturalist 134:288-310.

Nunes, S., P. A. Zuggar, A. L. Engh, K. O. Reinhart, and K. E. Holekamp. 1997. Why do female Belding's ground squirrels disperse away from food resources? Behavioral and Ecological Sociobiology 40:199-207.

Pinheiro, J. C. and D. M. Bates. 2000. Mixed-Effects Models in S and S-PLUS. Springer-Verlag, New York.

R Core Development Team. 2011. R: A Language and Environment for Statistical Computing. R Foundation for Statistical Computing, Vienna, Austria.

Readshaw, J. L. 1973. The numerical response of predators to prey density. Journal of Applied Ecology 10:342-351.

Rogers, D. J. 1972. Random search and insect population models. Journal of Animal Ecology 41:369-383.

Vanschoenwinkel, B., S. Gielen, H. Vandewaerde, M. Seaman, and L. Brendonck. 2008. Relative importance of different dispersal vectors for small aquatic invertebrates in a rock pool metacommunity. Ecography 81:567-577.

Wurtsbaugh, W.A. 1992. Food-web modification by an invertebrate predator in the Great Salt Lake (USA). Oecologia 89:168-175.

APPENDIX

1.A

This appendix section includes more in-depth versions of the model development and mathematical comparisons shown in the main text of Chapter 1.

Rearrangements of the Rosenzweig-MacArthur Model

Here I explain the modifications of the RM model shown in Table 1.1. These changes allow all of the population processes to be represented as independent terms, a necessary condition for both the PJP and SDE models to appropriately model the variances associated with changes in population sizes. I start with standard logistic population growth of prey (*N*):

$$rN\left(1-\frac{N}{K_N}\right) \qquad (1.A.1)$$

where *r* is the intrinsic rate of growth and K_N is the carrying capacity of the prey. This term encompasses two processes: prey birth and prey mortality (independent of predation). In order to include a separate term for prey mortality ($m_N N$), but have there be no overall change in the equation, we need to introduce an opposite-sign term as well. For example, X = X + aX − aX = (X + aX) − aX = X(1 + a) − aX. Thus, for the logistic term, we add and subtract mortality and have (after rearrangement):

$$rN\left(1-\frac{N}{K_N}\right)+\ m_N N-\ m_N N \qquad (1.A.2)$$

$$\left[rN\left(1-\frac{N}{K_N}\right)+\ m_N N\right]-\ m_N N \qquad (1.A.3)$$

$$N\left[N\left(1-\frac{N}{K_N}\right)+m_N N\right]-m_N N \qquad (1.A.4)$$

As a result, the prey birth (first term) occurs at a rate equal to the logistic growth rate plus the mortality rate, and death (second term) occurs at the mortality rate, thus overall population growth occurs at the logistic growth rate. Here I have formulated prey birth as density-dependent (it includes the logistic growth term) and mortality as density-independent (it does not include the logistic growth term). It is also possible to make birth density-independent and mortality density-dependent or to make both birth and death density-dependent (Pineda-Krch 2008).

Next, we split apart the predation term in the prey equation:

$$\frac{aNP}{N+h_N} \qquad (1.A.5)$$

where a is the maximum attack rate of the predator, P is the predator population size, and h_N is the half saturation constant of the predator. The issue is that this term does not directly match the term for predator birth in the predator equation:

$$\frac{caNP}{N+h_N} \qquad (1.A.6)$$

where c is the conversion rate of prey to predators.

A choice must be made regarding whether the birth of new predators should be linked to the consumption of prey or be treated as an independent process. Here I have assumed that the birth of a predator is linked to the consumption of a single (final) prey individual and all other predation events do not directly result in predator birth. This is accomplished by again

adding and subtracting the same value, here *caNP*, to the numerator of the prey-equation term (1.A.5).

Following rearrangements, we then achieve:

$$\frac{aNP - caNP + caNP}{N + h_N} \tag{1.A.7}$$

$$\frac{(1 - c)aNP + caNP}{N + h_N} \tag{1.A.8}$$

$$\frac{(1 - c)aNP}{N + h_N} + \frac{caNP}{N + h_N} \tag{1.A.9}$$

Now, the second term in (1.A.9) is identical to (1.A.6) and represents predation events that lead to the birth of new predators, whereas the first term represents all of the predation events that do not lead to the birth of new predators. Note that this rearrangement requires that *c* be less than or equal to one, which makes biological sense in many cases: predators need to consume at least one prey individual before giving birth to a new predator. If *c* equals one (one prey individual is all that is required to create a new predator), then the first term in (1.A.9) is equal to 0 and drops out of the model.

Relationship Between the ODE and PJP

In the main text, I assert that the ODE model is the mean-field approximation of the PJP model, so long as the product of the state change vector ($\mathbf{\Delta X}_k$) and propensity function ($p_k(\mathbf{X})$) is equal to the associated rates of change in the ODE for all population processes *k*. Here I give a slightly more involved, albeit somewhat heuristic, explanation of this statement and the general relationship between ODE and PJP models. Readers interested in a proper and

full derivation of this relationship and applications of PJP (and SDE) models should consult Kurtz (1970; 1971; 1978), Gillespie (1977; 2007), Nisbet and Gurney (1982), Pineda-Krch (2008), or Allen (2011).

A fundamental assumption of continuous-time Markov chain models is that all processes occur through "jumps" that cause population sizes to change by integer values (e.g., the birth of a whole individual). In a PJP, these processes are described by Poisson processes: events of process type k occur at rate $\lambda = p_k(\mathbf{X})$, where λ is the rate parameter of the Poisson distribution. Because the mean of a Poisson distribution is also equal to λ, if λ equals the rate of change in the ODE, then the mean rate of change in the PJP is what is expressed by the ODE (hence, the ODE is the mean-field approximation of the PJP). To fully realize this approximation, however, we need to address the consequence of the process (which populations change in size and in which direction) as well as the timing of specific events.

For example, take predator mortality in patch i, $p_k(\mathbf{X}) = \lambda = m_P P_i$. Thus far, we have only accounted for the rate of the process, not for the fact that predator mortality results in a *decrease* in predator population size in patch i, nor that this process does not change the population size of either prey subpopulation or the predator subpopulation in patch j. To handle this bookkeeping, we introduce the state change vector, which accounts for the directionality (increase or decrease) and identity (which trophic level and subpopulation) of the population size changes associated with the process. Thus, for the process of predator mortality in patch i, $\mathbf{\Delta X}_k = (0, -1, 0, 0)$, where the elements of $\mathbf{\Delta X}_k$ are $(\Delta N_i, \Delta P_i, \Delta N_j, \Delta P_j)$. Multiplying $\mathbf{\Delta X}_k$ and $p_k(\mathbf{X})$ for predator mortality in patch i results in $\mathbf{\Delta X}_k \times p_k(\mathbf{X}) = (0, -m_P P_i, 0, 0)$, which is how this process is represented in the ODE (as a negative term and only in the P_i equation).

The final piece of this relationship is the timing of events in the PJP. In the ODE (and the SDE) all events happen continuously through continuous time, whereas in the PJP, all events happen discretely through continuous time, with their exact realizations (when an event

occurs) being stochastic. To determine the waiting time until the next event, we call upon the relationship between the Poisson and exponential distributions: the waiting time between events of a Poisson process are exponentially distributed, with the same rate parameter (λ) as the Poisson and with the expected value equal to the inverse of the rate ($1/\lambda$). Thus, as long as we use an exponential distribution with a rate parameter equal to the rate parameter in the Poisson distribution to determine the timing of the next event, then the ODE is the mean-field approximation of the PJP.

We can then extend this to systems with multiple processes. We first account for all processes k by making sure that $\mathbf{\Delta X}_k \times p_k(\mathbf{X})$ is equivalent to how they are represented in the ODE model (in magnitude, sign, and identity), as was done for predator mortality in patch I above. It is straightforward to see that this is indeed the case for the model system described in the main text. Note that the ODE, as depicted in the main text, does not include the rearrangements as shown in Table 1 and described above, as they cancel back out (as stated in the main text).

Next, we determine the timing of events. If we have k processes, with corresponding propensities $p_1(\mathbf{X})$, $p_2(\mathbf{X})$, … $p_k(\mathbf{X})$, then the propensity of an event of *any* process type happening is simply the union (sum) of the individual propensities: $p_1(\mathbf{X}) + p_2(\mathbf{X}) + \ldots + p_k(\mathbf{X}) = p_0(\mathbf{X})$. The Poisson distribution with the rate parameter $\lambda = p_0(\mathbf{X})$ describes all of the individual process types *en masse*, and the waiting time until the next event (of any process type) occurs is given by the exponential distribution with $\lambda = p_0(\mathbf{X})$ and expected value = $(p_0(\mathbf{X}))^{-1}$. Because each process type k contributes to $p_0(\mathbf{X})$ in proportion to its own propensity $p_k(\mathbf{X})$, the identity of the next event to occur can be determined randomly, where the probability of the event being of type k is simply $p_k(\mathbf{X}) \div p_0(\mathbf{X})$. Using this approach, we can draw two random numbers to determine when the next event happens and what process type it is. As a result, the ODE approximates the PJP in mean-field.

As stated in the main text, the SDE can be thought of as the continuous Gaussian approximation of the PJP model generated by applying a Central Limit Theorem-type approximation for the net effect of the many discrete jumps that occur in a small time interval when the population size is large (Kurtz 1978). As a result, the SDE and PJP models have the same mean-field behavior. In the next section, I show that the ODE is also the mean-field approximation of the SDE. Thus, the ODE is an approximation of the SDE, which is an approximation of the PJP and the three models form a natural hierarchy with directly comparable outputs.

Articulation of the SDE Model

In the effort of simplification of presentation in the main text, the SDE model was given in matrix-vector form:

$$d\mathbf{X}_t = \mu(\mathbf{X}_t)\mathrm{d}t + \mathbf{C}(\mathbf{X}_t)\mathrm{d}\mathbf{B}_t \qquad (1.A.10)$$

which shows the change in each of the four population sizes ($\mathrm{d}\mathbf{X}_t$). Here I present the full versions of the matrices in the model.

First, the 4 × 1 matrix ($\mathrm{d}\mathbf{X}_t$), which represents the changes in the four population sizes at time *t*, is simply:

$$\mathrm{d}\mathbf{X}_t = \begin{bmatrix} \mathrm{d}N_i(t) \\ \mathrm{d}P_i(t) \\ \mathrm{d}N_j(t) \\ \mathrm{d}P_j(t) \end{bmatrix}$$

where, *e.g.*, $\mathrm{d}N_i(t)$ is the change in the size of the prey population in patch *i* at time *t*.

Next is the "drift vector" μ, which is the 4 × 1 matrix that describes the expected values of the changes in population sizes. First, I show the matrix in its full form, which includes all of the processes as displayed in Table 1.1:

$$\mu = \begin{bmatrix} \mu N_i \\ \mu P_i \\ \mu N_j \\ \mu P_j \end{bmatrix} = \begin{bmatrix} \left[m_N + r\left(1 - \frac{N_i}{K_N}\right)\right] N_i - m_N N_i - \frac{(1-c)aN_iP_i}{N_i + h_N} - \frac{caN_iP_i}{N_i + h_N} + \delta_N N_j - \delta_N N_i \\ \frac{caN_iP_i}{N_i + h_N} - m_P P_i + \delta_P P_j - \delta_P P_i \\ \left[m_N + r\left(1 - \frac{N_j}{K_N}\right)\right] N_j - m_N N_j - \frac{(1-c)aN_jP_j}{N_j + h_N} - \frac{caN_jP_j}{N_j + h_N} + \delta_N N_i - \delta_N N_j \\ \frac{caN_jP_j}{N_j + h_N} - m_P P_j + \delta_P P_i - \delta_P P_j \end{bmatrix}$$

However, because this component is deterministic, the algebraic rearrangements cancel back out, and we are left with the simplified version:

$$\mu = \begin{bmatrix} \mu N_i \\ \mu P_i \\ \mu N_j \\ \mu P_j \end{bmatrix} = \begin{bmatrix} rN_i\left(1 - \frac{N_i}{K_N}\right) - \frac{aN_iP_i}{N_i + h_N} + \delta_N\left(N_j - N_i\right) \\ \frac{caN_iP_i}{N_i + h_N} - m_P P_i + \delta_P\left(P_j - P_i\right) \\ rN_j\left(1 - \frac{N_j}{K_N}\right) - \frac{aN_jP_j}{N_j + h_N} + \delta_N\left(N_i - N_j\right) \\ \frac{caN_jP_j}{N_j + h_N} - m_P P_j + \delta_P\left(P_i - P_j\right) \end{bmatrix}$$

which matches the ODE representation of the two-patch R-M model. Hence, the ODE is also the mean-field approximation of the SDE.

We next have the 4 × 14 "diffusion matrix" **C**, where $\mathbf{C}^2$ is the covariance matrix that describes the variance associated with each of the 14 processes and any covariance among process (such as dispersal of prey from patch *i* to patch *j*). For each process, the variance is equal to the expected value, because we are taking the normal approximation to the Poisson

distribution (where mean = variance = λ). Obviously, only the populations affected by a given process will experience any (co)variance associated with it (*e.g.*, only prey in patch *i* are affected by the first process, which is the birth of prey in patch *i*). Negative signs indicate that the process results in a decreased population size. Any process affecting two populations (*e.g.*, dispersal of prey from patch *i* to patch *j*) is given a non-zero term in both rows, indicating covariance. In the RM system, all processes with covariance exhibit negative covariance (*e.g.*, dispersal of prey from patch *i* to patch *j* decreases population size in *i* but increases it in *j*), hence the opposite signs for the two terms.

To convert these variances to standard deviations (which is in proper units, and necessary to describe the diffusion process), we simply take their square roots. Although taking the square root of a matrix is often less trivial, it can be shown that if the matrix **C** is populated by the standard deviation of each process and correlations among process are accounted for (that is **C** is populated with the square roots of the variances and covariances, also moving the negative signs out of the square roots), as it is in this formulation (shown below), then it satisfies the property $\boldsymbol{CC}^{tr} = \mathbf{C}^2$ (Allen 2011).

Thus, the matrix **C** is (ellipses denote the continuation of the matrix):

$$\mathbf{C} = \begin{bmatrix} \sqrt{\left[m_N + r\left(1 - \frac{N_i}{K_N}\right)\right] N_i} & -\sqrt{m_N N_i} & -\sqrt{\frac{(1-c)aN_iP_i}{N_i + h_N}} & -\sqrt{\frac{caN_iP_i}{N_i + h_N}} & 0 & \cdots \\ 0 & 0 & 0 & \sqrt{\frac{caN_iP_i}{N_i + h_N}} & -\sqrt{m_P P_i} & \cdots \\ 0 & 0 & 0 & 0 & 0 & \cdots \\ 0 & 0 & 0 & 0 & 0 & \cdots \end{bmatrix}$$

$$\begin{bmatrix} \cdots & 0 & 0 & 0 & 0 & 0 & \cdots \\ \cdots & 0 & 0 & 0 & 0 & 0 & \cdots \\ \cdots & \sqrt{\left[m_N + r\left(1 - \frac{N_j}{K_N}\right)\right]N_j} & -\sqrt{m_N N_j} & -\sqrt{\frac{(1-c)aN_jP_j}{N_j + h_N}} & -\sqrt{\frac{caN_jP_j}{N_j + h_N}} & 0 & \cdots \\ \cdots & 0 & 0 & 0 & \sqrt{\frac{caN_jP_j}{N_j + h_N}} & -\sqrt{m_P P_j} & \cdots \end{bmatrix}$$

$$\begin{bmatrix} \cdots & -\sqrt{\delta_N N_i} & \sqrt{\delta_N N_j} & 0 & 0 \\ \cdots & 0 & 0 & -\sqrt{\delta_P P_i} & \sqrt{\delta_P P_j} \\ \cdots & \sqrt{\delta_N N_i} & -\sqrt{\delta_N N_j} & 0 & 0 \\ \cdots & 0 & 0 & \sqrt{\delta_P P_i} & -\sqrt{\delta_P P_j} \end{bmatrix}$$

Each of the 14 columns in the matrix corresponds to a different process *k*, and from left to right, the processes match with those listed from top to bottom in Table 1 in the main text.

The matrix **C** is then multiplied by the time-derivative of the 1 × 14 matrix **B**, which contains a separate term b_k for each process. Each b_k represents an independent continuous-time stochastic process with mean 0 and unit variance (Brownian motion). The product of these matrices is then a 4 × 1 matrix that describes the total variation (with appropriate correlation) for the change in size of each population.

REFERENCES

Allen, L. J. S. 2011. An introduction to stochastic processes with applications to biology. CRC Press, New York.

Gillespie, D. T. 1977. Exact stochastic simulation of coupled chemical reactions. Journal of Physical Chemistry 81:2340–2361.

Gillespie, D. T. 2007. simulation of chemical kinetics. Annual Review of Physical Chemistry 58:35–55.

Kurtz, T. G. 1970. Solutions of ordinary differential equations as limits of pure jump Markov processes. Journal of Applied Probability 7:49–58.

Kurtz, T. G. 1971. Limit theorems for sequences of jump Markov processes approximating ordinary differential processes. Journal of Applied Probability 8:344–356.

Kurtz, T. G. 1978. Strong approximation theorems for density dependent Markov chains. Stochastic Processes and their Applications 6:223–240.

Nisbet, R. M. and W. S. C. Gurney 1982. Modelling fluctuating populations. Wiley Publishing, New York.

Pineda-Krch, M. 2008. GillespieSSA: implementing the stochastic simulation algorithm in r. Journal of Statistical Software, 25:1–18.

1.B

This appendix section includes time series of simulations from the single-patch (Figure 1.B.1) and two-patch (Figure 1.B.2) versions of the PJP, SDE, and ODE models discussed in Chapter 1. Further, I have included representative time series of simulations from the two-patch ODE model where dispersal parameters generated long-term, but still transient anti-phase dynamics (Figures 1.B.3, 1.B.4). For all time series, local parameter values are as described in the main text.

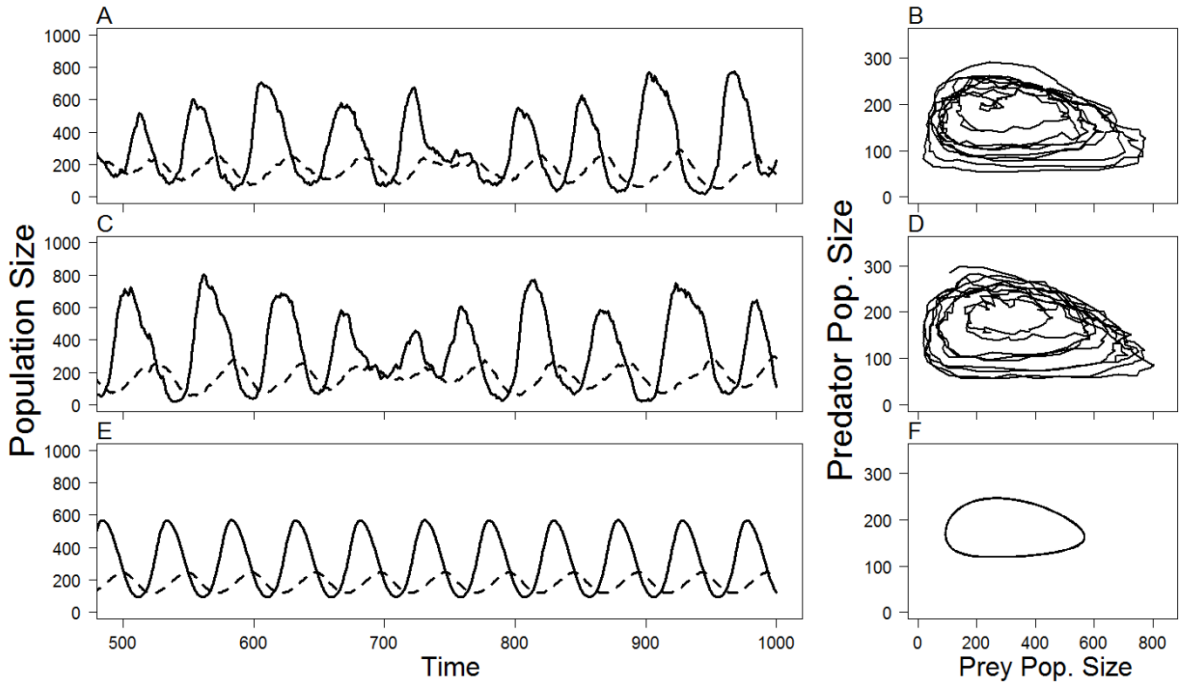

Figure 1.B.1. Typical dynamics from the single-patch versions of the PJP (A, B), SDE (C, D), and ODE (E, F) models, shown as time series (A, C, E) and corresponding phase planes (B, D, F) for days 500-1000. In the time series plots, prey are represented by the solid line, predators by the dashed line.

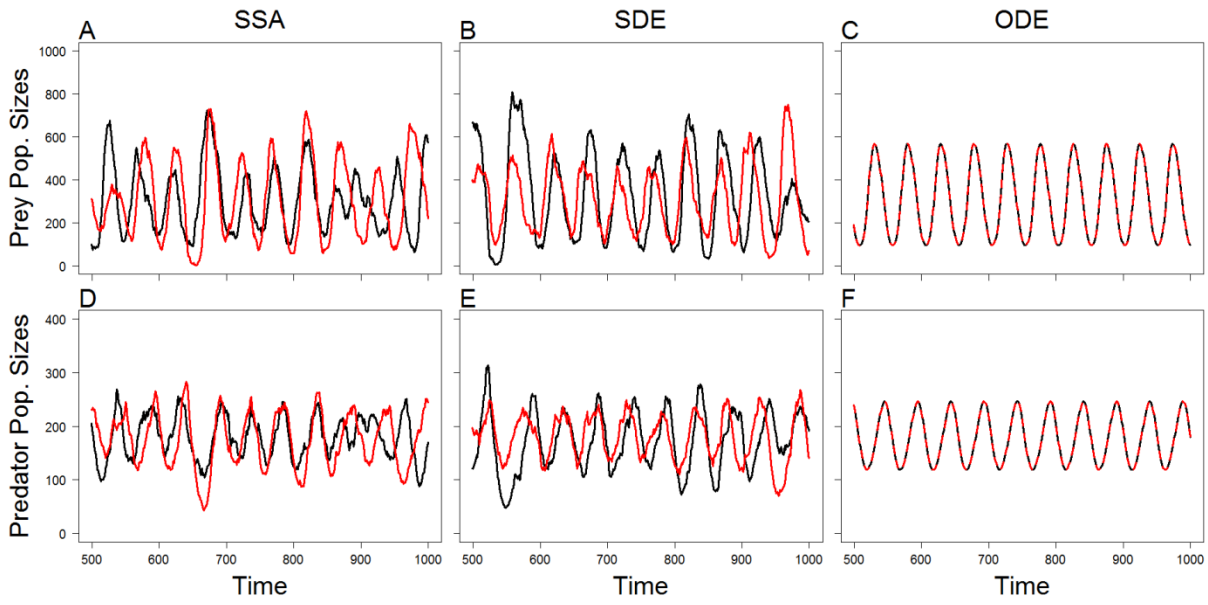

Figure 1.B.2. Typical prey (A, B, C) and predator (D, E, F) dynamics from the second half of simulations of the two-patch versions of the PJP (A, D), SDE (B, E), and ODE (C, F) models with $\delta_N = \delta_P = 0.00599$ (one of the combinations used in the main text simulations). For all three models, one patch is delineated by the black lines and the other by the red lines. (In the ODE, the red line was dashed to make it stand out.) The PJP simulation resulted in second-half correlations of 0.379 (prey) and 0.397 (predators), compared to the mean second-half correlations of 0.468 (prey) and 0.441 (predators), as displayed in Figure 1.1. The SDE simulation resulted in second-half correlations of 0.467 (prey) and 0.456 (predators), compared to the mean second-half correlations of 0.440 (prey) and 0.397 (predators), as displayed in Figure 1.1. The ODE simulation shown resulted in correlations of 1.0 for both prey and predators.

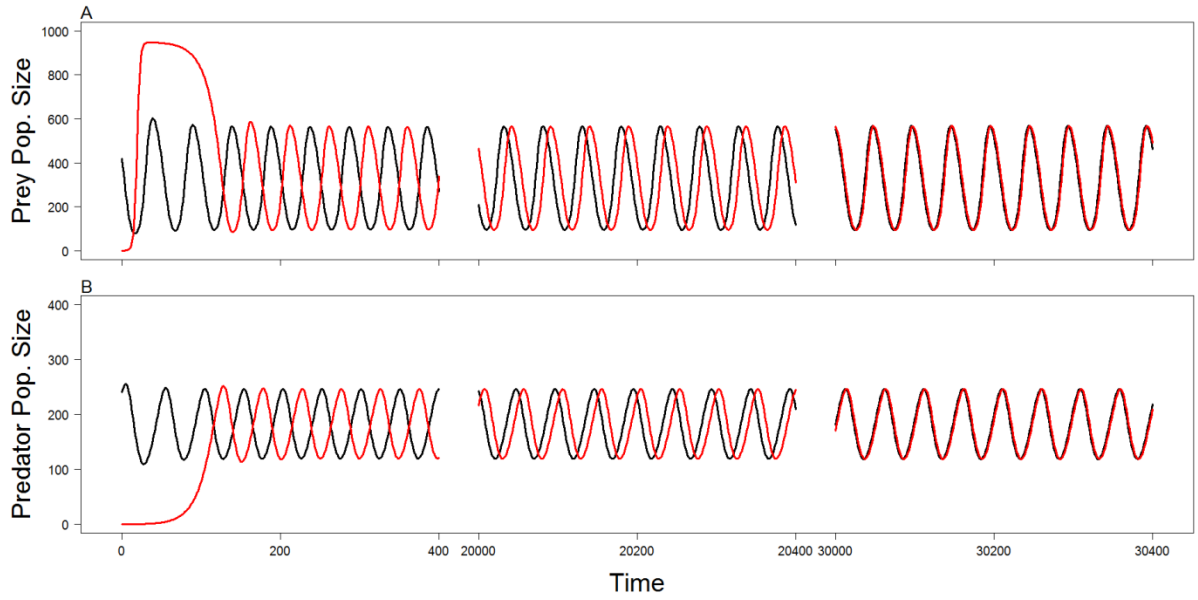

Figure 1.B.3. Transient anti-phase dynamics for prey (A) and predator (B) in the two-patch ODE model generated when $\delta_N = \delta_P = 0.0001$. One patch is delineated by the black lines and the other by the red lines. Note the breaks in time along the x-axis.

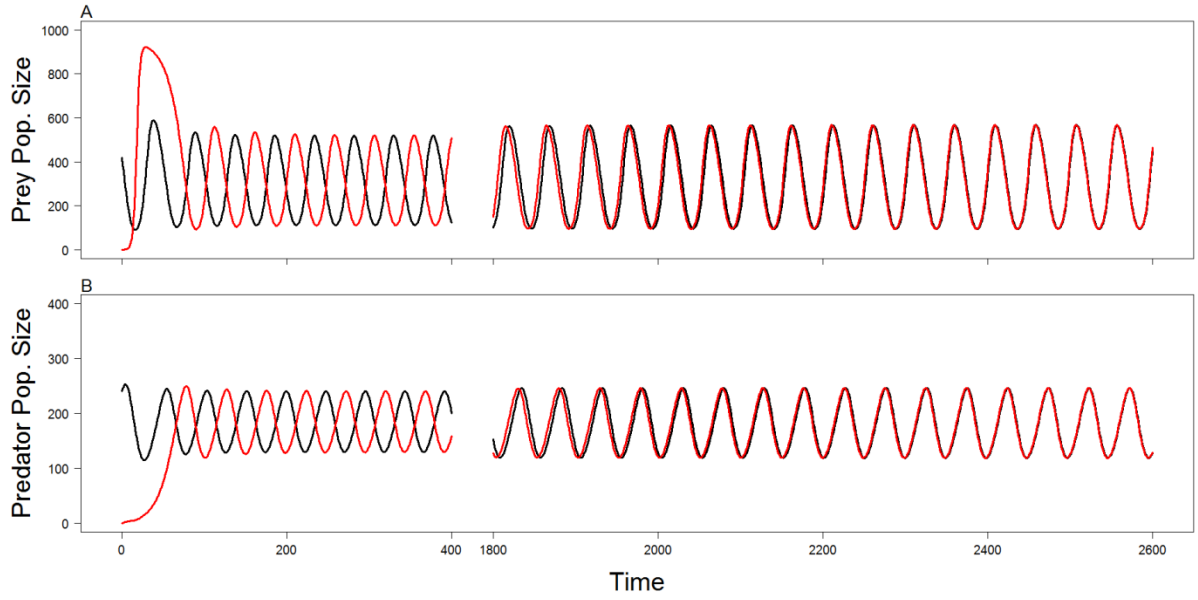

Figure 1.B.4. Transient anti-phase dynamics for prey (A) and predator (B) in the two-patch ODE model generated when $\delta_N = 0.00022$ and $\delta_P = 0.0025$. One patch is delineated by the black lines and the other by the red lines. Note the breaks in time along the x-axis.

1.C

This appendix section details the replicate-to-replicate variation of the PJP and SDE models discussed in the main text of Chapter 1 and shows that (1) the mean was a suitable statistic for summarizing the correlations of the replicates and (2) 10 replicate simulations were adequate for each dispersal parameter combination.

The Mean as an Appropriate Summary Statistic for Replicate Simulations

For each of two combinations of dispersal rates ($\delta_N = \delta_P = 0.0001$ d^{-1} and $\delta_N = \delta_P =$ 0.01668 d^{-1}), I conducted 50 replicate simulations with each of the two models. For all simulations, I used the same procedures and local parameter values as discussed in the main text and started with one patch empty and the other full. I calculated the correlations between the prey and predator subpopulations for each simulation using the second half of the time series, and plotted the distributions of these correlations for the two dispersal values (Figures 1.C.1 and 1.C.2 for the PJP and 1.C.3 and 1.C.4 for the SDE). For both trophic levels at both dispersal rates, the correlations were approximately normally distributed, symmetrical, and not strongly bi-modal, indicating that the mean correlation was an adequate summary statistic for a series of replicate simulations. The correlation distributions were generally similar for the two model types.

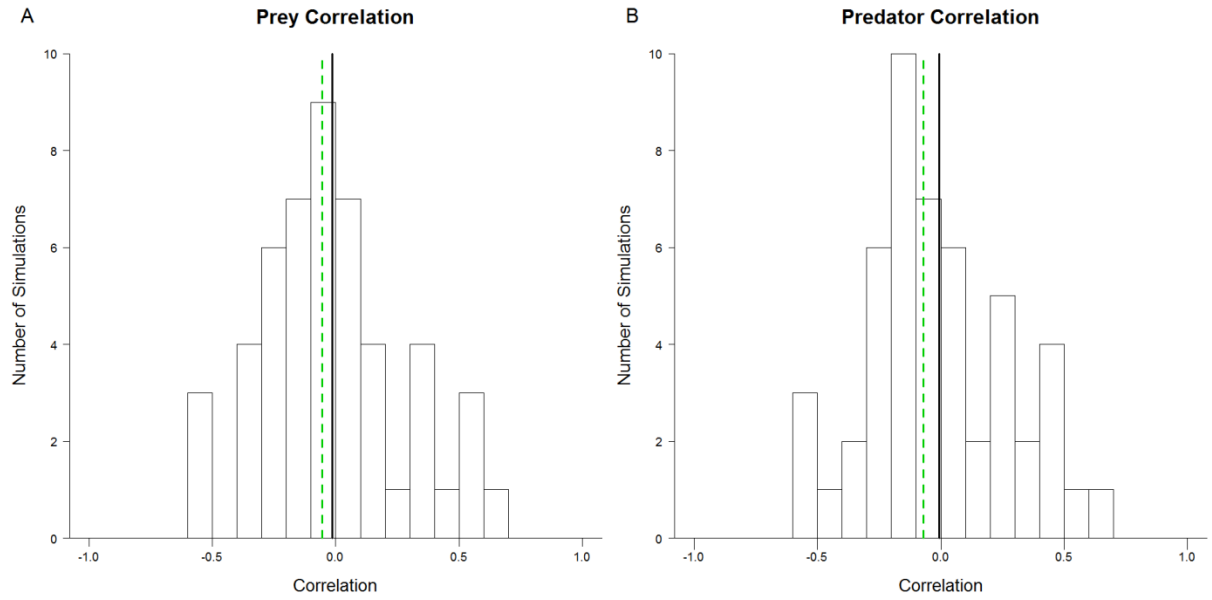

Figure 1.C.1. Histogram of the between-patch correlation values for the prey (A) and predators (B) in each of the 50 simulations of the PJP model when $\delta_N = \delta_P = 0.0001$ d^{-1}. The solid black lines indicate the mean correlation of the 50 simulations (prey = -0.015, predators = -0.007) and the dashed green lines indicate the value used in the main text Figure 1.1 (prey = -0.055, predators = -0.070).

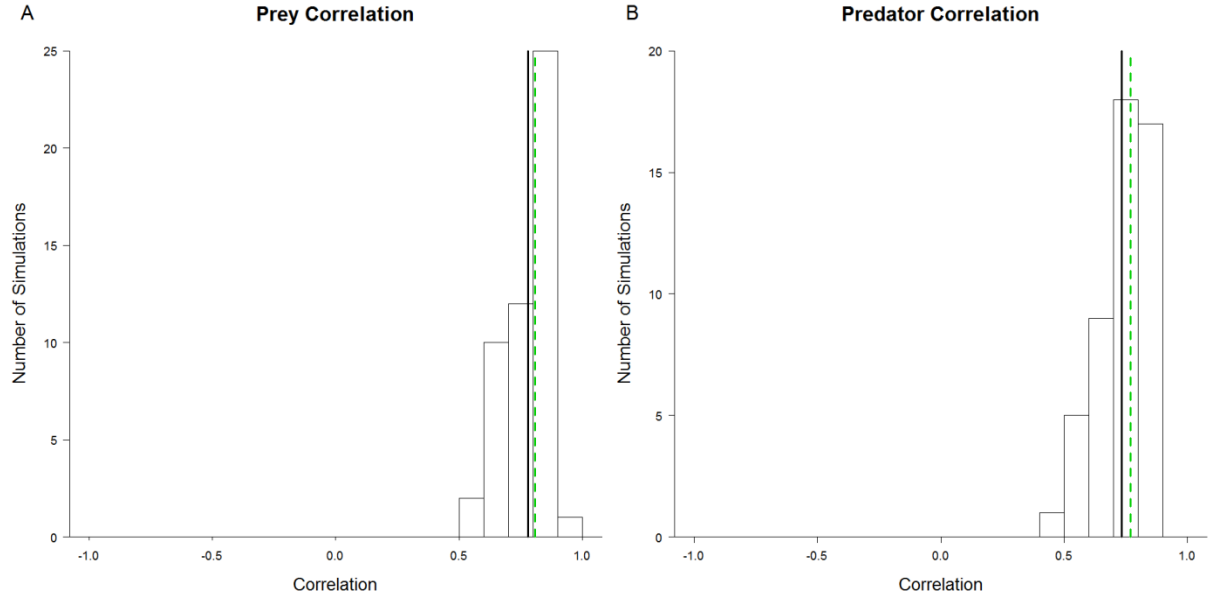

Figure 1.C.2. Histogram of the between-patch correlation values for the prey (A) and predators (B) in each of the 50 simulations of the PJP model when $\delta_N = \delta_P = 0.01668$ d^{-1}. The solid black lines indicate the mean correlation of the 50 simulations (prey = 0.779, predators = 0.735) and the dashed green lines indicate the value used in the main text Figure 1.1 (prey = 0.809, predators = 0.771).

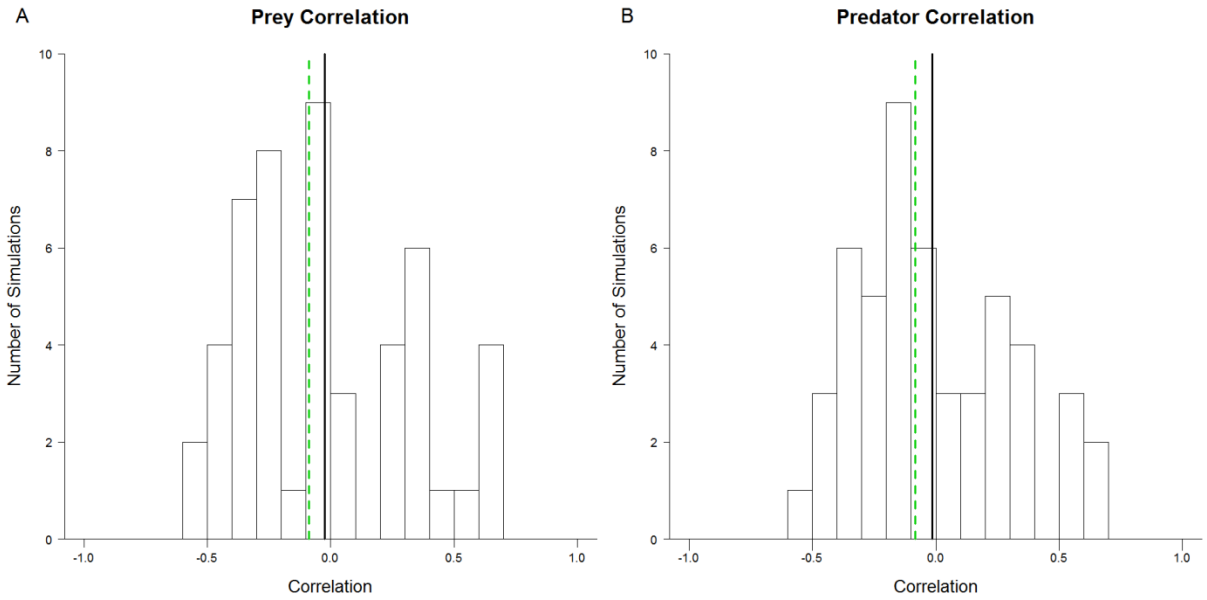

Figure 1.C.3. Histogram of the between-patch correlation values for the prey (A) and predators (B) in each of the 50 simulations of the SDE model when $\delta_N = \delta_P = 0.0001$ d^{-1}. The solid black lines indicate the mean correlation of the 50 simulations (prey = -0.024, predators = -0.014) and the dashed green lines indicate the value used in the main text Figure 1.1 (prey = -0.088, predators = -0.082).

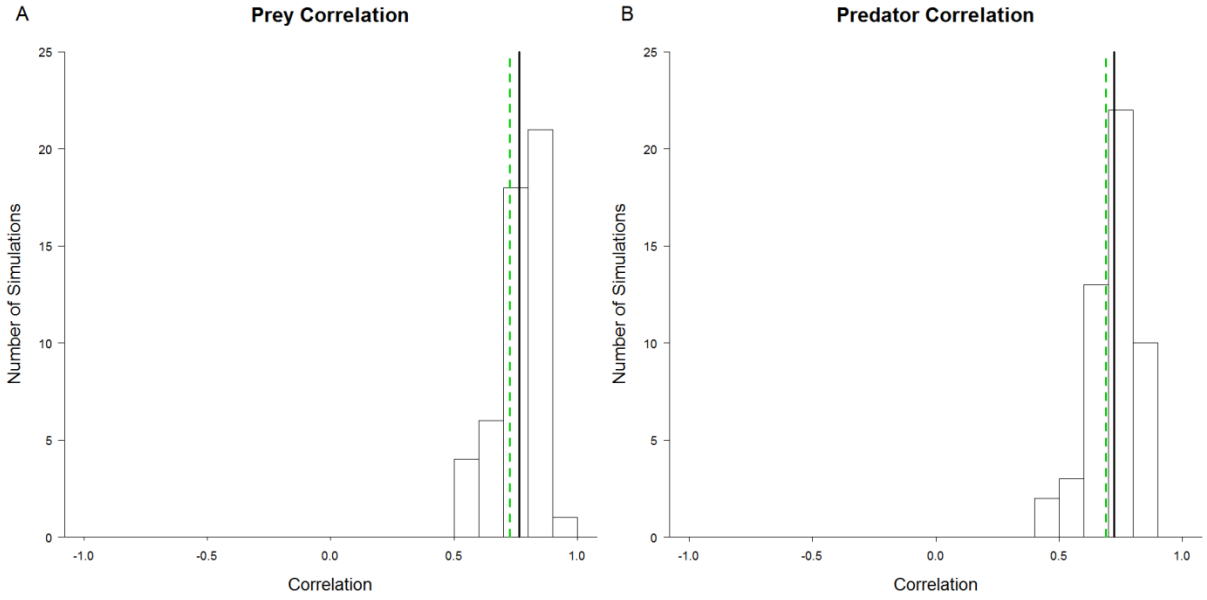

Figure 1.C.4. Histogram of the between-patch correlation values for the prey (A) and predators (B) in each of the 50 simulations of the SDE model when $\delta_N = \delta_P = 0.01668$ d^{-1}. The solid black lines indicate the mean correlation of the 50 simulations (prey = 0.765, predators = 0.724) and the dashed green lines indicate the value used in the main text Figure 1.1 (prey = 0.727, predators = 0.692).

Appropriate Number of Replicate Simulations

To determine the appropriate number of replicate simulations for the two stochastic models, I conducted a simple random sampling procedure. I used the same procedure independently for both models using the correlation values calculated from the simulations run previously and described above. Again, I analyzed the data separately for each of the trophic levels at both of the dispersal rates (0.0001 d^{-1} and 0.01668 d^{-1}). For each possible sample size X (all integers from 1 to 50), I drew X correlation values at random with replacement from the list of 50 possible values, and calculated the mean of the X correlations. I conducted 20 such random drawings for each sample size to determine the range and repeatability of the means. I graphed the 20 means for each sample size in Figures 1.C.5 and 1.C.6 for the PJP and Figures 1.C.7 and 1.C.8 for the SDE (1.C.5 and 1.C.7: dispersal = 0.0001 d^{-1} and 1.C.6 and 1.C.8: dispersal = 0.01668 d^{-1}).

For both models at both dispersal levels, fewer than five replicates gave high variation among the means, but 10 or more replicates tended to give repeatable mean correlations. Increasing the number of replicates beyond ten did not substantially decrease the variation among mean correlation values. Thus, I used 10 replicates for each parameter combination shown in Figure 1.1 in the main text. Note that for both models at both dispersal levels, the mean correlations for both predators and prey used in Figure 1.1 in the main text were very close to the overall mean of the 50 values (green vertical lines compared to black vertical lines in Figures 1.C.1−1.C.4) and well within the range of the possible means for 10 replicate samples (green dots compared to horizontal lines in Figures 1.C.5−1.C.8).

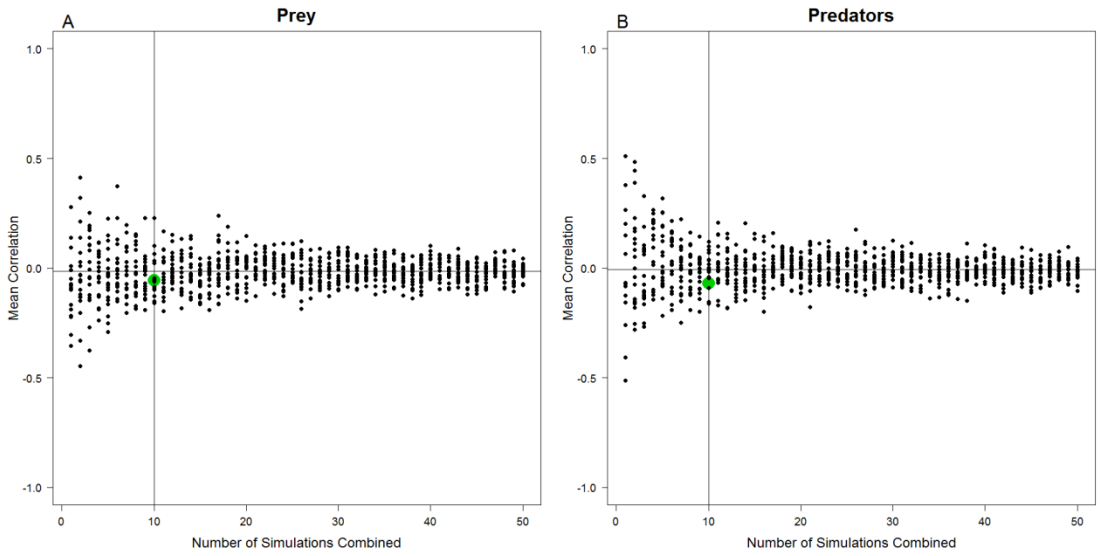

Figure 1.C.5. Distribution of the mean correlation of 20 samples at each size from 1 to 50 simulations of the PJP model for prey (A) and predators (B) when $\delta_N = \delta_P = 0.0001$ d^{-1}. The vertical lines indicate a sample size of 10 (used to create Figure 1.1), the horizontal lines show the mean correlations for the 50 simulations (pre = -0.015, predators = -0.007), and the green points indicate the correlation values used in the main text Figure 1.1 (prey = -0.055, predators = -0.070).

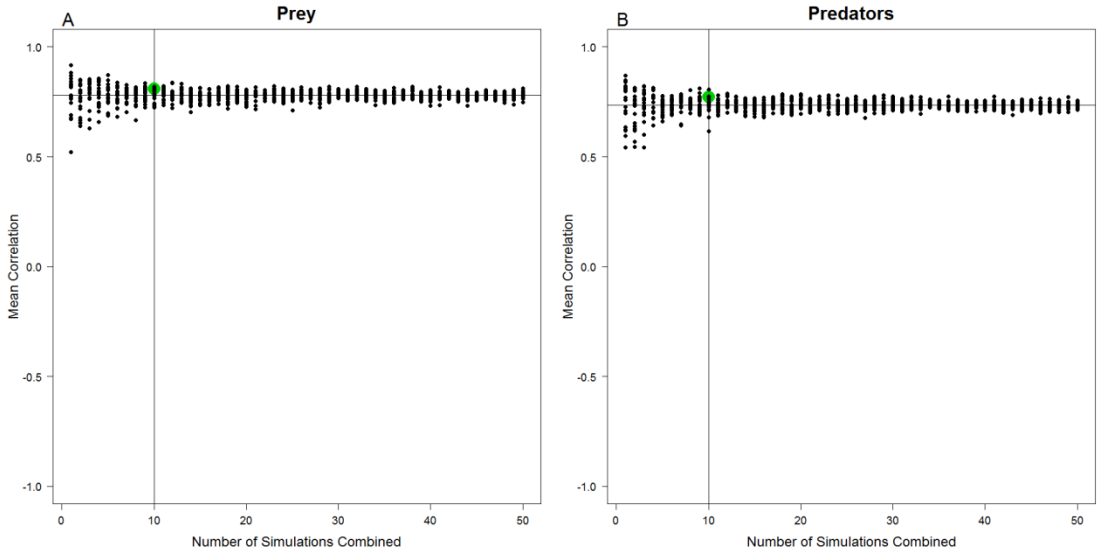

Figure 1.C.6. Distribution of the mean correlation of 20 samples at each size from 1 to 50 simulations of the PJP model for prey (A) and predators (B) when $\delta_N = \delta_P = 0.01668$ d^{-1}. The vertical lines indicate a sample size of 10 (used to create Figure 1.1), the horizontal lines show the mean correlations for the 50 simulations (pre = 0.779, predators = 0.735), and the green points indicate the correlation values used in the main text Figure 1.1 (prey = 0.809, predators = 0.771).

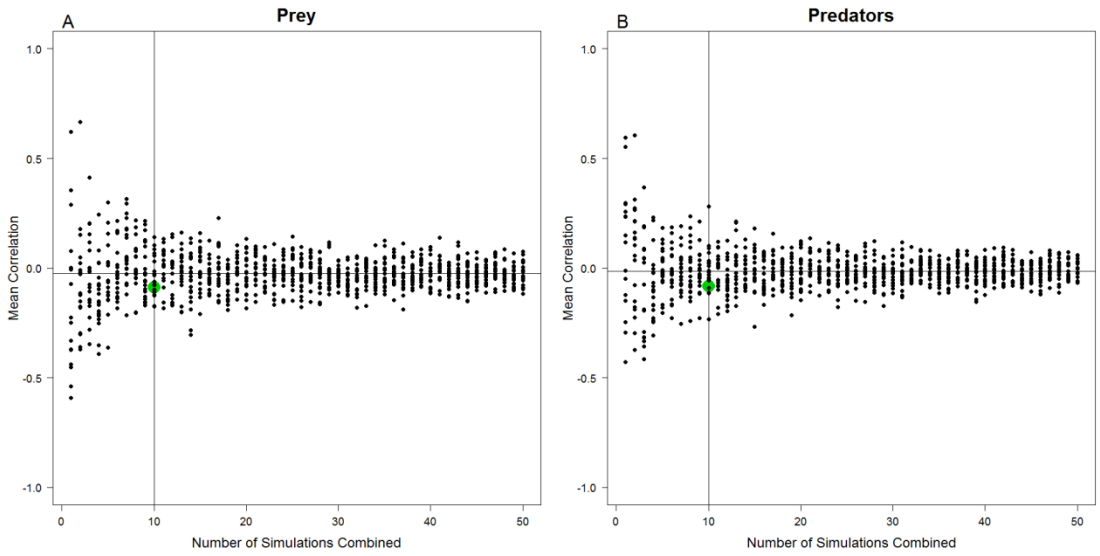

Figure 1.C.7. Distribution of the mean correlation of 20 samples at each size from 1 to 50 simulations of the SDE model for prey (A) and predators (B) when $\delta_N = \delta_P = 0.0001$ d^{-1}. The vertical lines indicate a sample size of 10 (used to create Figure 1.1), the horizontal lines show the mean correlations for the 50 simulations (pre = -0.024, predators = -0.014), and the green points indicate the correlation values used in the main text Figure 1.1 (prey = -0.088, predators = -0.082).

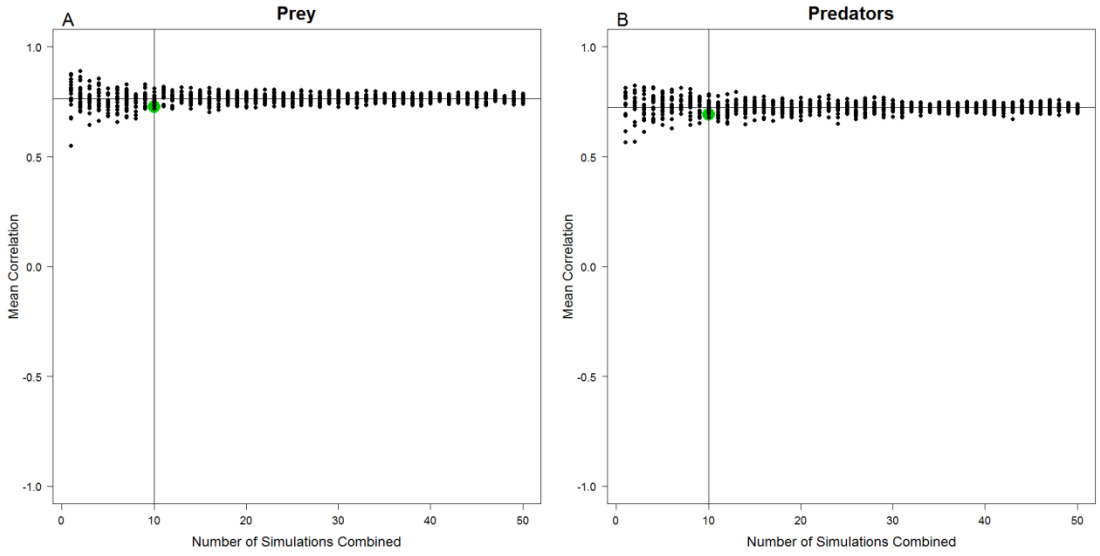

Figure 1.C.8. Distribution of the mean correlation of 20 samples at each size from 1 to 50 simulations of the SDE model for prey (A) and predators (B) when $\delta_N = \delta_P = 0.01668$ d^{-1}. The vertical lines indicate a sample size of 10 (used to create Figure 1.1), the horizontal lines show the mean correlations for the 50 simulations (pre = 0.765, predators = 0.724), and the green points indicate the correlation values used in the main text Figure 1.1 (prey = 0.727, predators = 0.692).

1.D

This appendix section addresses the sensitivity of the three models of Chapter 1 to initial conditions.

First, I graphically compared the correlations generated by the two initial conditions for each of the three models (Figures 1.D.1-1.D.6). Both the PJP (Figures 1.D.1, 1.D.2) and the SDE (Figures 1.D.3, 1.D.4) gave very similar results for the two initial conditions, whereas the ODE model generated distinctly different correlations under the two initial conditions (Figures 1.D.5, 1.D.6). In particular, the initial condition of one patch full and one patch empty generated lengthy antiphase dynamics (areas of negative correlation) for some parameter combinations, whereas the initial condition of both patches full generated complete synchrony for all dispersal levels.

Next, I ran the three models using a set of 100 randomly chosen initial conditions. For each of the starting points, I drew the initial densities of all four subpopulations independently and at random from a uniform distribution (between 0 and 420 individuals for prey and 0 and 240 for predators). I then ran the PJP, SDE, and ODE models using prey and predator dispersal rates of 0.001 d^{-1} and the rest of the parameters as described in the main text of Chapter 1, and calculated the between-patch correlations for the prey and the predators using the last 501 data points in the time series. The same 100 random initial conditions were used for all three models. I conducted ten replicate PJP and SDE simulations for each initial condition and computed the mean correlation for the replicates. The distributions of correlations are shown in Figures 1.D.7 (PJP), 1.D.8 (SDE), and 1.D.9 (ODE).

The initial conditions did not substantially affect the correlation values generated by the PJP model (Figure 1.D.7) or the SDE (Figure 1.D.8). For the PJP, the distribution of mean correlations was not strongly skewed, had a slightly positive expected value (mean for prey = 0.081, for predators = 0.070), and had a small amount of variance, which was due to the

stochastic nature of the model (as to be expected, see Appendix 1.C). Generally all of initial conditions led to the same result in the PJP: approximately asynchrony (or slight positive synchrony). The mean correlations ranged between -0.098 and 0.332 for prey and between -0.103 and 0.301 for predators. Similarly for the SDE, the distribution of mean correlations was not strongly skewed, had a slightly 28 positive expected value (mean for prey = 0.091, for predators = 0.082), and had a small amount of variance. Generally all of initial conditions led to the same result in the SDE: approximate asynchrony (or slight positive synchrony). The mean correlations ranged between -0.178 and 0.302 for prey and between -0.180 and 0.282 for predators.

In contrast, the initial conditions dictated the between-patch correlation generated by the ODE model (Figure 1.D.9). Approximately half of the initial conditions led to strong in-phase synchrony in the ODE model (53 of 100 simulations gave prey and predator correlations over 0.9), yet the correlations ranged between -0.967 and 1.000 for prey and between -0.978 and 1.000 for predators. The wide range of correlations was due to the initial conditions generating various degrees of phase lag between the two patches. At the extreme end, the initial conditions generated complete antiphase between the patches which may persist for over 30,000 model days. More often they led to a less than perfect phase offset, and dispersal was able to slowly overcome the difference in population density between the patches, generating medium-length transients with intermediate correlations.

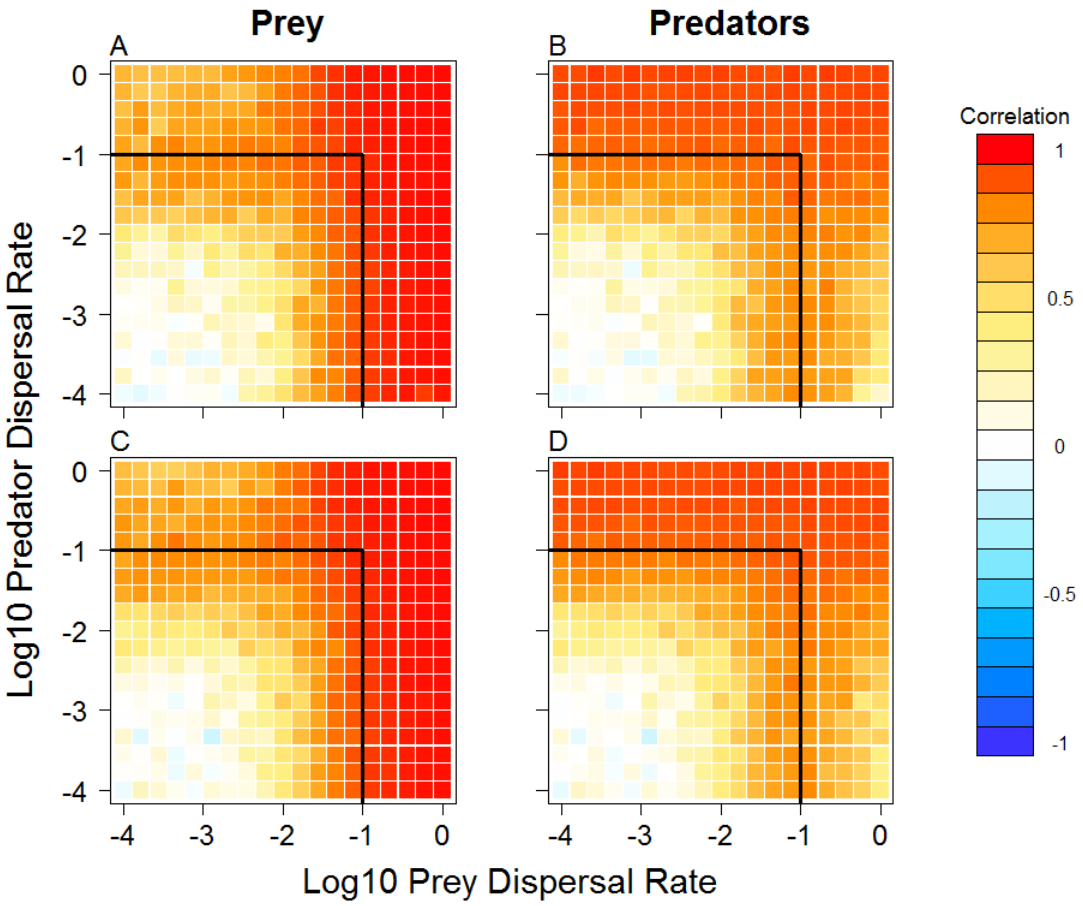

Figure 1.D.1. Correlation in densities between the two subpopulations for the prey (A, C) and predators (B, D) as a function of prey and predator dispersal rates (on a log10 scale) for the PJP model. Data are from simulations initiated with one patch full and one empty (A, B) or initiated with both patches full (C, D). Correlations are from the second half of the time series and are the means of 10 replicate simulations for each dispersal parameter combination. The thick lines mark mortality rates, (0.01 d^{-1} for both trophic levels). A and B are what were presented in Figure 1.1 in the main text of Chapter 1.

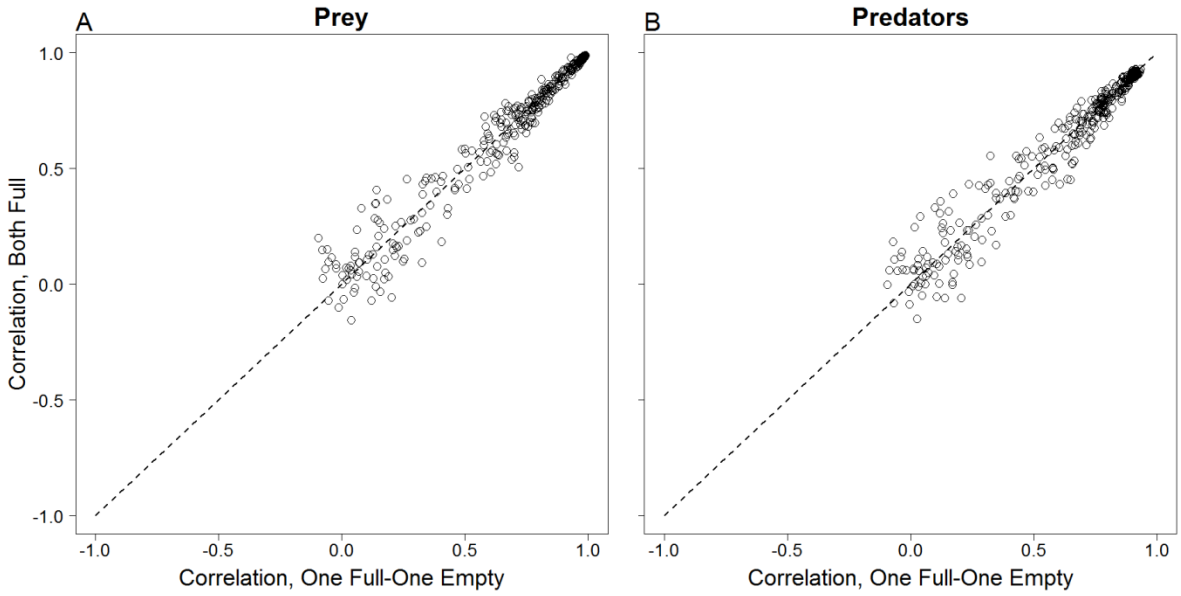

Figure 1.D.2. Relationship between the correlations generated by the PJP model under the two initial conditions (both patches full on the Y axis vs. one patch empty-one patch full on the X axis) for prey (A) and predators (B). Data points are the mean correlations for the ten replicate simulations run for a given set of dispersal parameters. The 1:1 line was added for comparison.

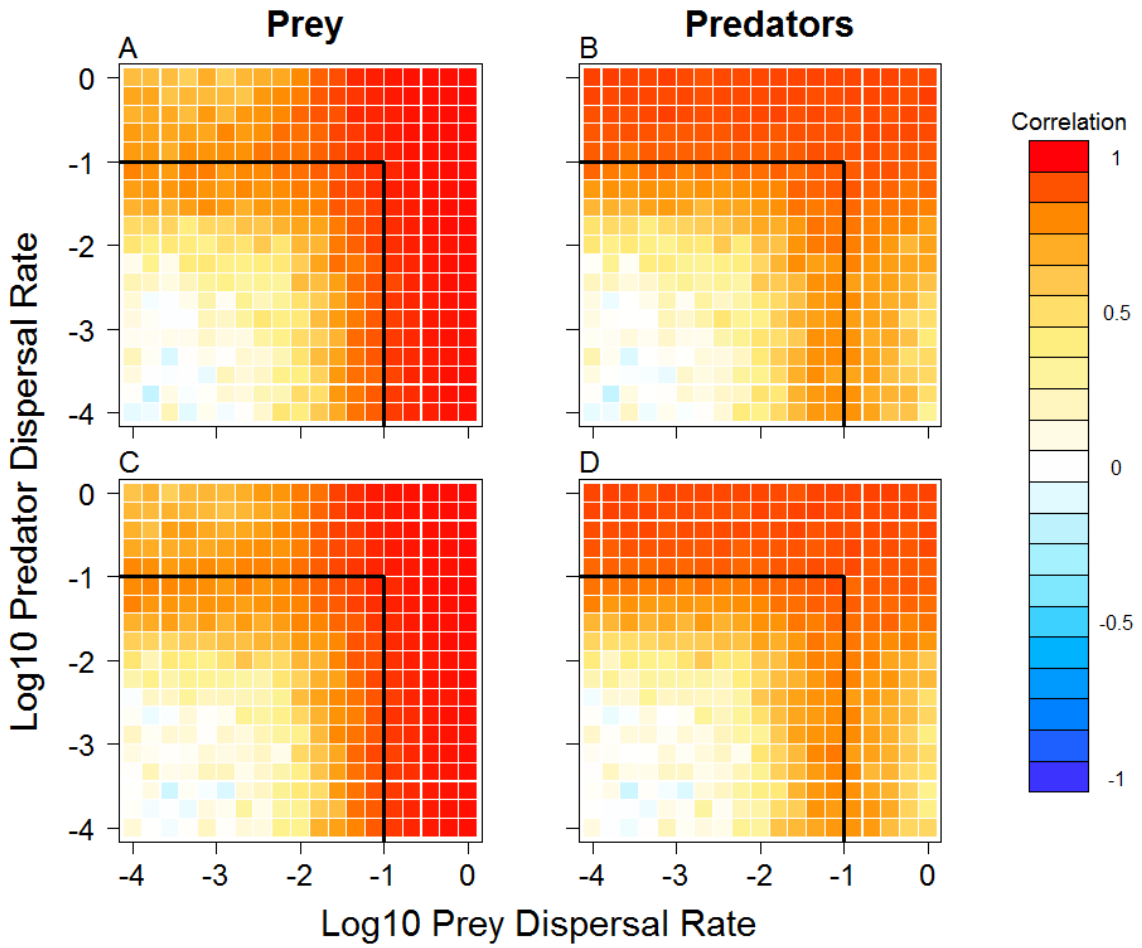

Figure 1.D.3. Correlation in densities between the two subpopulations for the prey (A, C) and predators (B, D) as a function of prey and predator dispersal rates (on a log10 scale) for the SDE model. Data are from simulations initiated with one patch full and one empty (A, B) or initiated with both patches full (C, D). Correlations are from the second half of the time series and are the means of 10 replicate simulations for each dispersal parameter combination. The thick lines mark mortality rates, (0.01 d^{-1} for both trophic levels). A and B are what were presented in Figure 1.1 in the main text of Chapter 1.

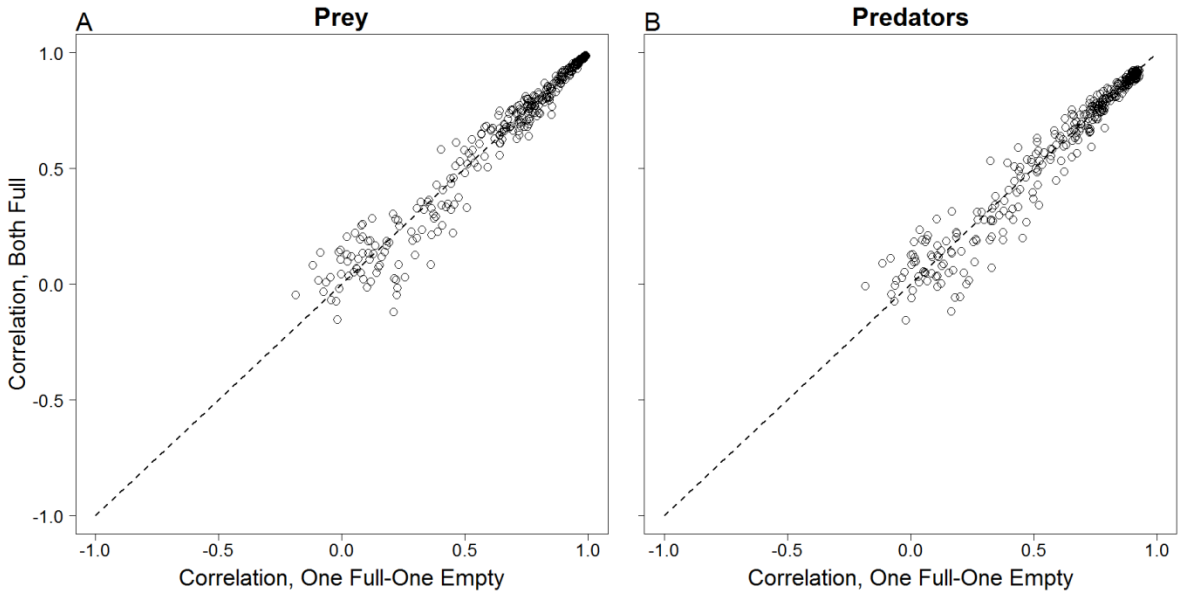

Figure 1.D.4. Relationship between the correlations generated by the SDE model under the two initial conditions (both patches full on the Y axis vs. one patch empty-one patch full on the X axis) for prey (A) and predators (B). Data points are the mean correlations for the ten replicate simulations run for a given set of dispersal parameters. The 1:1 line was added for comparison.

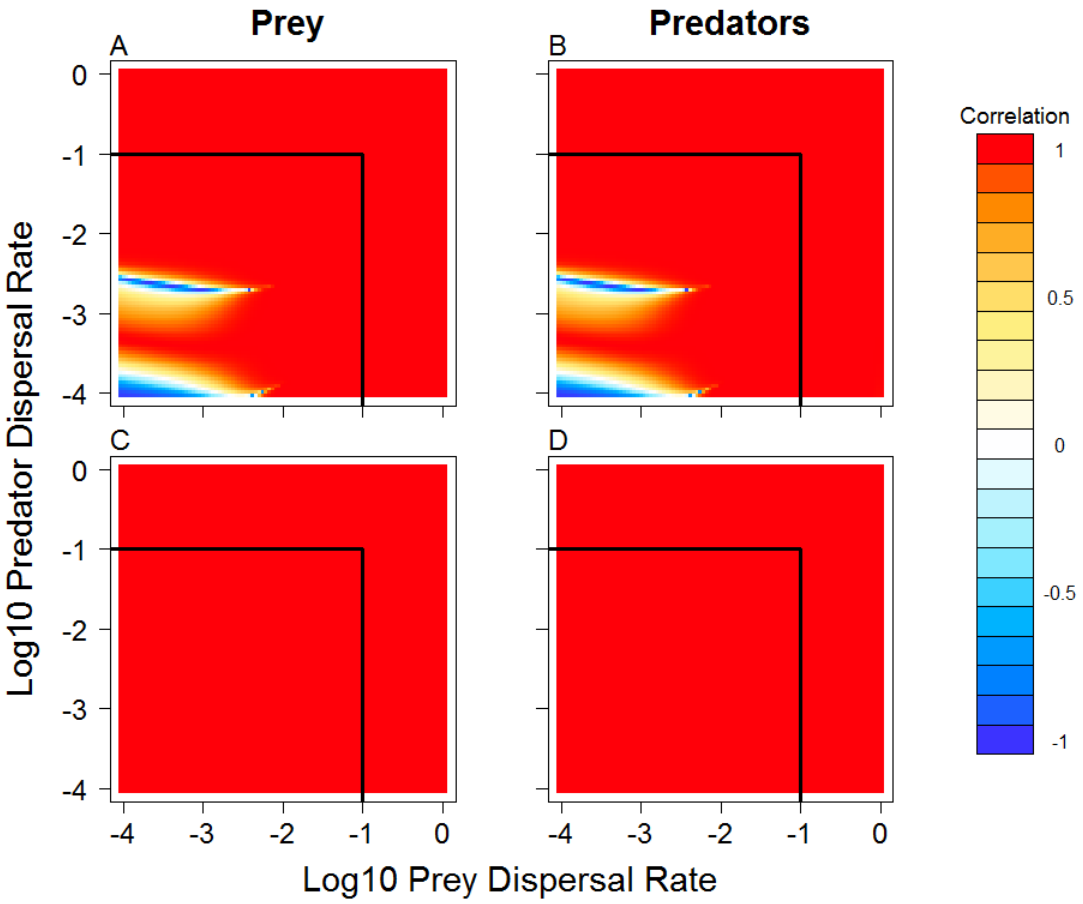

Figure 1.D.5. Correlation in densities between the two subpopulations for the prey (A, C) and predators (B, D) as a function of prey and predator dispersal rates (on a log10 scale) for the ODE model. Data are from simulations initiated with one patch full and one empty (A, B) or initiated with both patches full (C, D). Correlations are from the second half of the time series and are the means of 10 replicate simulations for each dispersal parameter combination. The thick lines mark mortality rates, (0.01 d^{-1} for both trophic levels). A and B are what were presented in Figure 1.1 in the main text of Chapter 1.

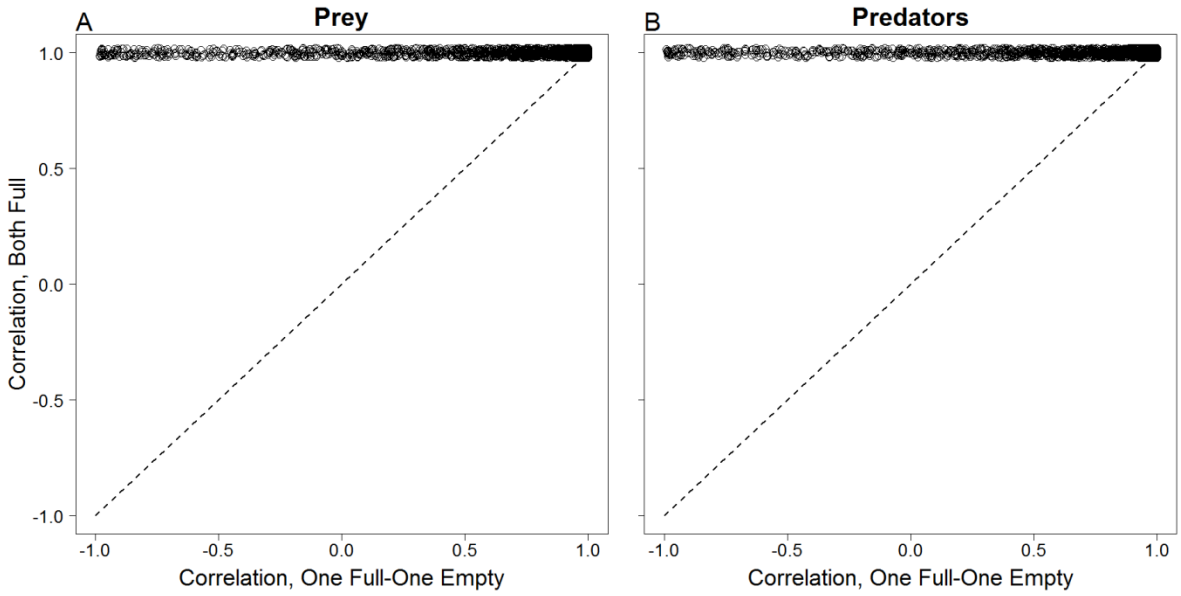

Figure 1.D.6. Relationship between the correlations generated by the ODE model under the two initial conditions (both patches full on the Y axis vs. one patch empty-one patch full on the X axis) for prey (A) and predators (B). Data points are the mean correlations for the ten replicate simulations run for a given set of dispersal parameters. The 1:1 line was added for comparison.

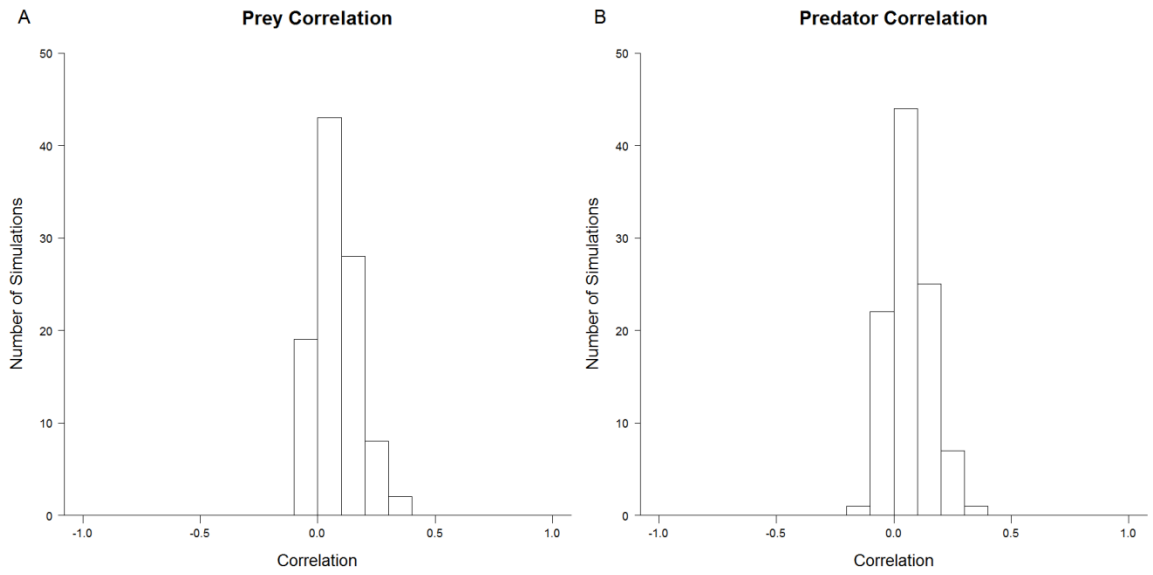

Figure 1.D.7. Distribution of correlation values for prey (A) and predators (B) in the PJP with random initial conditions and dispersal = 0.001 d^{-1} for both trophic levels. Data are mean correlations from 10 replicate simulations conducted for each initial condition.

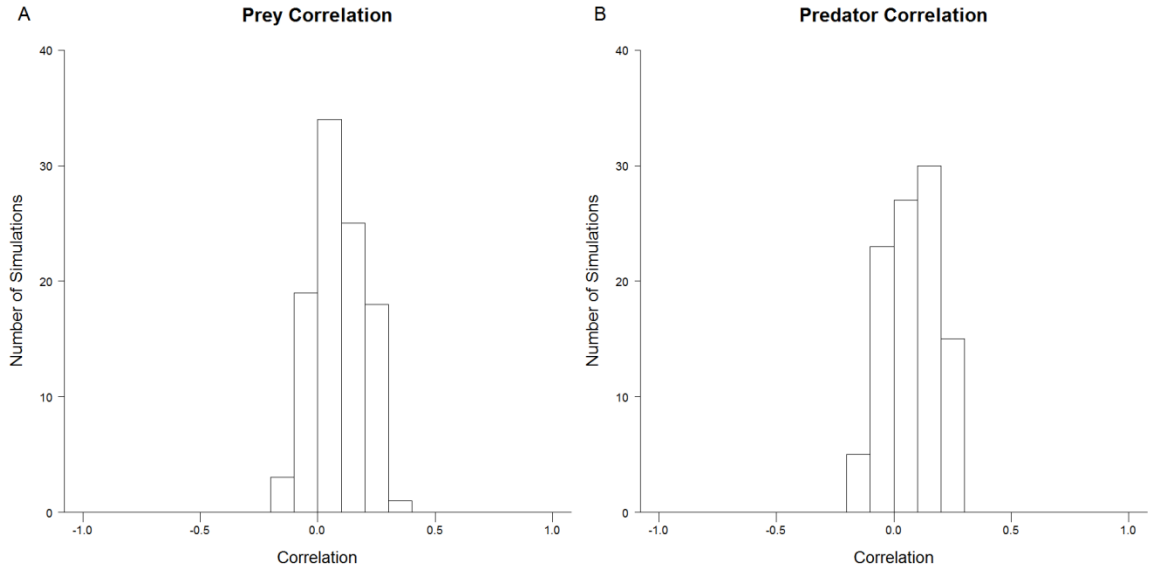

Figure 1.D.8. Distribution of correlation values for prey (A) and predators (B) in the SDE withrandom initial conditions and dispersal = 0.001 d^{-1} for both trophic levels. Data are mean correlations from 10 replicate simulations conducted for each initial condition.

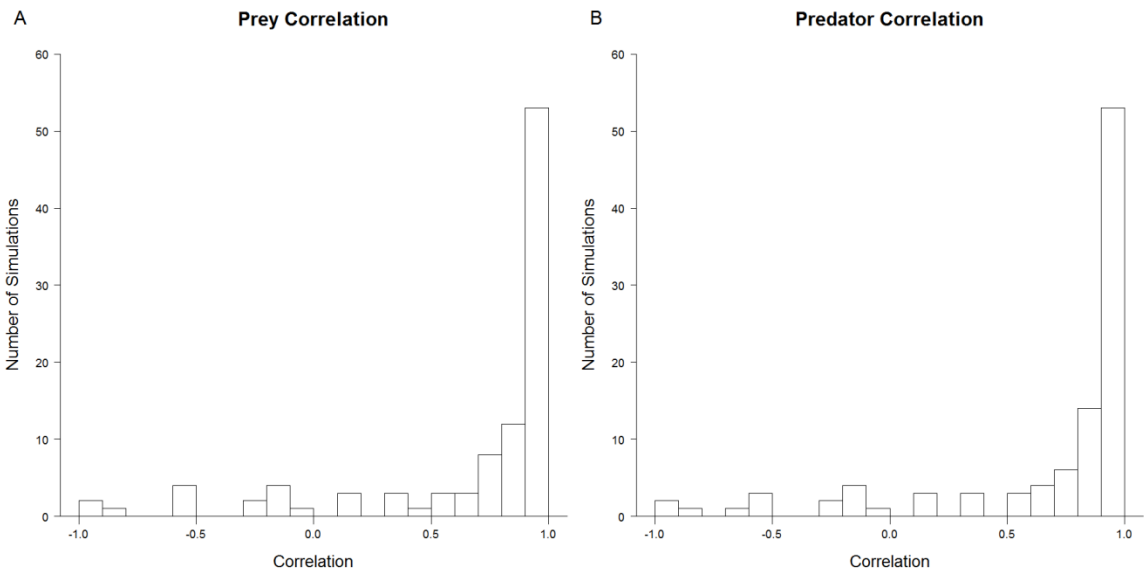

Figure 1.D.9. Distribution of correlation values for prey (A) and predators (B) in the ODE with random initial conditions and dispersal = 0.001 d^{-1} for both trophic levels. Data are mean correlations from 10 replicate simulations conducted for each initial condition.